Final Report

Investigation of Crystal Growth from Solutions

National Aeronautics and Space Administration
George C. Marshall Space Flight Center
Contract Number NAS 8-28098
November 22, 1971 - August 21, 1975

by

Ichiro Miyagawa
Project Director
Professor of Physics
University of Alabama-Tuscaloosa

University, Alabama 35486

October 1975

Final Report

Investigation of Crystal Growth from Solutions

National Aeronautics and Space Administration
George C. Marshall Space Flight Center
Contract Number NAS 8-28098
November 22, 1971 - August 21, 1975

by

Ichiro Miyagawa
Project Director
Professor of Physics
University of Alabama-Tuscaloosa

University, Alabama 35486

October 1975

TABLE OF CONTENTS

PREFACE

This project was motivated by the program "Space Processing Applications", the effort which was, and still is, being actively performed in the George C. Marshall Space Flight Center, National Aeronautics and Space Administration. There is no doubt that the core projects of "Space Processing Applications" should be concerned with metals and semi-conductors because of their industrial importance. This contractor believes, however, that studies on solution crystal growth such as that given in this report is also important, especially for understanding the fundamental mechanisms of material processing in space.

This report presents the results of all work performed for NASA contract number NAS 8-28098 "Investigation of Crystal Growth from Solutions". The primary accomplishments made during this project are as follows: proof of the degrading effect of convection currents, demonstration of the effect of a zero-gravity environment on solution crystal growth by an experiment on Skylab-4, identification of growth rate as the most important factor for dopant concentration, and suggestion and demonstration of a new solution growth technique under vacuum. Other accomplishments include: an improved convection-current observation technique using a Hellium-Neon laser and formulation of a theory of the effect of cavities on a ferroelectric hysteresis curve.

In addition to the contract reports the following papers have been published as a result of work performed during this contract period.

1. Tom Hunter "Procedure for Drilling Small Holes in Fragile Crystals", Review of Scientific Instruments, in press.

2. Y. Kotake and I. Miyagawa, "Negative ENDOR Study of Triglycine Sulphate and its Ferroelectric Transitions", Journal of Chemical Physics, in press.

In addition, two papers dealing with the degradation effect of convection and the effect of growth rate on dopant concentration are being prepared.

LIST OF FIGURES

List of Tables

ABSTRACT

This report describes the results of three years and nine months work on studies of crystal growth from solution. Growth of organic compounds from solution, in particular Rochelle salt and triglycine sulphate, was investigated. Ground-based experiments showed the strong influence that gravity-driven convection currents in the growth solution has on defect production in crystals. Ferroelectric quality is also degraded by defects which result from convection currents. The results of these experiments indicated that an experiment done in a zero-gravity environment where convection is practically absent would be useful in understanding the basic mechanisms of crystal growth and defect production. For this reason, a crystal of Rochelle salt was grown on board Skylab-4. The quality of this crystal was compared to earth-grown crystals and some of its unusual features were studied. The results of the Skylab experiment showed that (i) a typical defect produced in this convection-free environment was a long straight tube extending in the direction of the c crystal axis; these tubes were much longer and more regularly arranged than in similar earth-grown crystals (ii) the crystal was actually several crystals whose corresponding axes were parallel to each other. Ferroelectric hysteresis experiments showed that some parts of the crystal had many defects, while other parts were of extremely good quality.

Supporting studies on techniques of characterization were performed; for example, a theory which describes the effect of defects on the shape of the hysteresis curve was formulated. In addition, ground-based studies on

the effect of convection on growth rate, macroscopic and microscopic quality, and dopant concentration resulted in several new growth and characterization techniques.

ACKNOWLEDGEMENTS

This investigator acknowledges efforts of the people who worked for this project. Their names, positions, and primary roles are as follows:

Dr. Estelle F. Helms, Research Physicist: Growth experiments and characterizations.

Dr. Roderic B. Davidson, Research Physicist: Preliminary work and planning.

Dr. Bob A. Wilkinson, Graduate Assistant: Characterization techniques, especially for ferroelectric domains.

Dr. Ikuo Suzuki, Research Physicist: Characterization and growth techniques.

Dr. Yashige Kotake, Research Physicist: Characterization techniques.

Mr. Harold A. Helms, Jr., Graduate Assistant: Characterization and growth techniques, photographs and ferroelectric hysteresis measurements.

Mr. John R. Neergaard, Graduate Assistant: Characterization techniques, especially for ferroelectric hysteresis.

Mr. Jenn-Luen Yeh, Graduate Assistant: Characterization and growth techniques.

Mr. Thomas C. S. Chen, Graduate Assistant: Characterization techniques.

Mr. Tom Hunter, Machinist: Instrumentation.

The staff and this investigator are grateful to Mr. Tommy Bannister of SSL, George C. Marshall Space Flight Center, for his suggestions in various stages of this investigation. We are particularly grateful to Astronaut Col. Pogue for performing our experiment on Skylab-4.

Summary and Conclusions

Crystal growth of organic compounds from solution, in particular Rochelle salt and triglycine sulphate (TGS), was investigated. The investigation included growth study, observation of visible and microscopic defects, study of convection currents responsible for defect production, study of copper and L-alanine doping, measurement of ferroelectric hysteresis and domains, and characterization of crystal quality in general. A crystal of Rochelle salt was grown on board Skylab-4 in a near-zero gravity experiment and some of its unusual features were studied.

By growth studies and observation of convection currents it was proven that convection currents produce defects, both visible and microscopic, which are usually cavities and inclusions of solution. In addition it was concluded that sensitivity to convection depends on the crystal axis along which growth occurs. In the case of Rochelle salt, the c-axis was found to be the most sensitive.

The convection responsible for visible and microscopic defects is essentially a gravity-driven, concentration induced one. More accurately, convection was shown to arise from motion of solution layers adjacent to the growing crystal surface. Evidence was also found to indicate the presence of weak, invisible convection currents.

It was shown, by studying ferroelectric hysteresis curves and domains in several different parts of a crystal, that convection currents degrade ferroelectric quality. It was also shown that different parts of a crystal can be greatly different in ferroelectric quality, even though these parts show no visible defects.

A microscopic study was performed in order to gain insight into the nature of the degradation effect of convection. It was found that in general crystals have many microscopic defects, even if they appear perfect to the unaided eye. It was also found that these microscopic defects can usually be classified into two groups; relatively large, empty cavities, and relatively small cavities containing solution. Dissolved air in the growth solution was shown to be one of the reasons for the formation of both types of cavities. In addition, it was found that convection increases the relative number of solution-containing cavities compared to empty cavities in a crystal.

A crystal of Rochelle salt was grown from solution on Skylab-4 in a near-zero gravity environment. This crystal offered the first opportunity to experimentally examine the effect that the absence of gravity would have on solution crystal growth. Two important results of the experiment on Skylab were: (i) a typical defect in this crystal was a long straight tube extending in the direction of the c-axis; these tubes were far more regularly arranged than in earth-grown crystals; (ii) the crystal was actually a composite consisting of several single crystals whose corresponding axes were parallel to each other, this arrangement is most unusual in earth-grown composite crystals.

An investigation was performed to identify the factors which determine the dopant concentration in a crystal. One such factor was found to be the growth rate. The concentration of the doping copper ion in Rochelle salt increased with increasing growth rate, while no appreciable doping occurred in the case of extremely slow growth.

A basically new technique of crystal growth from solution was suggested by some of the results discussed above. We found that it is possible to achieve consistently high doping concentrations by growing crystals from a solution in a low-pressure or vacuum environment and increasing the growth rate to such an extent that many cavities would be produced if the crystal were grown under atmospheric pressure. This technique resulted in crystals of TGS with consistently high L-alanine doping concentrations.

The observation of convection currents during solution crystal growth has been greatly improved by a new method of illumination. A Helium-Neon laser beam was used as a source with a Schlieren type observation technique.

A theory for the shape of the ferroelectric hysteresis curve was formulated. It was found that the shape of a hysteresis curve is sensitive to the concentration of cavities in the crystal.

List of Publications

I. Contract Reports

Bi-monthly reports were prepared and distributed by the Principle Investigator to the National Aeronautics and Space Administration, George C. Marshall Space Flight Center, Huntsville, Alabama, on the following dates during the contract period.

1. February 1, 1972
2. March 4, 1972
3. June 6, 1972
4. August 7, 1972
5. October 6, 1972
6. December 7, 1972
7. April 4, 1973
8. June 6, 1973
9. August 6, 1973
10. October 9, 1973
11. December 7, 1973
12. April 9, 1974
13. June 6, 1974
14. August 7, 1974
15. October 7, 1974
16. December 5, 1974
17. April 1, 1975
18. June 4, 1975

In addition, yearly Technical Summary Reports were prepared and distributed on the following occasions.

1. February, 1973
2. May, 1974

II. Publications: Journals and Others

This work has led to the publishing of the following papers during the contract period.

(1) Procedure for Drilling Small Holes in Fragile Crystals", by Tom Hunter - The Review of Scientific Instruments, in press.

(2) "Negative ENDOR Study of an Irradiated Single Crystal of Triglycine Sulphate and its Ferroelectric Phase Transition" by Y. Kotake and I. Miyagawa - Journal of Chemical Physics, in press.

III. To Be Published

Work during this contract period has resulted in the following papers which will be published in the near future.

(1) "Copper Doping in Single Crystals of Rochelle Salt", by E. F. Helms and I. Miyagawa.

(2) "Effect of Convection in Rochelle Salt", by I. Miyagawa.

Section 1. Introduction

1.1 Aim of Study

This project was funded to study crystal growth from solutions as one of the programs in "Space Processing Applications". Thus, our work had several important goals: first, to investigate whether or not convection currents in growth solutions degrade the quality of the resulting crystal; second, if the degrading effect of convection were firmly established, to perform a crystal growth experiment in zero-gravity surroundings and to analyze the results; and third, to apply the results obtained during the course of these investigations to materials of practical importance.

We believe this project has accomplished most of these goals: It was proven that strong convection produces defects in crystals grown from solution; a Rochelle salt crystal was grown in the zero-gravity environment of Skylab-4; the crystal was analyzed and compared to similar earth-grown crystals; and the information gathered during these investigations has been applied to one material, triglycine sulphate, which may be improved by growth in a zero-gravity environment.

1.2 Scope of Work

A. Work Statement - The work statement stipulated for this contract is as follows: The contractor shall study growth characteristics and resulting crystal quality of various crystals with the purpose of defining flight experiments utilizing extended freefall conditions. Candidate materials will be selected on the basis of scientific and industrial significance and may represent a new material or a significantly improved product. The study should be potential or employ the advantages of freefall conditions.

Emphasis will be placed on growth from solution. Studies will be performed to ascertain the effect of a space environment on growth phenomena and resulting quality. Effects of crystal weight and thermal convection will be studied under controlled conditions and related to crystal quality for different growth conditions, i.e., rate of cooling, mixing, temperature of saturation, etc.

Candidate materials will be selected on the basis of their potential technological impact. Dopant distribution, crystal quality, and crystal size are factors which effect the utility of many materials. For example, doping homogeneity is an important factor in electronic transport properties, and crystal size and quality is important in the utility of many ferroelectric, piezoelectric, and electrooptic crystals.

Characterization of the crystals will include determination of optical properties, spin resonance data, and electronic properties. Other techniques will be used where appropriate to the particular material (i.e., electrooptic, electromagnetic, and etc).

Expected Results. The contractor shall define crystals with growth techniques amiable for flight operation. The contractor will pursue a laboratory growth program on candidates selected as having a high potential for inclusion in the MS/MS including definition of optimum growth techniques, and definition of practical characterization techniques that can be used to elucidate the role of space environment. Data from the results of ground-based studies on growth parameters versus crystal perfection will be applied.

The contractor shall apply the characterization and growth techniques developed in the course of this project to materials of practical interest. Suggestions for future space processing experiments are important.

B. Summary of Procedure - In order to examine the effect of convection on crystal quality, many organic crystals of L-alanine, glycine, acetylglycine, Rochelle salt, and triglycine sulphate were grown from pure solutions and those containing doping ions. It became evident after these preliminary experiments that effort should be concentrated on one material, in order to establish the degrading effect of convection. Studies with many materials in a short time appeared to result only in possible suggestions, but not in a firm conclusion. Rochelle salt was selected because of its ferroelectricity, the property which is potentially interesting but has not been fully exploited industrially. Triglycine sulphate, another ferroelectric material, was also studied rather intensively.

Many growth studies and observations of convection currents were also made. The results of these experiments proved that gravity-driven convection currents in the growth solution produce defects in the resulting crystal.

On the basis of the above conclusion, the contractor recommended that solution-growth experiments be performed in a zero-gravity environment. Thus, a crystal of Rochelle salt was grown from solution on Skylab-4. This crystal offered the first opportunity to experimentally examine the significance of a zero-gravity environment in the case of solution crystal growth. The unusual characteristics of cavity-type defects in the crystal indicated that the growth process in zero-gravity experiments greatly differed from that in ground-based laboratories.

An extensive study was performed on copper ion doping in Rochelle salt crystals. The primary purpose of this study was to identify the factors which determine the dopant concentration in a crystal. One such factor was found to be the growth rate.

On the basis of the above conclusion and some of the results obtained in this project, a basically new technique of crystal growth from solution was suggested and demonstrated. We found that it is possible to achieve consistently high doping concentrations by growing crystals from a solution under a low-pressure atmosphere and increasing the growth rate to such an extent that many cavities would be produced if the crystal were grown under normal atmospheric pressure. This technique resulted in crystals of triglycine sulphate (TGS) with consistently high L-alanine doping concentrations. L- lanine doped TGS is believed to be a potentially excellent infrared detector material.

The observation of convection currents during solution crystal growth has been greatly improved by a new method of illumination employing a Helium-Neon laser.

Finally, a theory for the shape of the ferroelectric hysteresis curve was formulated. The shape of a hysteresis curve was found to be sensitive to the concentration of cavity defects in the crystal.

Section 2. PRELIMINARY GROWTH STUDIES - CONVECTION CURRENTS (FIRST YEAR'S WORK)

2.1 Experimental Procedures

As is indicated in the Introduction, Rochelle salt was used in most of the experiments for this section. The dry chemical was obtained commerically from Eastman Organic Chemicals.

2.1-1 Growth Experiment Technique

A. Preparation of seed crystals - Crystals were grown by slow evaporation of a saturated solution at room temperature without special precautions. A crystal of relatively high quality was selected for preparation of seed crystals. The crystal was sliced by a wet thread method. The plane of each resulting piece was perpendicular to the desired crystal axis. Then each piece was carefully ground with sand paper to a desired size, typically 2 x 3 x 4 mm. Many seed crystals, identified for the a, b, and c axes, respectively, were prepared and stored for growth experiments.

Slicing of crystals in this report was performed by a Microtech crystal cutting machine.

Crystals of relatively low quality were used for preparation of the saturated solutions for growth experiments.

B. Preparation of saturated solutions - 10 grams of Rochelle salt and 7.5 cc of distilled water were heated in a vial to about 60°C for about 30 minutes. When the Rochelle salt dissolved completely and the solution became uniform, a small crystal of low quality was added to the solution, and the vial was placed in a constant-temperature water bath at 34°C. In this condition, a crystal in general grows rather rapidly for first one or two hours

and then crystal growth almost ceases several hours later. The solution is now only slightly supersaturated and ready for the next step of the growth experiment.

Dimensions of the vial used in the present work were 29 mm diameter by 62 mm.

C. Growth experiment: preparation - The vial with the solution was then taken from the bath and the solution was transferred into another clean vial, leaving the crystal, or crystals, which had grown in the original vial. Then the solution was heated to 40-45°C. Next, a seed crystal with the desired axis vertical was added to the solution, and finally, the vial was returned to the water bath.

The heating to 40-45°C is needed to destroy invisible nuclei which exist in any supersaturated solution. The seed crystal was washed in benzene, then in acetone, and finally in a small amount of distilled water.

D. Preliminary growth experiment - In the preliminary experiment, the c-axis of the seed crystal was held vertical and, as was done in all the other experiments, placed at the bottom of the solution. The cooling rate of the water bath, which was controlled manually, was kept uniform for some periods but changed continuously for some other periods. Growth of the crystal was determined by taking photographs every two to four hours over a period of 73 hours. The result of this observation is given in Fig. 1. It was found that when the cooling rate was uniform, the growth rate was essentially uniform, both in the a and c-axes (see periods I and II in Fig. 1).

E. Proportional temperature controller - Based on the preceding conclusion, a standard type[1] proportional temperature controller unit was designed and built. The sensor was a negative temperature coefficient

Figure 1. Preliminary Growth Study of Rochelle Salt.
Growth of a Rochelle salt crystal with the c-axis held vertical under manual operation. The upper curves show the linear growths along the a anc c-axes against time. The lower curve shows temperature of the bath against time.

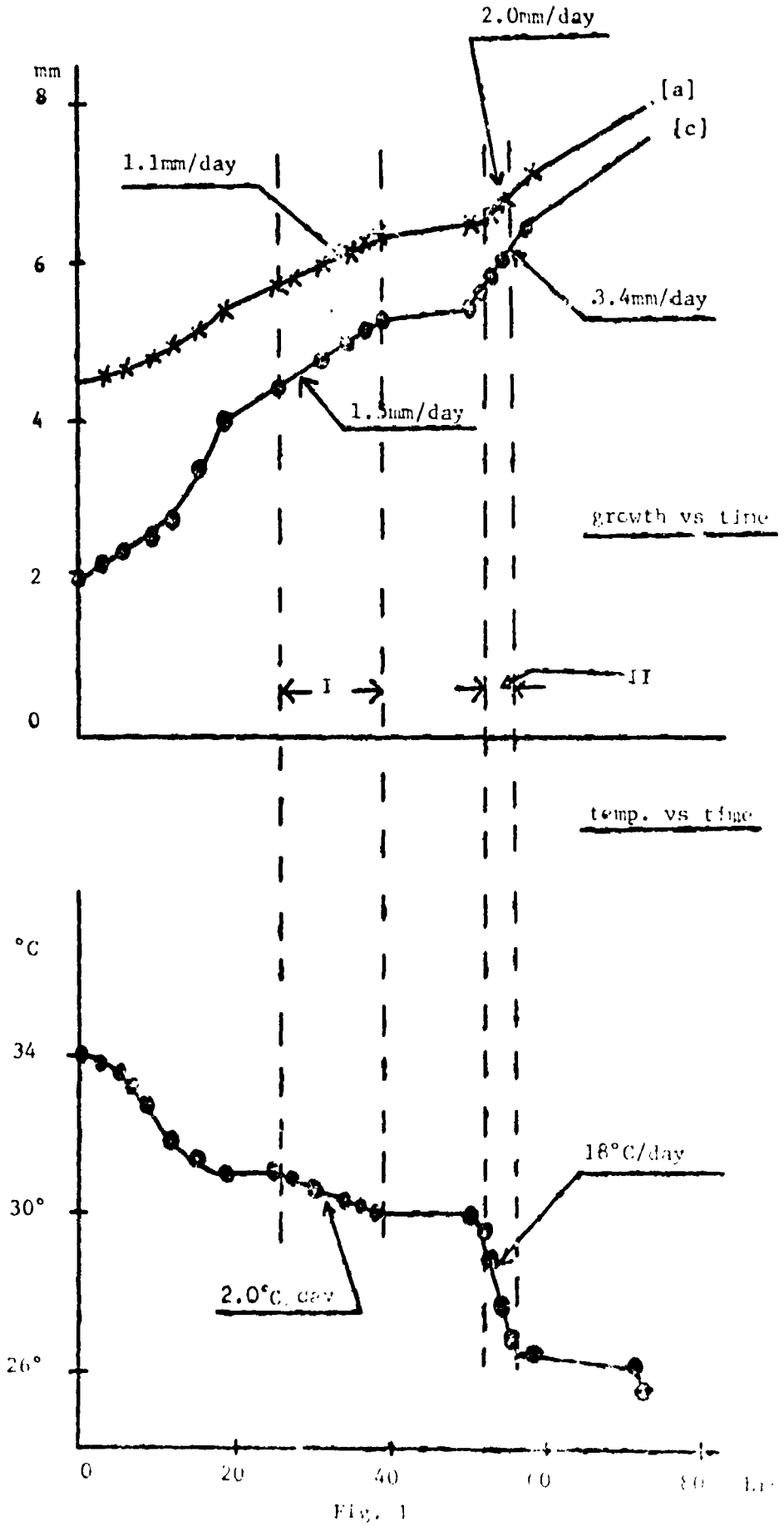
2.0mm/day
mm
8
[a]
[c]
1.1mm/day
6
3.4mm/day
4
1.5mm/day
growth vs time
2
I
II
0
temp. vs time
°C
34
18°C/day
30°
2.0°C/day
26°
0
20
40
60
80

Fig. 1

chermister, Fenval JA35J1, 5000 ohms. A 1000 ohm, 10-turn potentiometer, which is connected in series with the sensor, was driven by a clock-motor of variable rotation rate. An example of the performance of this unit is given in Fig. 2. This result shows a uniform cooling rate even in the case of 54°C/day, predicting a uniform growth rate over a range of several degrees in °C. The growth experiment hereafter was done with the use of this unit.

2.1-2 Observation of Ferroelectric Domains

One finds a good review of ferroelectricity in a book by Joan and Shirane.[2] A brief discussion will be given in 2.4-1, for convenience. A Leitz Ortholux microscope with camera was used to observe and take photographs of ferroelectric domains. A sample crystal was placed on a water jacket kept at 5°C, since Rochelle salt is ferroelectric only for the temperature range of -18 to +24°C.

2.1-3. Observation of Ferroelectric Hysteresis

The circuit shown in Fig. 3 was used to observe ferroelectric hysteresis in the present work. In Fig. 1, $C_o >> C_s$, the capacitance of the capacitor with a sample, so that the voltage across the sample is approximately the supply voltage. The electric field is proportional to the applied voltage, thus if a fraction of the supply voltage is used as the horizontal axis of the scope, this axis is proportional to the electric field. The voltage at A is across the capacitor C_o on the left and is proportional to the charge passing through the circuit containing the sample. The voltage at B is across the capacitor C_o on the right and is proportional to the charge passing through the circuit containing a variable capacitor which has a pure dielectric behavior. The variable capacitor is adjusted so as to produce

Figure 2. Cooling Curve.

Bath temperature against time under automatic operation.

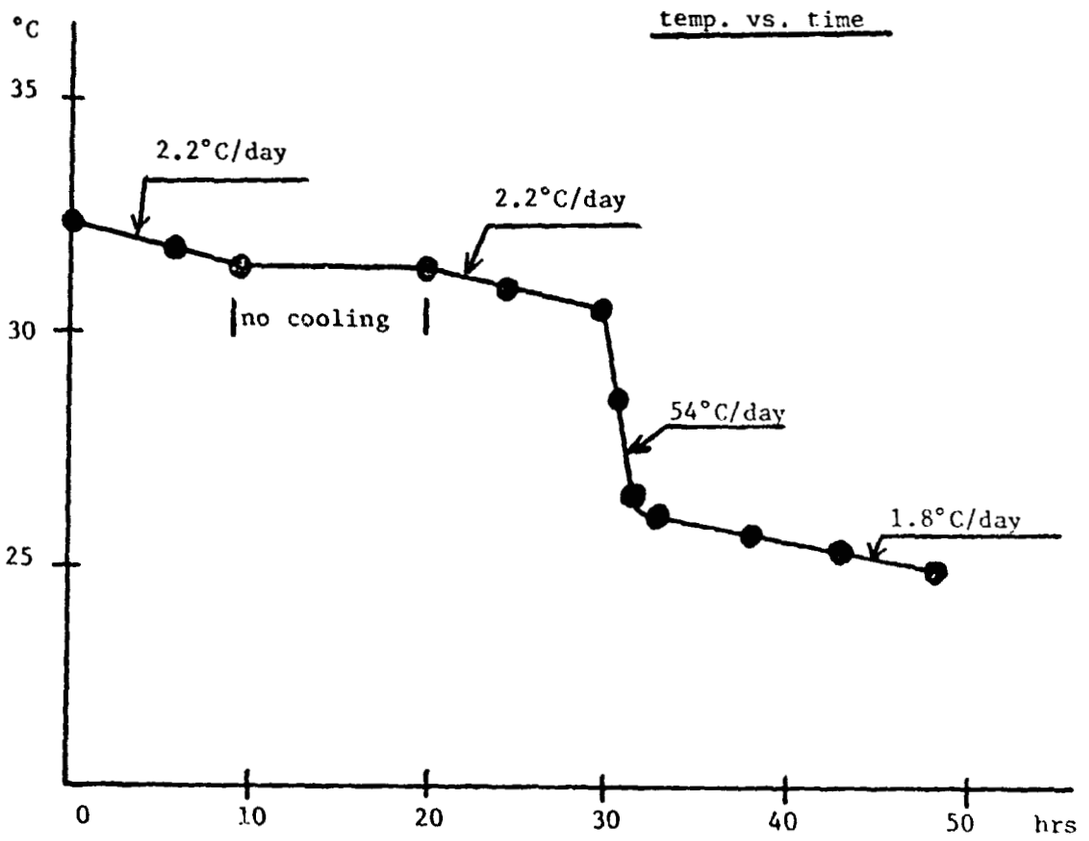
temp. vs. time
°C
35
30
25
2.2°C/day
2.2°C/day
no cooling
54°C/day
1.8°C/day
0
10
20
30
40
50
hrs

Fig. 2

Figure 3. Circuit Diagram for Observation of Ferroelectric Hysteresis.

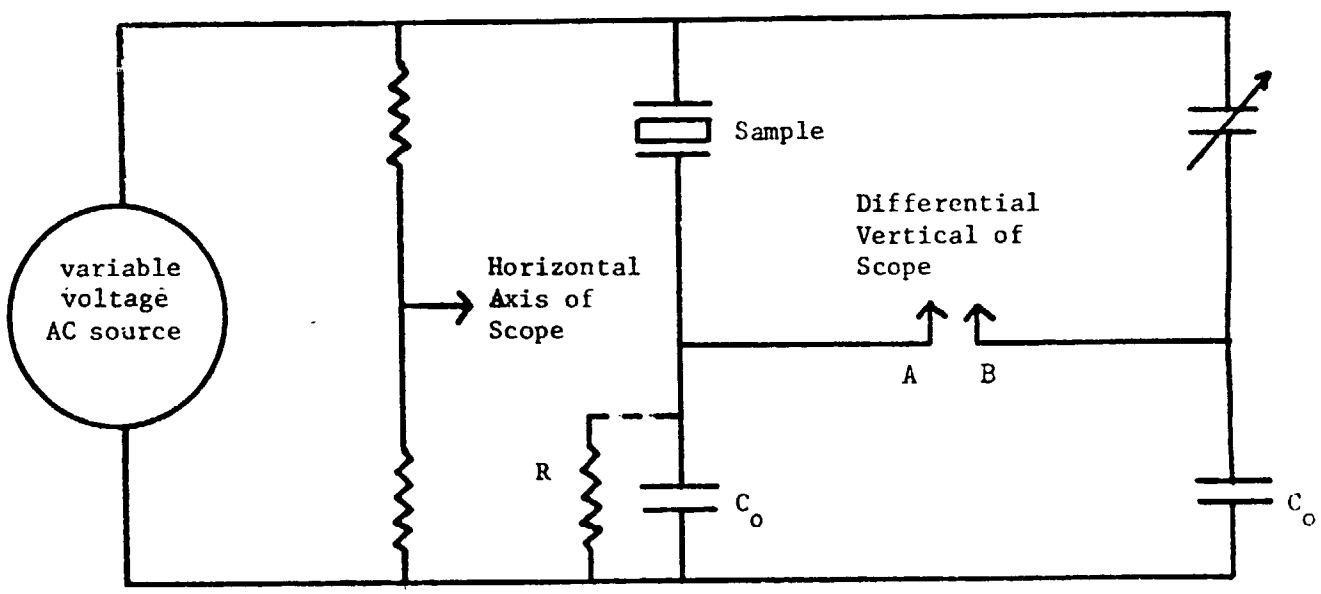
variable
voltage
AC source
Horizontal
Axis of
Scope
Sample
Differential
Vertical of
Scope
A
B
R
C_o
C_o

Fig. 3

the same dielectric current in the right circuit as the sample does in the left. If the vertical axis is taken as the voltage at A minus the voltage at B, then the dielectric contributions of the sample is subtracted off and the vertical axis will contain only the ferroelectric contributions. If the sample conducts, a suitable resistor can be placed in parallel with the capacitor C_o on the left to compensate for this so long as the required parallel resistor $R >> 1/2\pi fC_o$, where f is the frequency of the voltage source. All measurements were made at 60 Hz. The resulting vertical axis is then proportional to the polarization charge, P, of the sample. If a large enough electric field is applied to the sample the polarization is saturated to a value P_s. As the voltage is varied from a large negative value to a large positive value, the polarization goes from $-P_s$ to $+P_s$ as shown by the upper figure in Fig. 11.

2.2 Visible Defects Arising From Convection

2.2-1 Appearance of Defects

Three crystals, whose vertical axes were a, b, and c-axes, respectively, were grown at the same time under the same conditions. The cooling rate was 2.2°/day. Examples of the photographs taken during this growth experiment are given in Fig. 4. The upper figure shows many defects along the c-axis which is vertical, while the lower figure shows no defects along the c-axis which is horizontal. Thus this result suggests that convection produces the defects (I). In addition, the lower figure shows fewer defects along the vertical, a-axis compared to those along the vertical c-axis in the upper figure. A similar result was obtained for the crystal with the b-axis vertical. Thus it is suggested that growth along the c-axis is most sensitive to convection (II).

Figure 4. Photographs of Growing Crystals.

In the upper figure, the c-axis is vertical, while in the lower figure the a-axis is vertical.

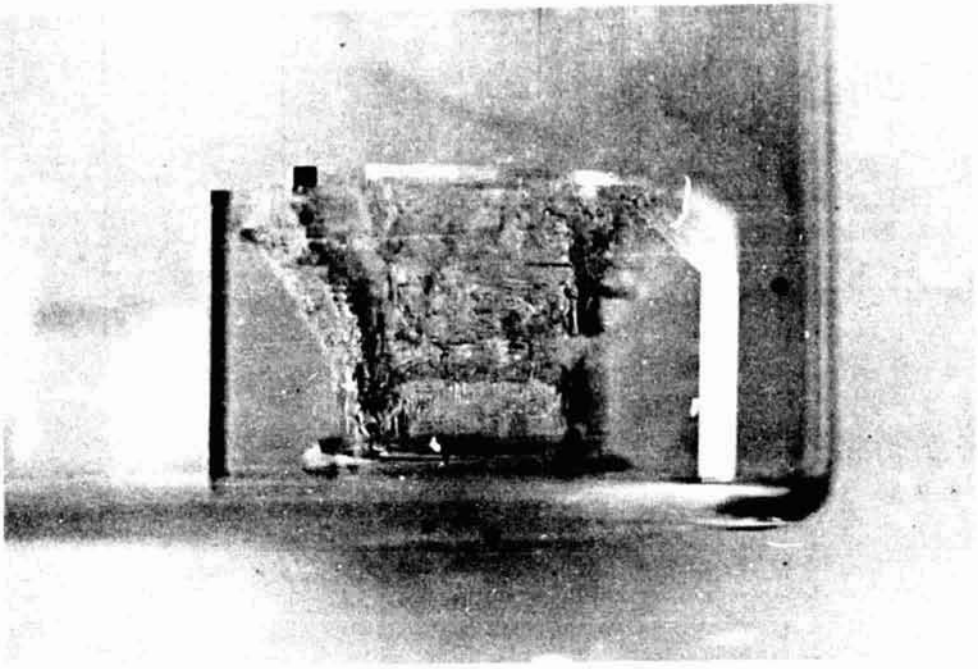

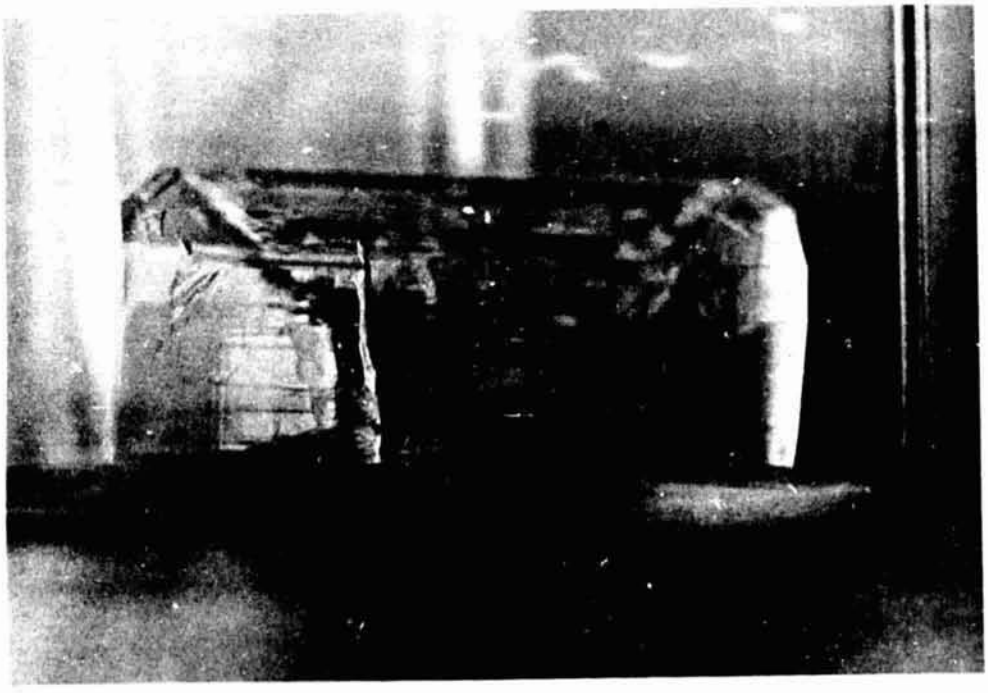

Fig. 4

2.2-2 Observation of Convection

The two suggestions, (I) and (II), are supported by observation of convection. Figure 5 shows an example of convection in the case of a cooling rate of 25°C/day. The photograph was taken by illuminating with a light source placed on the right side. One sees convection from the upper surface of the crystal, but no evidence is seen in the side surfaces or in any other region in the solution. Thus it is concluded that convection is much stronger at the upper surface of a growing crystal compared to the side surfaces. This conclusion supports the suggestion (I), since defects appear on the upper surface along the vertical axis of a crystal.

The white spot indicated by the arrow in Fig. 5 is a fiber from some tissue paper. Motion of this spot and its significance will be discussed in 2.3-3.

2.2-3 Further Evidence of the Effect of Convection

The photographs in Fig. 6 present direct evidence for correlation between convection and production of the defects. The upper photograph shows a strong convection current concentrated in the narrow top area of the crystal. In addition, this photographs shows that defects appear in the narrow region along the current. In the lower photograph, the defects are emphasized: the defects appear along a narrow vertical region at the top of the crystal. The lower photograph was taken 24 hours before the upper one. Comparison of the two photographs shows that the narrow defects grow along a vertical line.

Figure 7 shows a sketch of the same crystal after the growth experiment. The defects were found to be concentrated in a thin, vertical planar region.

Figure 5. Examples of Convection.

Notice no evidence for convection at the side surfaces. The white spot indicated by an arrow is a fiber from a tissue paper.

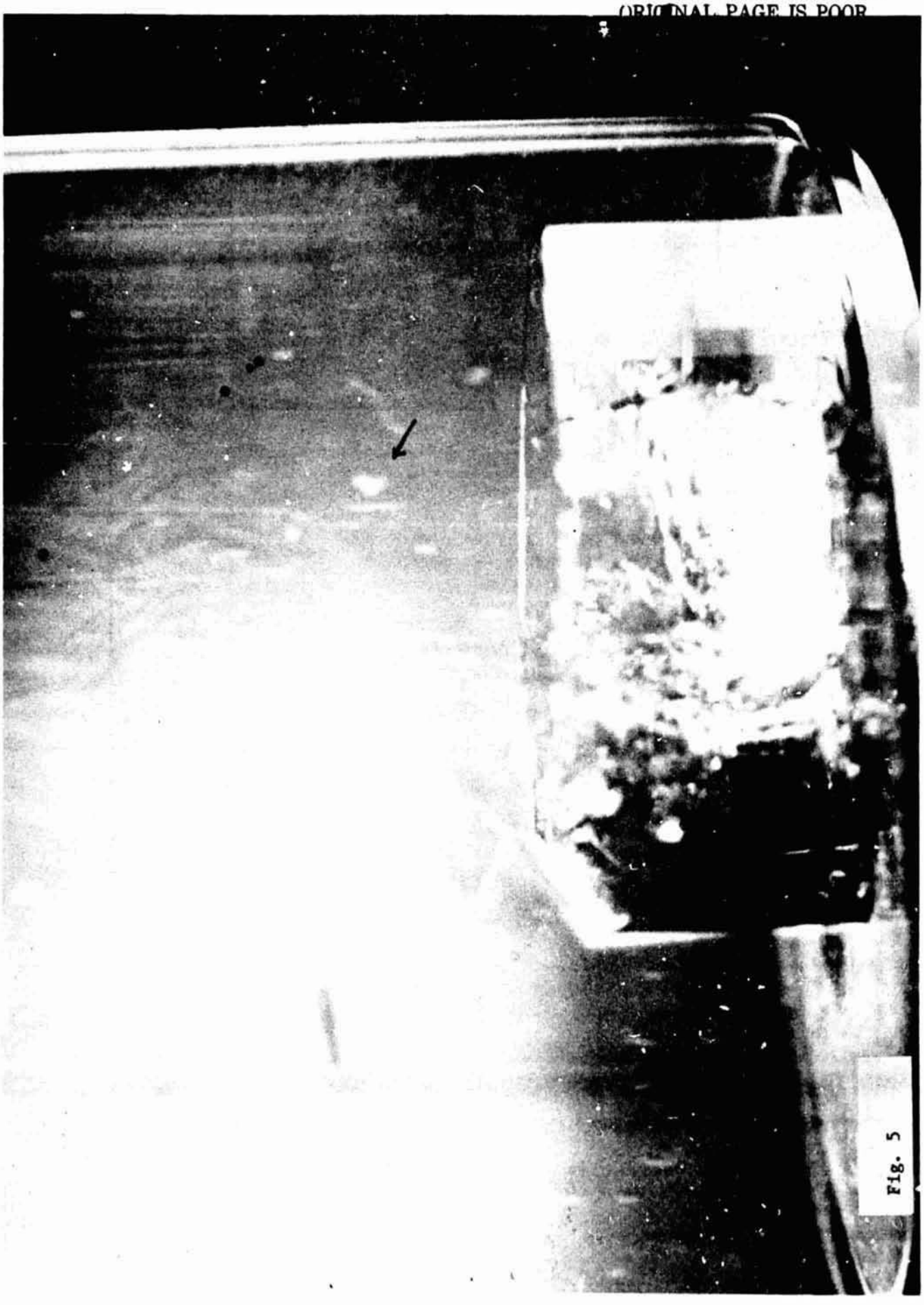

Fig. 5

Figure 6. Convection Currents and Defects.

Concentration convection currents and defects in the case of a growing crystal with the a-axis held vertical. In the upper photograph, the convection current is emphasized. In the lower photograph, the defects are emphasized. The lower one was taken 24 hours before the upper one.

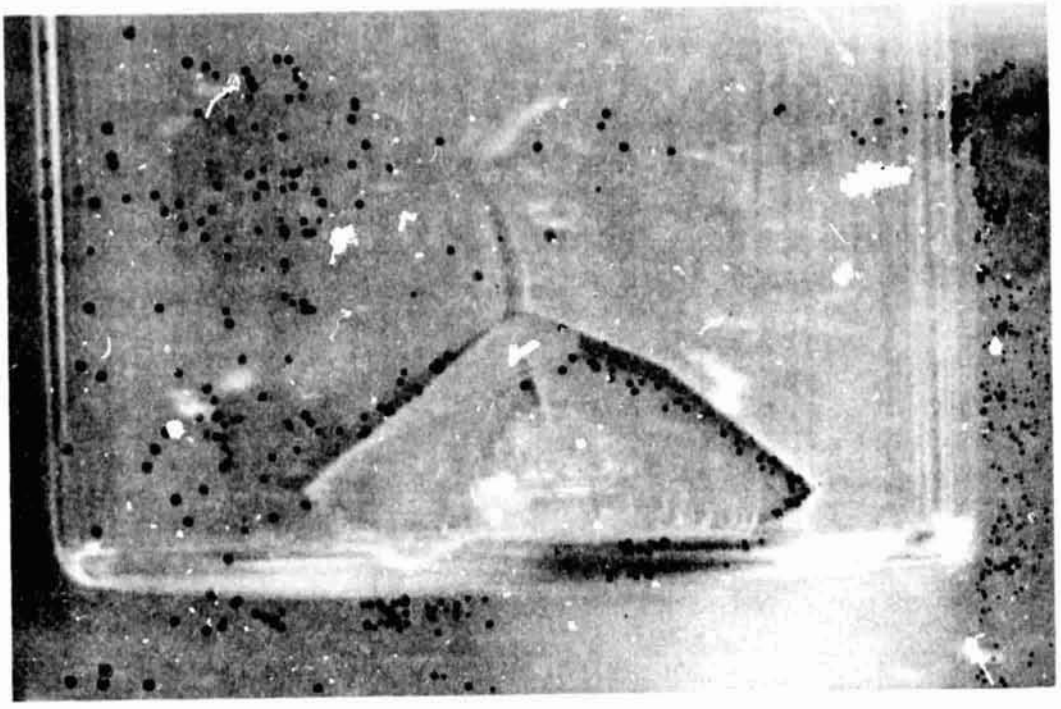

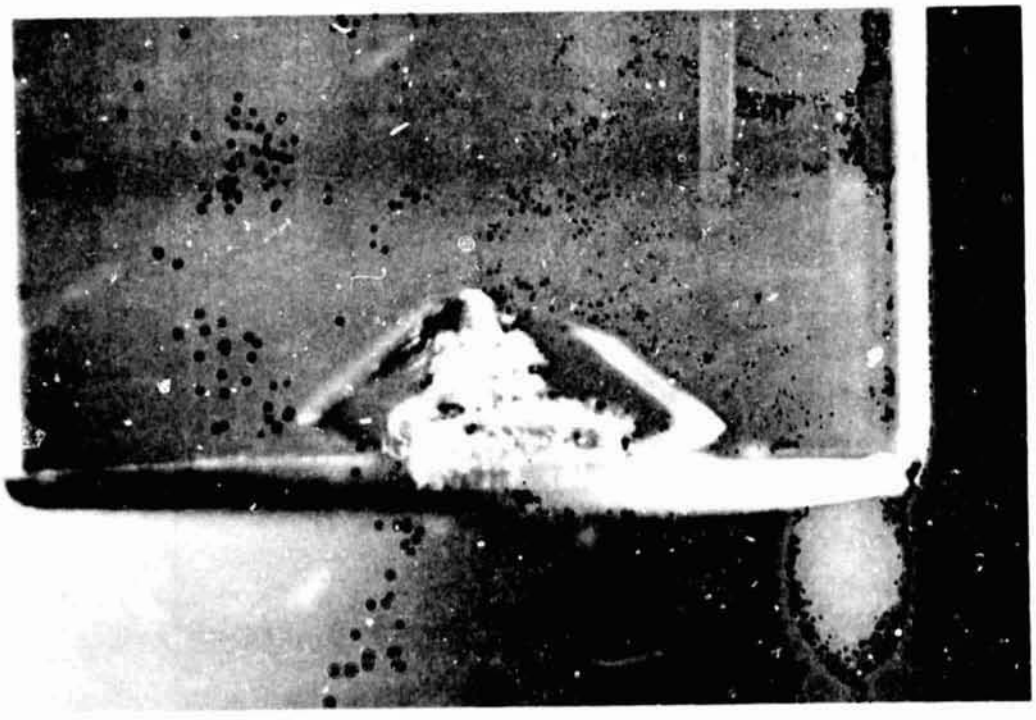

Fig. 6

Figure 7. Illustration of Figure 6.

Sketch of the same crystal as in Fig. 6 after the growth experiment. Notice the defects are concentrated in a thin, vertical plane.

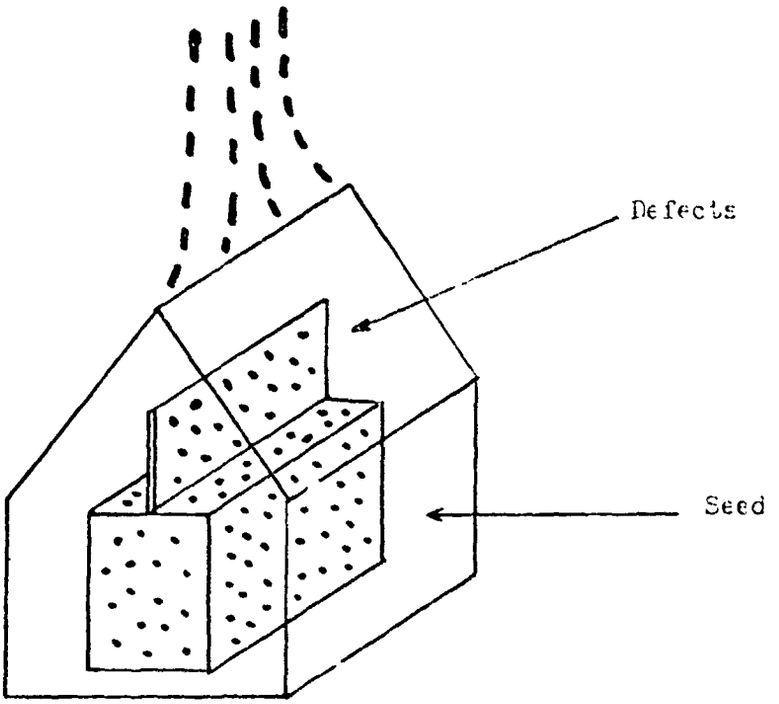

Fig. 7

2.2-4 Conclusion

In view of the evidence presented in this section, that given in 2.2-3 in particular, we believe, it has been proven that (i) strong convection currents produce defects. In addition, it is undoubted that (ii) sensitivity to convection depends on the crystal axis along which crystal growth occurs. In the case of Rochelle salt, growth along the c-axis is most sensitive. Sensitivity to convection is about the same for growth along the a and b axes, and less than that for growth in the c axis direction.

2.3 Study of Convection

2.3-1 Nature of Convection

In general, convection in liquids is induced by three factors, they are temperature gradient, concentration gradient, and surface tension. Temperature gradient and concentration gradient can induce convection only in the gravitational field. Convection by surface tension can occur even in the absence of gravitational field.[3]

The convection which is related to the observed production of defects is essentially the one induced by a concentration gradient.

Figure 8a shows a picture focused at the top surface of a growing crystal. The convection occurred shortly after the cooling of the water bath was started at a rate of 18°C/day. These photographs were taken every 4 seconds, the top one was first and the bottom one was last. Important features of the convection are illustrated in Fig. 8b: The protrusion indicated by an arrow expanded gradually and finally detached itself from the surface, rising as a small sphere. Density of the liquid inside the sphere

Figure 8a. Photographs of a Growing Crystal.

Photographs of the convection from a crystal with the c-axis held vertical. The photographs were taken every 4 seconds beginning with the top one and ending with the bottom one.

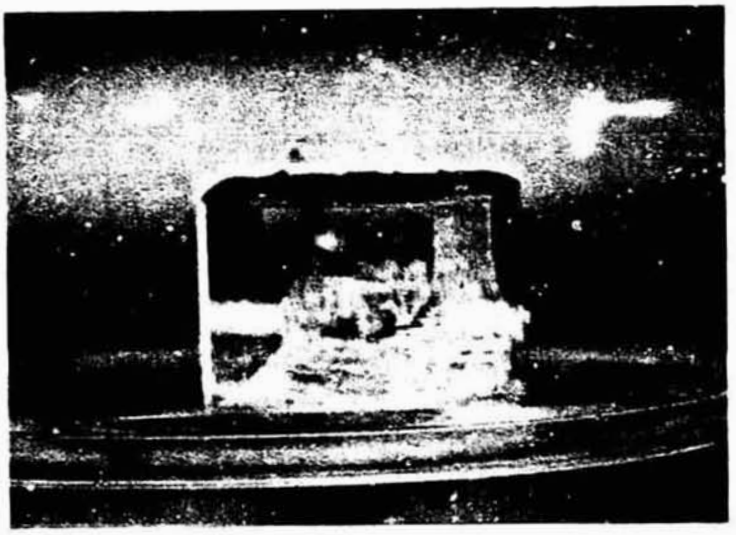

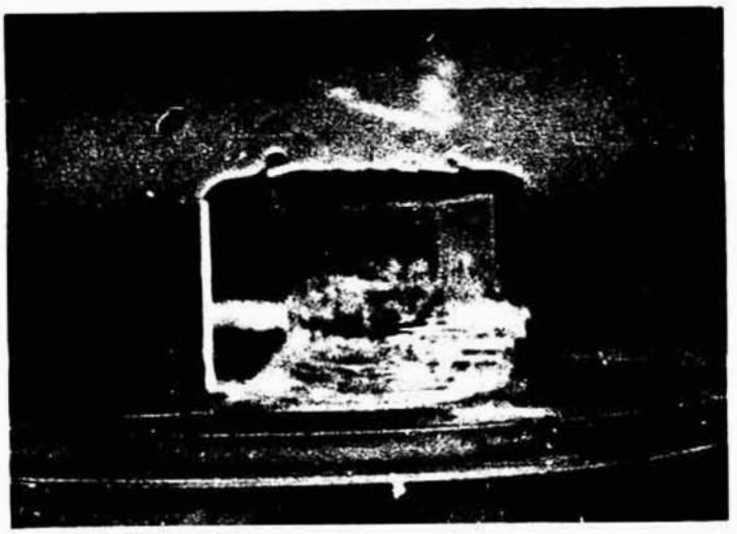

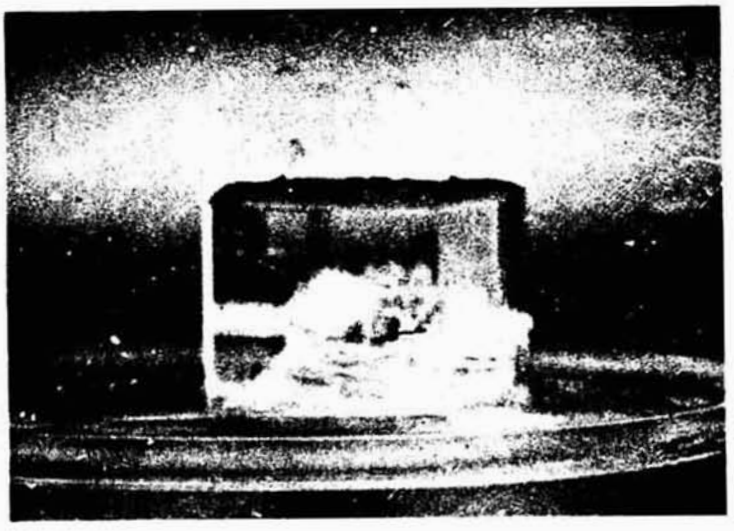

Fig. 8a

Figure 8b. Illustrations of the Photographs Given in Figure 8a.

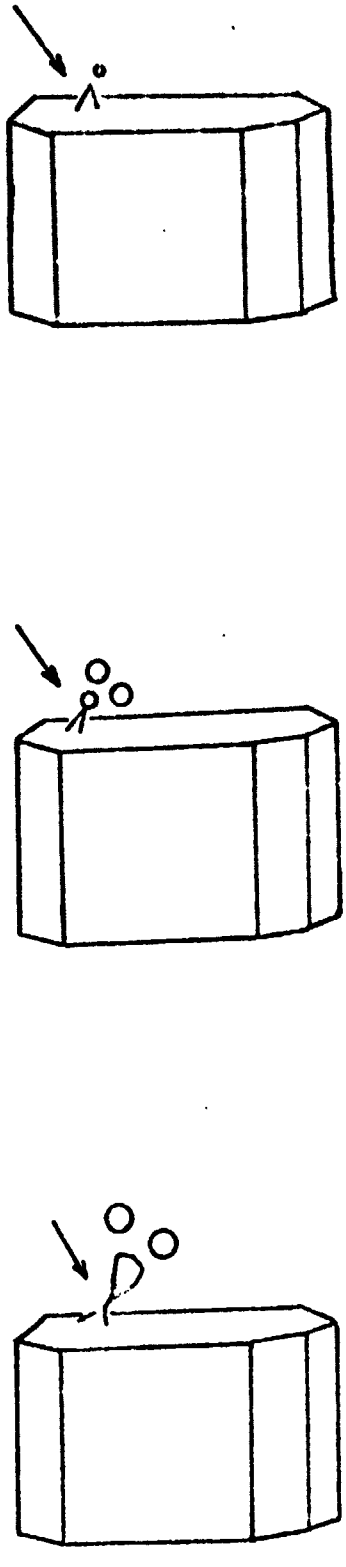

Fig. 8b

should be slightly lower than that of the solution. Thus this result suggests that convection occurs as a result of motion of solution layers adjacent to the crystal surface. As the crystal grows, concentration in the layer would decrease compared to that of the bulk solution. Thus, finally the layer would move under the effect of gravity. In other words, the convection should occur as a result of a concentration discontinuity produced in the vicinity of the surface of a growing crystal.

2.3-2 Concentration Discontinuity

It is possible to estimate approximately the concentration discontinuity which results in the convection current. For this purpose, motion of the spheres in Fig. 8b was studied. Upward speed and radius of the sphere were found to be approximately 0.5 mm/sec and 0.5 mm, respectively. It is noted that the Stokes force on the sphere should be equal to the buoyancy,

$$6\eta\pi av = \frac{4\pi}{3} a^3 (d_o - d)g,$$

where

η = viscosity of the solution,

a = radius of the sphere,

v = speed of the upward motion,

d_o = density of the solution,

d = density of the liquid inside the sphere,

g = gravitational acceleration.

One must remember, however, that Stokes law applies to the present case only with poor accuracy for several reasons: For example, the sphere is not rigid but deforms as it moves; secondly, radius of the sphere increases with time because of diffusion (see Fig. 8a); for the same reason, density, d,

increases with time, etc. It would be possible and interesting to formulate a theory which applies to the present case more accurately. Such an effort is beyond the scope of the present investigation, however.

For the reasons cited, use of the above equation allows one to obtain only an order-of-magnitude approximation to the concentration discontinuity. With the use of $\eta = 0.0286$ gm/cm-sec for a saturated solution at 20°C,[4,5] and the observed values of v and a, it was found that

$$d_o - d \tilde{=} 0.001.$$

Or the concentration difference Δc is

$$\Delta c \tilde{=} 0.1\%.$$

Concentration of a saturated solution, C_o, at 28°C, where the experiment was done, is about 100%.[4,5] Thus in terms of $\Delta c/C_o$, the concentration discontinuity $\tilde{=} 10^{-3}$. Although there is, to our knowledge, no way to examine dependability of the above calculation, it would be interesting to note that the calculated concentration discontinuity is very small, as one might expect.

2.3-3 Evidence for Weak Convection Currents

The experimental evidence presented so far indicates strong convection currents only in the narrow vertical region above the upper surface, or the peak, of a growing crystal. There is some evidence, although indirect, indicating weak convection in other regions of the solution.

As was already described, the white spot indicated by the arrow in Fig. 5 is a fiber from a tissue paper. The tissue was used to dry the vial, in which the fiber happened to be trapped. Motion of this fiber was studied by taking 10 photographs, one every 20 seconds. This study revealed

invisible, weak convection currents which are illustrated by broken curves in Fig. 9. The solid curves in the same figure show visible, strong convection currents.

2.3-4 Conclusions

The convection responsible for production of the visible defects was shown to arise from motion of solution layers adjacent to the crystal surface. The concentration discontinuity, which induced the convection and made its detection possible, was found to be of the order of magnitude of 10^{-3}, in terms of a normalized concentration difference. In addition, evidence was obtained to indicate weak, invisible convection currents.

2.4 Effect of Convection on Ferroelectric Qualtiy

2.4-1 S-value and Characterization of Ferroelectric Quality

Since the defect-producting effect was proven, a more definitive characterization of crystal quality is required. In particular, it is important to characterize the ferroelectric quality in which we are interested.

In the case of a ferroelectric material,[2] the crystal has a structure which consists of regions (called domains) with opposite, or nearly opposite, directions of electric polarizations (see the upper figure in Fig. 10). In the case of Rochelle salt which is ferroelectric between -18°C and 24°C, the different polarizations are found to be not exactly in opposite directions, although both directions are nearly parallel (or anti-parallel) to the a-axis. For this reason, a domain with positive polarization and one with negative polarization rotate a polarized light beam propagating along the a-axis by different angles. As a result, one can distinguish domains of opposite polarization using a microscope with polarized light.

Figure 9. Convection Currents Around a Growing Crystal.

Convection induced by a growing crystal. Broken curves show weak convection currents which are not visible but detected by other means. Solid curves show visible, strong convection currents.

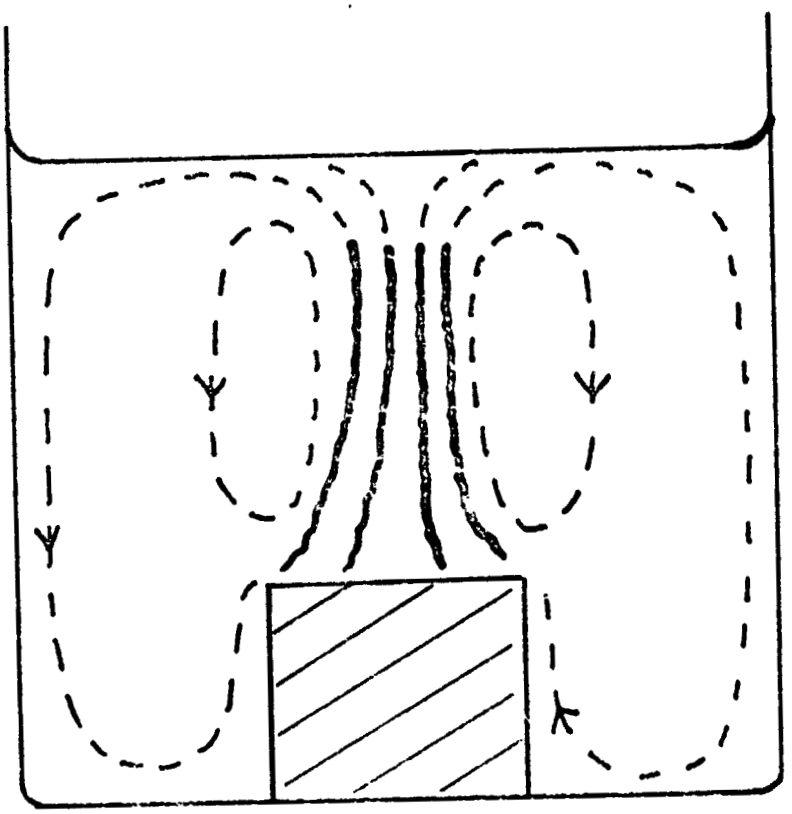

Fig. 9

Figure 10. Ferroelectric Domains.

The lower figure illustrates expansions of some domains and contractions of others by an applied electric field.

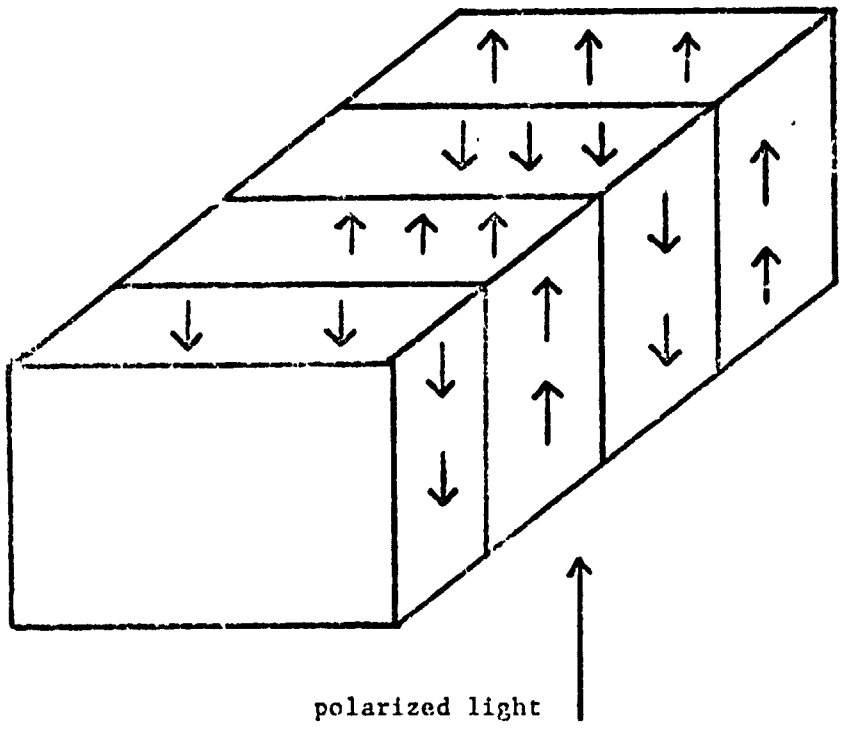

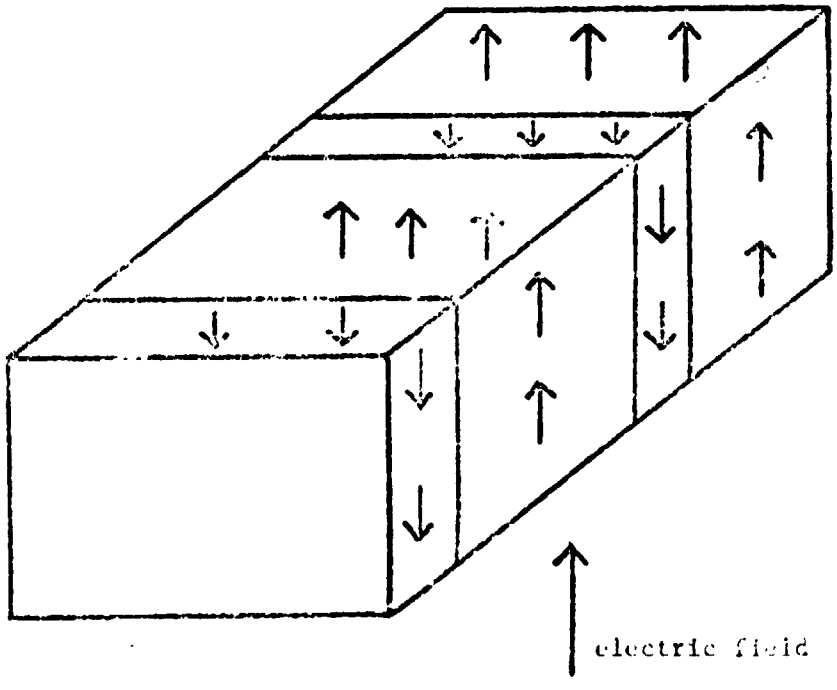

Fig. 10

When an electric field is applied along the positive polarization direction (the lower figure in Fig. 10), the positive domain expands and the negative domain contracts. In general, switching of polarization occurs gradually and discontinuously, as the electric field increases. Consequently the hysteresis curve given in the upper figure in Fig. 11 is observed for a ferroelectric crystal in general. For a hypothetical, perfect ferroelectric crystal, the switching would occur at a certain electric field value throughout the crystal. Consequently, the hysteresis curve would be a rectangular loop such as that shown in the lower figure in Fig. 11. Thus a higher value of tan α would be expected for a better crystal. Since the shape of the hysteresis loop depends on observation conditions, a normalized tangent, or S-value, was defined (see the upper figure):

$$S = (\tan \alpha)(P_s/V_o)^{-1}.$$

For the reason given above, S-value should represent ferroelectric quality: a higher value corresponds to better quality, the value for a perfect crystal being infinity.

2.4-2 Quality Distribution in a Crystal

Figure 12 shows a photograph of the sample crystal. A diagram of the same crystal is shown below the photograph with some of its growth characteristics shown for clarity. This crystal is the product of the first growth experiment shown in Fig. 1. The lower diagram in Fig. 12 also illustrates the crystal growth in time, the latter being given by the number in hours in parentheses. Growth was relatively slow between 18 hours and 37 hours. The rate was found to be 1.1 mm/day along the horizontal, a-axis and 1.5 mm/day along the vertical, c-axis (Fig. 1). As is shown by the

Figure 11. Ferroelectric Hysteresis Curves.

The upper loop represents a typical curve. The lower one represents a loop from a perfect crystal.

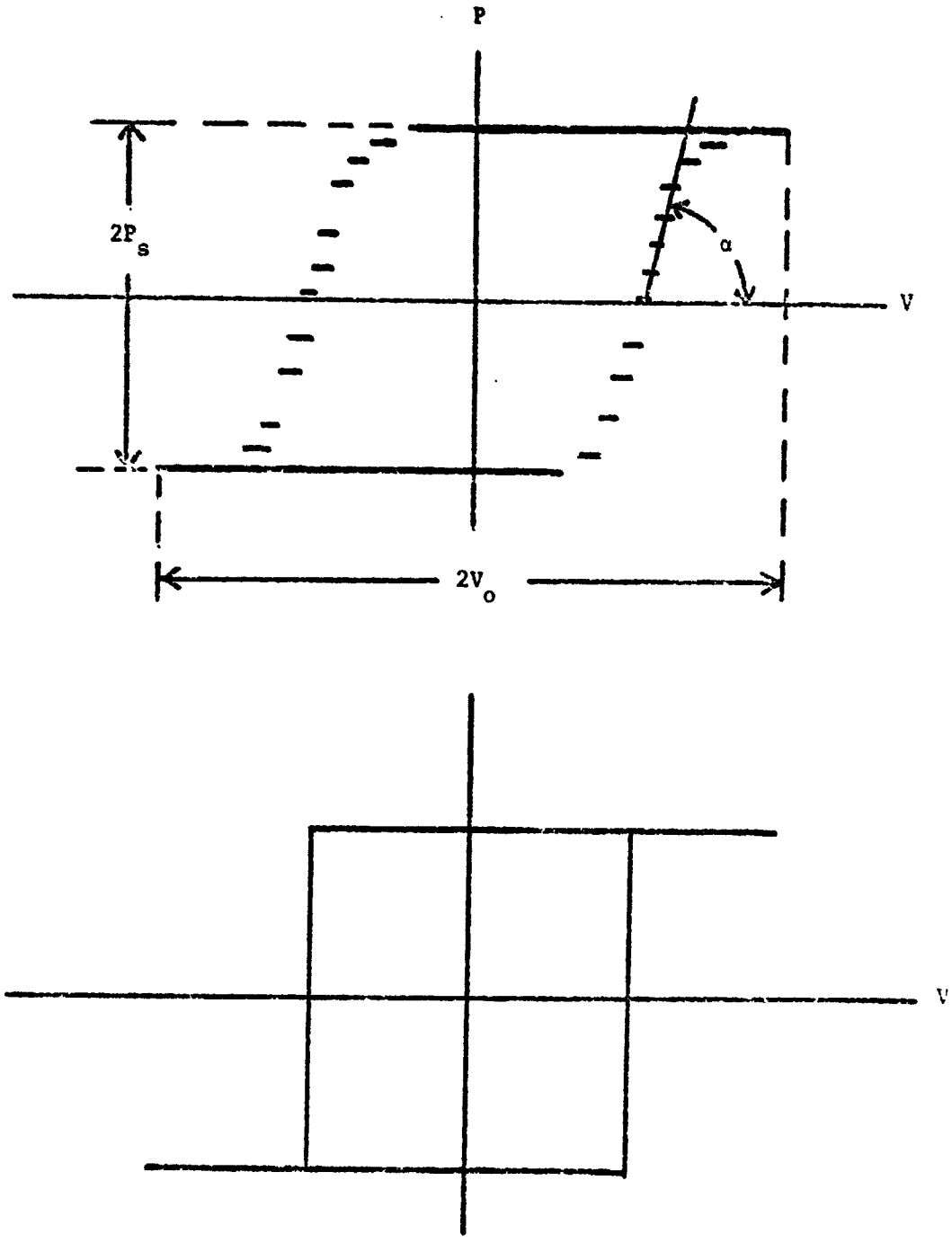

Fig. 11

Figure 12. A Sample Crystal.

Growth of the crystal against time is illustrated by the lower figure. The number in parentheses indicates time in hours. The 6 specimens taken are shown by broken lines.

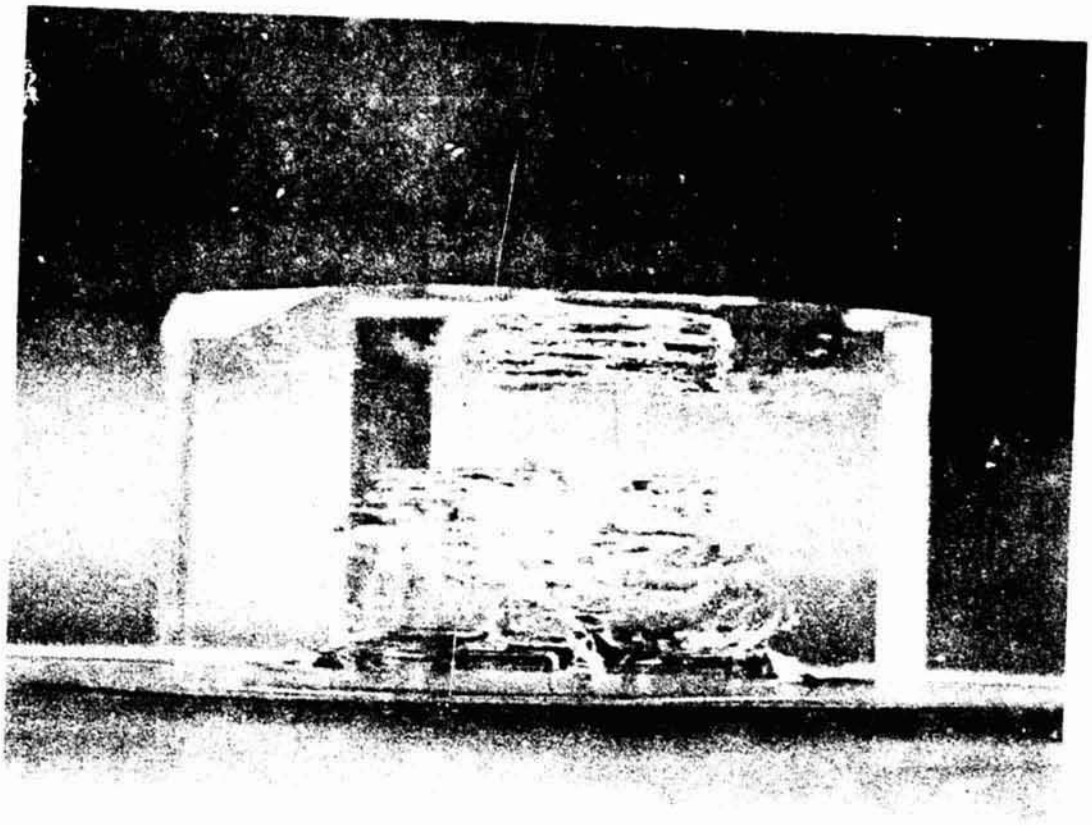

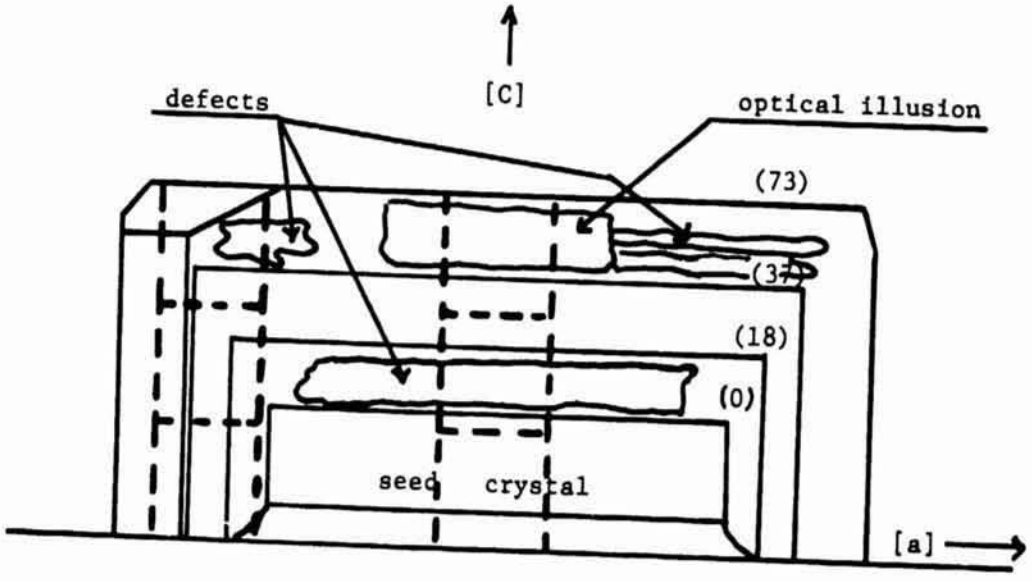

Fig. 12

illustration, no defect appeared during this time of growth. In contrast, the growth was irregular for the next period from 37 hours to 73 hours, the end of growth (see Fig. 1). In particular between 50 hours and 57 hours, the rate was relatively high, that is 2.0 mm/day along the horizontal axes and 3.4 mm/day along the vertical axes. As a result of this high growth rate, many defects appeared along the vertical axis, although no defect appeared along the horizontal axis.

As is shown by broken lines in the illustration, two slices were taken from this crystal: one at the center and the other at the left side, each being further cut into three pieces. The crystal cutting machine (see 4.2-3E) was used for this process.

Figure 13 shows two examples of the observed hysteresis curves: the upper one is for the top part of the central slice, and the lower is for the bottom part of the lefthand slice. The tangents of these two curves are quite different.

Figure 14 shows S-values for the six specimens. The top part of the central slice has the lowest S-value of 3.7, while the bottom part of the left-side slice has the highest S-value of 15.9. In addition, the S-value for any specimen in the left hand slice is higher than that for any in the central slice. These results would be reasonably expected from the observed convection currents. The central slice is predominantly a product of growth along the vertical axis which is sensitive to convection currents. In contrast, the left-hand slice is predominantly a product of growth along the horizontal axis which is less sensitive to convection currents. Moreover, in the same central slice, the top part influenced by a higher growth rate and hence strong convection currents, has a lower S-value (3.7) as compared

Figure 13. Hysteresis Curves.

Observed hysteresis curves from the sample cyrstal in Fig. 12. The upper curve, which is from the top part of the central slice, has a small tangent and S = 3.7. The lower one, which is from the bottom part of the left slice, has a large tangent, and S = 15.9.

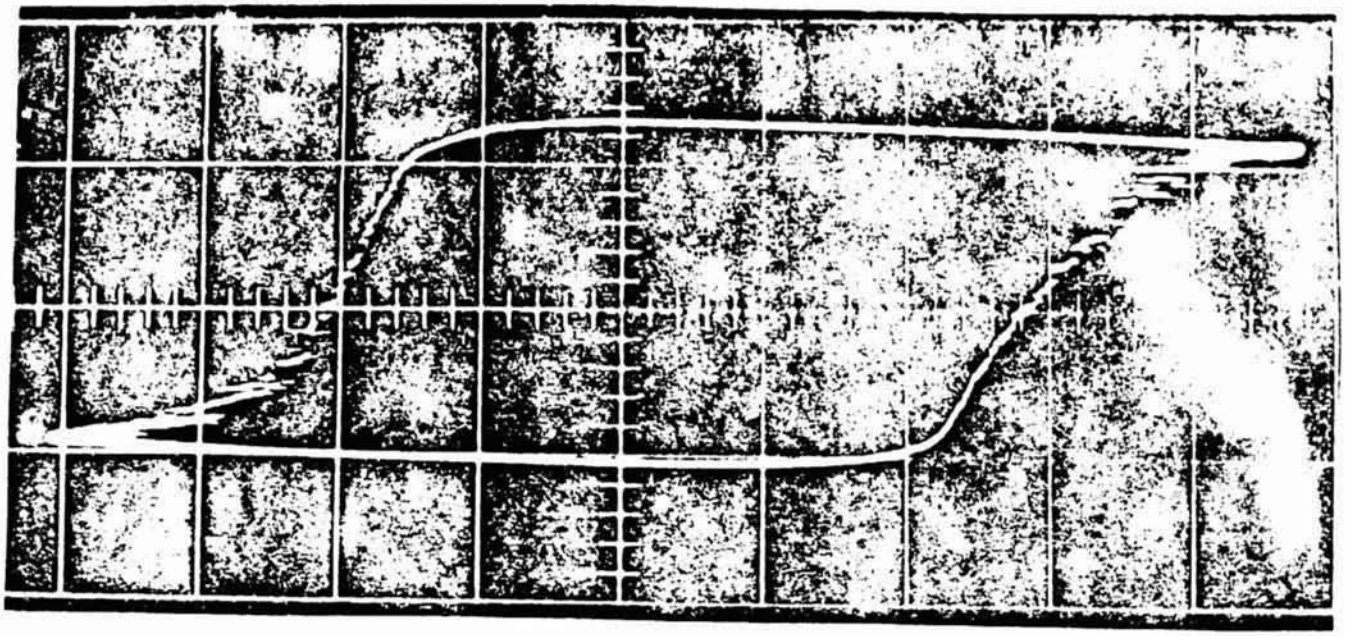

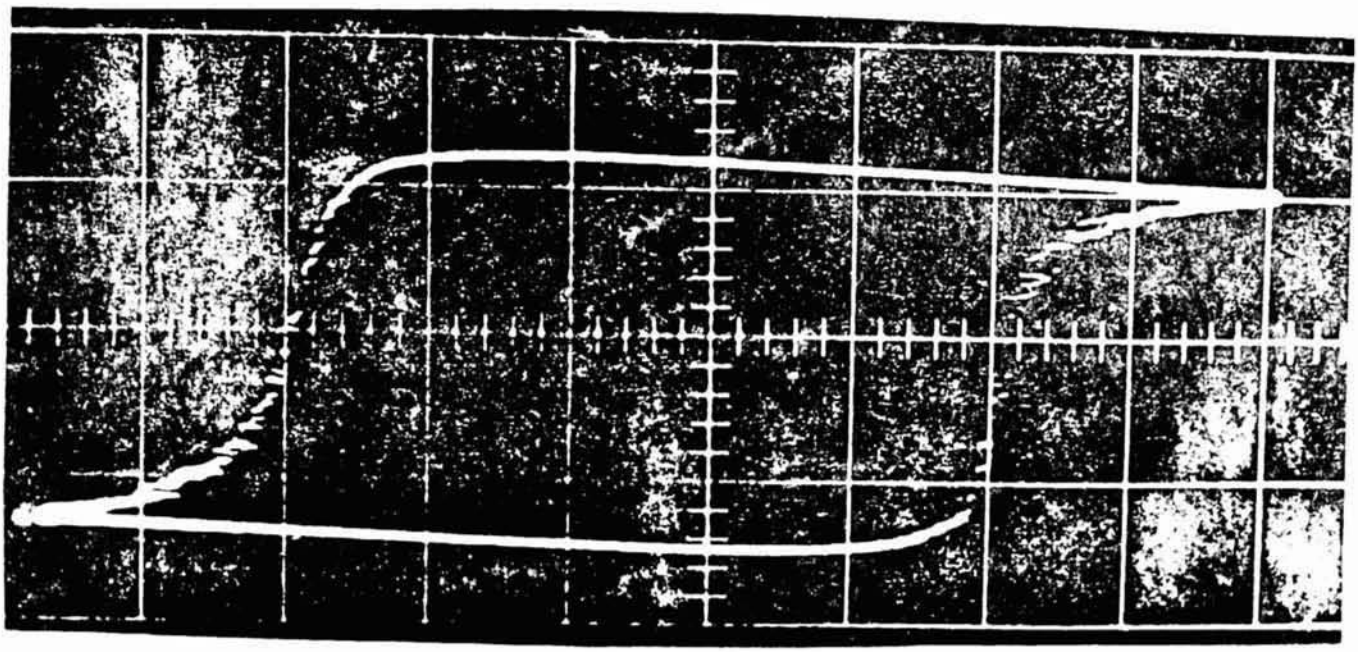

Fig. 13

Figure 14. S-values of the Sample Crystal in Fig. 12.

S-VALUE

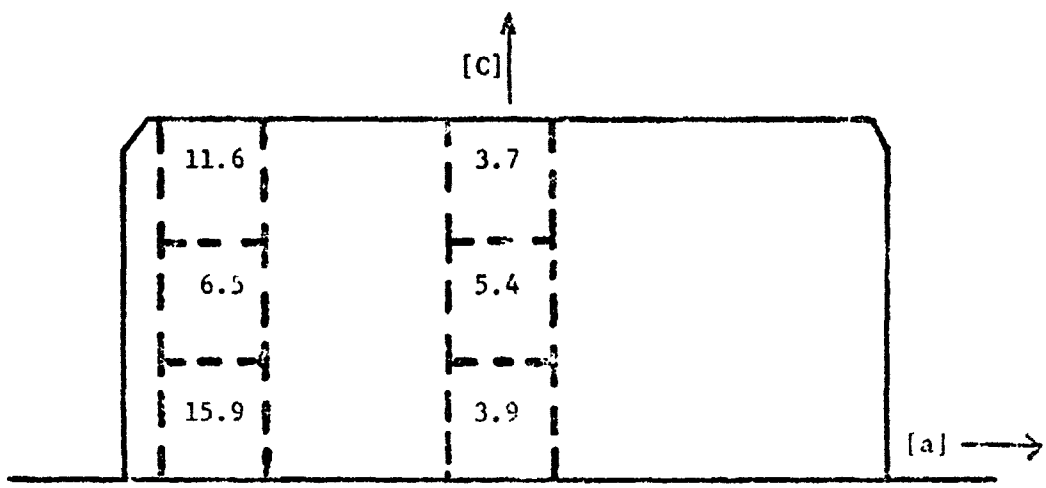

Fig. 14

to the central part, where S = 5.4. This is also the case for the left-hand slice, that is, the top part which grew under strong convection currents had a lower S-value (11.6) as compared to the bottom part of the slice where S = 15.9.

In the left hand slice, the center part has the lowest S-value in the slice. It is noted that the present convection study predicts an intermediate value in contrast to the observation. Thus it was important to confirm dependability of the characterization by hysteresis method by another entirely different techniques. For this reason, domain photographs for the six specimens were taken, and three examples are given in Fig. 15. The top figure, which is from the top part of the central slice shows domains greatly different in width. The central one and the bottom one are from the center part and the bottom part of the left-hand slice, respectively.

Both domain structures are fairly uniform in width but the central one shows greatly deformed domains. The photograph from the top part of the left hand slice, which is not given, shows a domain structure similar to that in the top figure but much less irregular. Consequently, the result of domain structure observation is in accordance with the result of hysteresis observation, as far as characterization of crystal quality is concerned. In particular in the case of the left-hand slice, there is no doubt that the center part is of relatively poor quality. Explanation for this fact has not been found. More sensitive techniques to detect convection such as Schrieren method, might help to interpret this result. It is important to note, however, that both parts show no visible defects and yet the two parts are greatly different in ferroelectric quality.

Figure 15. Ferroelectric Domains

Domain structures of the sample crystal in Fig. 12. The magnification factor is 300. The top figure, which is from the top part of the central slice, shows domains which are greatly different in width. The central one and bottom one are from the center part and the bottom part of the left slice, respectively. Both domain structures are fairly uniform in width but the central one shows greatly deformed domains.

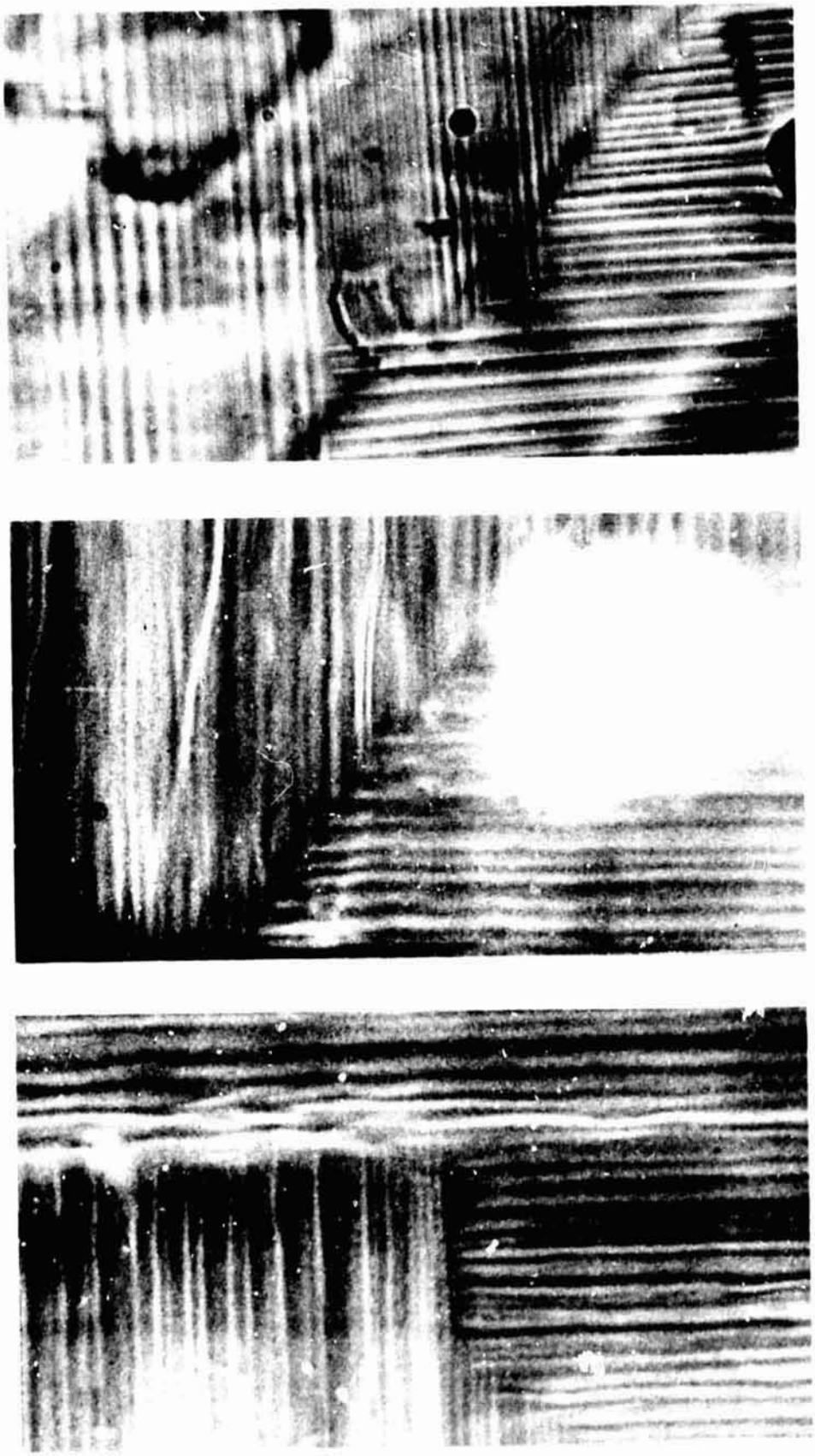

Fig. 15

2.4-3 Conclusions.

It was concluded that convection currents degrade ferroelectric quality. It was shown also that different parts of a crystal can be greatly different in ferroelectric quality, even though these parts show no visible defects. No study has been conducted, however, to determine degrees of the convection, those of ferroelectric quality, and concentrations of the visible defects.

2.5 Metal Ion Doping-Preliminary Study

2.5-1 Significance of the Study

Since we have shown the degrading effect that convection currents have on ferroelectricity, one might expect that convection would effect many other crystal qualities as well. Distribution of the doping metal ions in an organic crystal is one of the possible qualities to be examined. Many metal ions such as Cu^{++} and Cr^{+++} have strong characteristic colors, and hence examination of the doping distribution should be fairly easy. For this reason, several organic crystals doped by varied metal ions were grown to obtain preliminary information.

2.5-2 Results of the Preliminary Study

Doped crystals were grown by a slow evaporation technique at room temperature. The concentration of a doping compound was usually about 1 weight percent of the solution saturated by a crystal material. A slow cooling technique was used supplementarily in some cases.

The crystals doped are as follows:

Rochelle salt;

triglycine sulphate;

L-alanine;

acetyl-N-glycine;

glycine.

These crystals were doped with the following metal ions:

Cu^{++};

Cr^{++}, Cr^{+++};

Co^{+++};

Fe^{++}, Fe^{+++};

Ni^{+++}.

Chlorides and nitrates of these metals were used as doping compounds.

The doped crystals were examined with the unaided eye and under a microscope. Some crystals, for example those of Cu^{++} doped L-alanine showed marked inhomogeneities even for a visual inspection. Some other crystals, for example those of Cr^{+++} doped L-alanine appeared uniform for a visual inspection, but showed inhomogeneities under a microscope examination. In many cases, a slow evaporation technique produced a crystal higher in concentration of the doping ions and better in the doping uniformity.

2.5-3 Concluding Remarks

It was shown that many organic crystals can be doped with metal ions by growing crystals from solutions containing these doping ions. It is noted that several workers have published on some doped crystals.[6,7] The present investigation is, however, believed to be the first extensive study in which many doping compounds were examined.

The effect of convection on doping homogeneity was not investigated, as of yet, however.

2.6 Summary and Conclusions

Crystal growth from solutions was studied in the case of organic compounds, Rochelle salt in particular. The investigation included growth study, observation of visible defects, study of the convection currents responsible for defect production, and study of ferroelectric qualities. In addition, many metal ion doped organic crystals were grown from solutions.

By the growth study and observation of convection currents, it was proven that a convection current produces visible defects, which are flaws and inclusions of solution. In addition, it was concluded that sensitivity to convection depends on the crystal axis along which crystal growth occurs. In the case of Rochelle salt, growth along the c-axis is most sensitive.

The convection responsible for visible defects is essentially a concentration induced one. More accurately, the convection was shown to arise from motion of solution layers adjacent to the growing crystal surface. The concentration discontinuity between the layers and the bulk solution induced the convection. This discontinuity was found to be of the order of magnitude of 10^{-3} in terms of a normalized concentration difference. In addition, evidence was found to indicate weak, invisible convection currents.

It was shown, by studying ferroelectric hysteresis curves and domain in several different parts of a crystal, that convection currents degrade ferroelectric quality. It was shown also, that different parts of a crystal can be greatly different in ferroelectric quality, even though these parts show no visible defects.

Since the convection currents were shown to produce visible defects and degrade ferroelectric quality, many other crystal qualities are expected to be degraded by the convection currents. It is noted that the convection

responsible for the degradations can primarily occur in a gravitational field, as the study of its nature indicates. Consequently it is expected that a solution growth in a zero gravitational environment can result in a crystal of a very high quality.

Section 3. Further Growth Experiments - Convection and Growth Rate (Second Year's Work)

3.1 Introduction

This project was intended to study crystal growth from solutions as one of the programs for "Space Processing Applications". The work during the preceding contract period had proven that strong convection in a solution produces defects in the resulting crystal.[8] The aim of the current project was to clarify the nature of the defects, to identify some important factors affecting crystal qualities, and if possible to apply these results to improve qualities of crystals with scientific and industrial significance.

The current investigation has achieved this aim to some extent, though rather accidentally and in a modest degree: For example, interpretation of the newly observed facts resulted in the discovery of a useful technique "crystal growth under vacuum". This technique was applied to growth of L-alanine-doped triglycine sulphate which has been suggested to be possibly an excellent infrared detector material.[9] L-Alanine doping concentrations of between 2% and 4% was obtained consistently compared to 2% which is the highest previously reported concentration.[10]

Many useful properties of crystals can be obtained by doping. Thus an investigation was planned to identify the factor which determines the dopant concentration of a crystal. By studying copper ion doped Rochelle salt, the factor was found to be the growth rate.

It has been found that convection degrades ferroelectric quality.[8] Thus the next step was to gain some insight into the nature of the ferroelectric degradation. For this purpose, microscopic studies of many crystals were performed. It was found that convection increases the relative

number of solution-holding microscopic cavities compared to empty microscopic cavities. The solution trapped in a crystal is expected to absorb electromagnetic energy and hence to degrade electrical properties including the ferroelectric property.

A further study revealed that the microscopic cavities, empty or containing solution, are filled with gaseous air. Interpretation of this and preceding results suggested a new technique of crystal growth under vacuum. This technique was actually investigated and was applied successfully to grow a triglycine sulphate crystal highly doped with L-alanine, as will be described.

In view of the results obtained during the preceding and current projects, there is now no doubt about the degradation effect of convection. Thus some preparatory work on flight experiments was performed. This work included preparation of suitable growth materials and seed crystals of good quality.

Interpretation of the effect of convection suggested the possibility of suppression of convection by an inhomogeneous magnetic field. A preliminary analysis supporting this possibility was attempted.

3.2 Effect of Growth Rate on Metal Ion Doping

3.2-1 Correlation between Growth Rate and Dopant Concentration

A. Experimental - We have already done experiments to show the correlation between defects in the resulting crystal and rate of growth.[8] Since a metal ion, such as copper, would be a kind of defect in the Rochelle salt crystal lattice, it seems possible that there is a similar correlation between rate of growth and concentration of metal ion dopant.

Preliminary experiments were done with Rochelle salt grown in a solution of water, Rochelle salt and $CuCl_2$. Figure 16 shows the glass vial with growth solution and crystal in the temperature bath. The saturation temperature for the experiment shown in Fig. 17 was slightly above 34°C. In the first part of the experiment (region I in the figure), the temperature was kept at 34°C where convection currents were visible but not strong. After more than 12 hours of slow growth, the original convection currents were barely visible. The crystal that had grown in this time looked transparent, uncolored, and had no visible defects. Next, the system was cooled 10° in two hours. Very strong convection currents were observed while the temperature was kept at 24°C. After four hours of this rapid growth, region II in Fig. 17, many defects had appeared near the top, growing surface of the crystal, roughly in the ab plane. The temperature was then raised until those vigorous currents stopped. Next, the system was cooled at a rate of about 0.08°C/hr (region III in Fig. 17). After about 40 hours of this moderate growth, the crystal was removed from the growing solution. A slice was made perpendicular to the ab plane and the crystal surfaces were polished with several grades of grinding compound. Finally, the crystal was washed in a mixture of water and methanol.

B. Results - The slice of crystal resulting from this preparation presented a cross section for study which clearly showed three different regions. Photographs were taken with a microscope camera and the results are shown in Fig. 18. The different regions of growth are called I, II, and III, and correspond to the regions I, II, and III in Fig. 17, that is, region I of the crystal slice grew in the time called I in Fig. 17 and so on. The growth rates for regions I, II, and III were slow, fast, and moderate, respectively.

Figure 16. Crystal Growth Vial.

A glass vial with a plastic stopper was used to hold the growth solution for the copper-doped Rochelle salt experiments. A brass weight was used to stabilize the vial in the plastic support stand. Temperature of the growth solution was held at a desired value by heating or cooling the rapidly circulating water in the temperature bath.

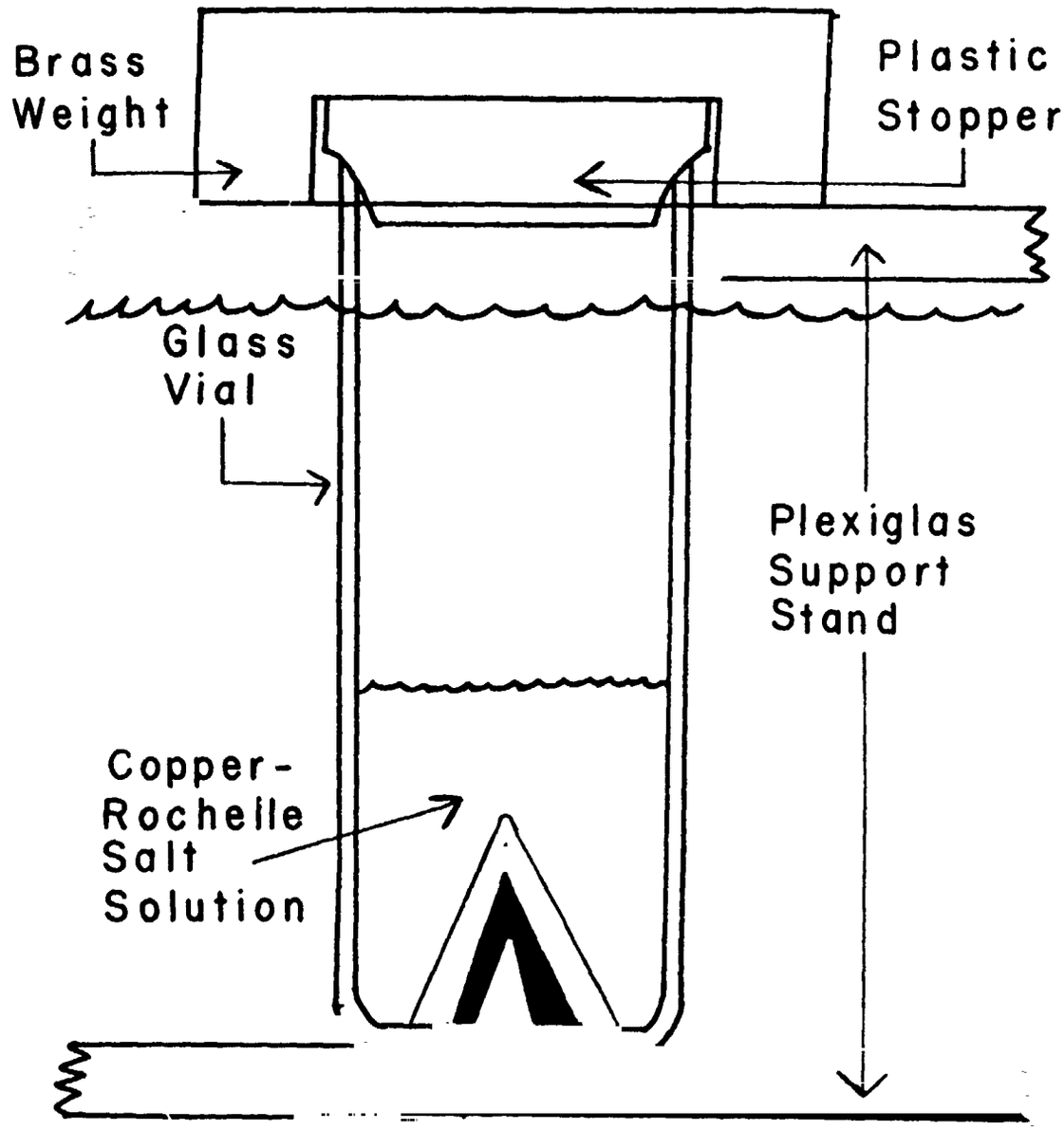
Brass
Weight
Plastic
Stopper
Glass
Vial
Plexiglas
Support
Stand
Copper-
Rochelle
Salt
Solution

Figure 17. Cooling Curve for Preliminary Experiment CuRS #1

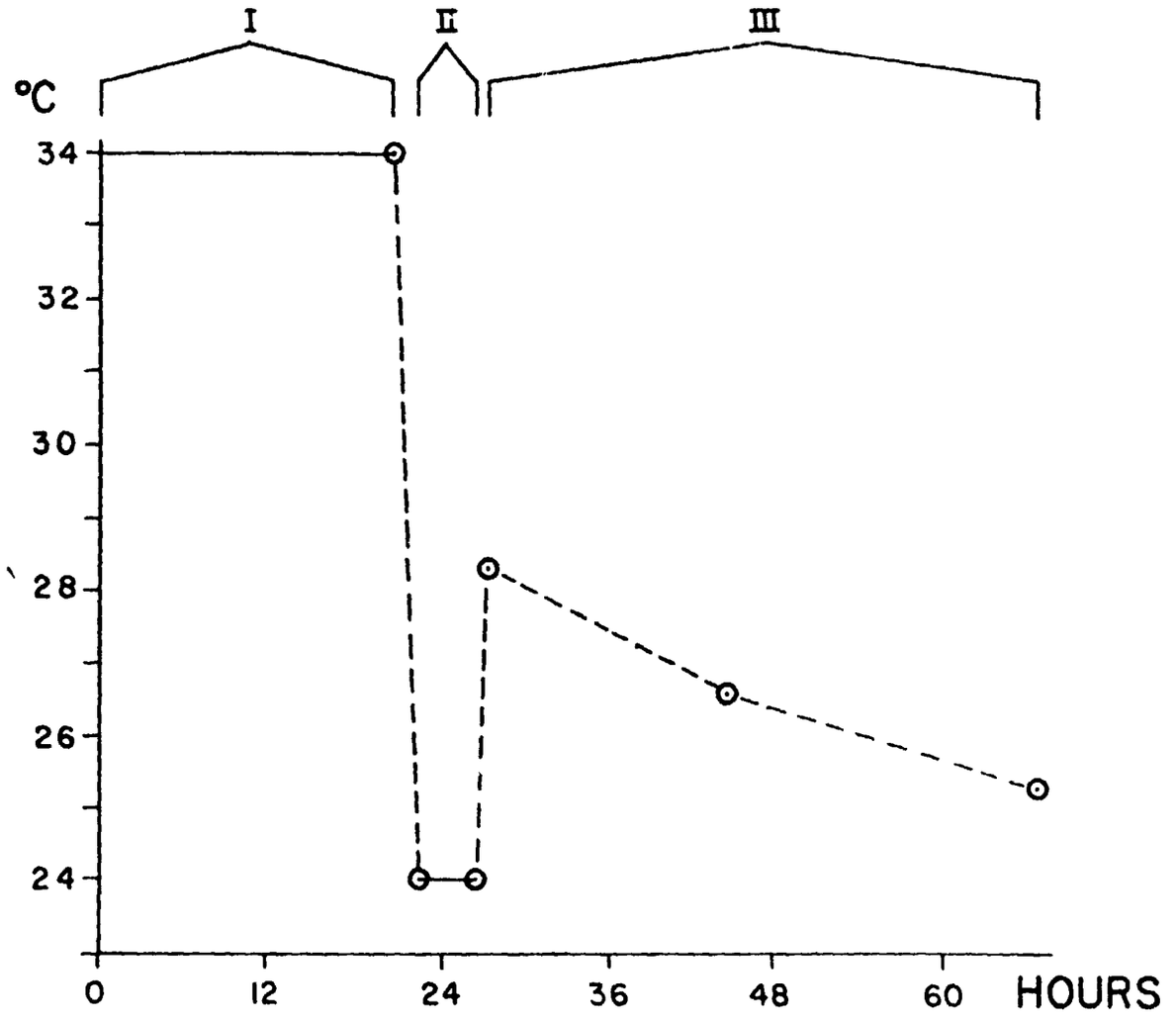
I
II
III
°C
34
32
30
28
26
24
0
12
24
36
48
60
HOURS

Figure 18. Microscopic Cross Section of Crystal CuRS #1.

A thin slice of the crystal grown as described in Fig. 16. The layers shown as I, II, and III correspond to the growth periods I, II, and III in Fig. 16. The slice was grown vertically, from the bottom of region I to the top of region III. The thickness of the slice, from the top of region III to the bottom of region I, is 3 mm.

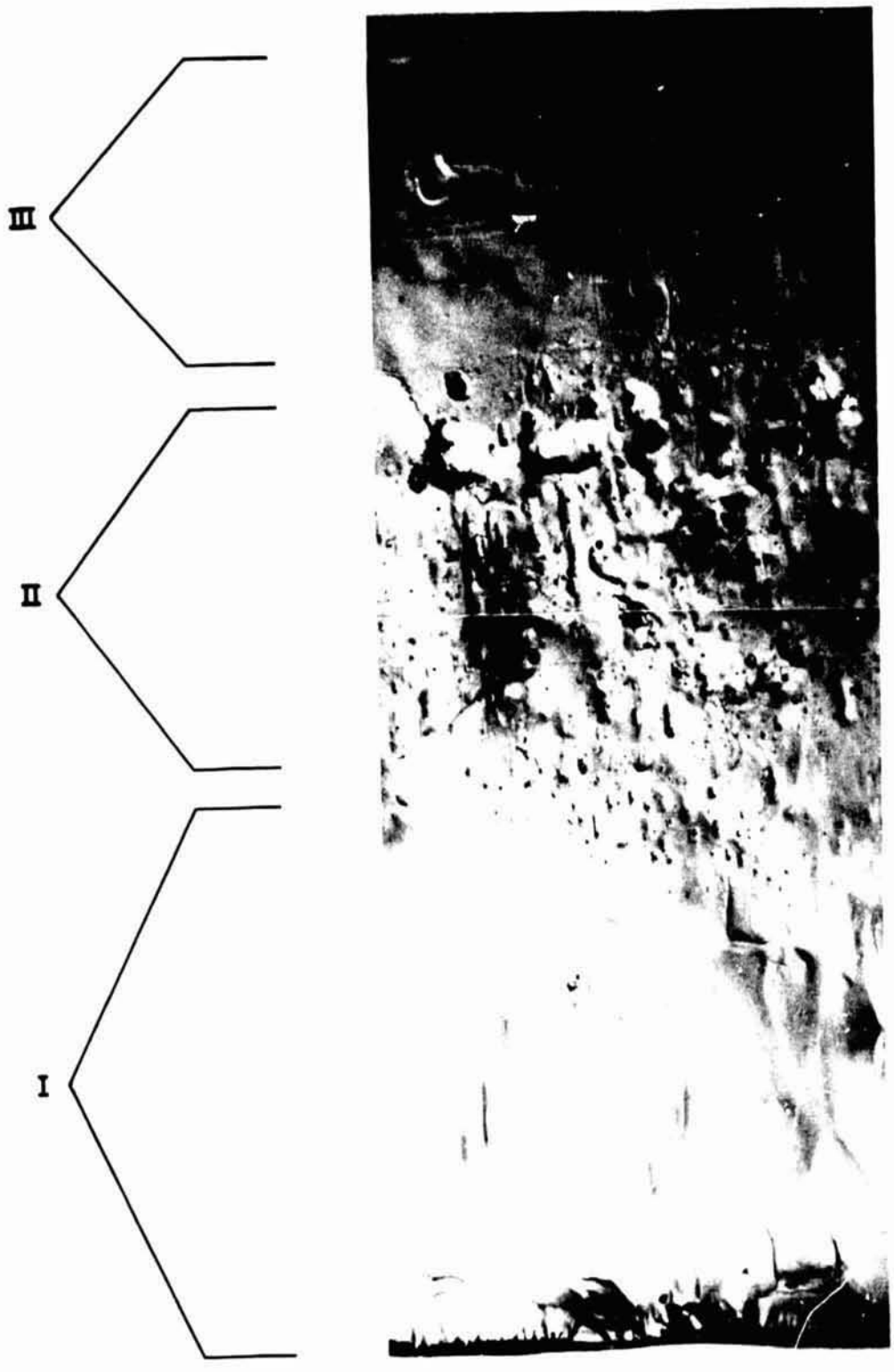

Region III was transparent and blue, II was opaque and mostly white, and I was transparent and uncolored. Thus it appears from the blue color that the copper dopant was present only in region III.

It is possible for copper to be present in small amounts without giving a blue color to the crystal, so it was necessary to make a more accurate measure of copper ion concentration. An electron spin resonance (ESR) spectrometer was used to make this measurement. The slice shown in Fig. 18 was divided into two parts by a cut made through the center of region II. Each of these two pieces was then further ground and polished to remove the material from region II. Thus we were left with two samples; one was transparent and blue in color and came entirely from region III, the other was transparent with no visible color, and came from region I.

Both samples were oriented in the microwave cavity with the c-axis approximately parallel to the static field. The resulting ESR spectra were recorded and are shown in Fig. 19. From this we can see that the concentration of copper is at least ten times as great in the blue sample from region III as in the uncolored one from region I.

C. Conclusions - From these preliminary studies we can see that there is some correlation between concentration of metal ion dopant and growth rate. Further experiments are needed to prove this correlation.

D. Further Studies - A growth solution was prepared by mixing the following materials at 40°C: 15 grams of water, 25.5 grams of Rochelle salt, and 0.15 gram of copper chloride. Further, by adding 0.1 gram of NaOH (anhydrous) pH of the solution was adjusted approximately to 7.5. This solution was used for the following growth experiments.

Figure 19. ESR Study of Crystal CuRS #1.

Comparison of the ESR spectra of Region III [shown in (A) of Fig. 19] with Region I [shown in (B) of Fig. 19]. The concentration of paramagnetic copper ions is clearly greater in Region III which was grown at the higher rate.

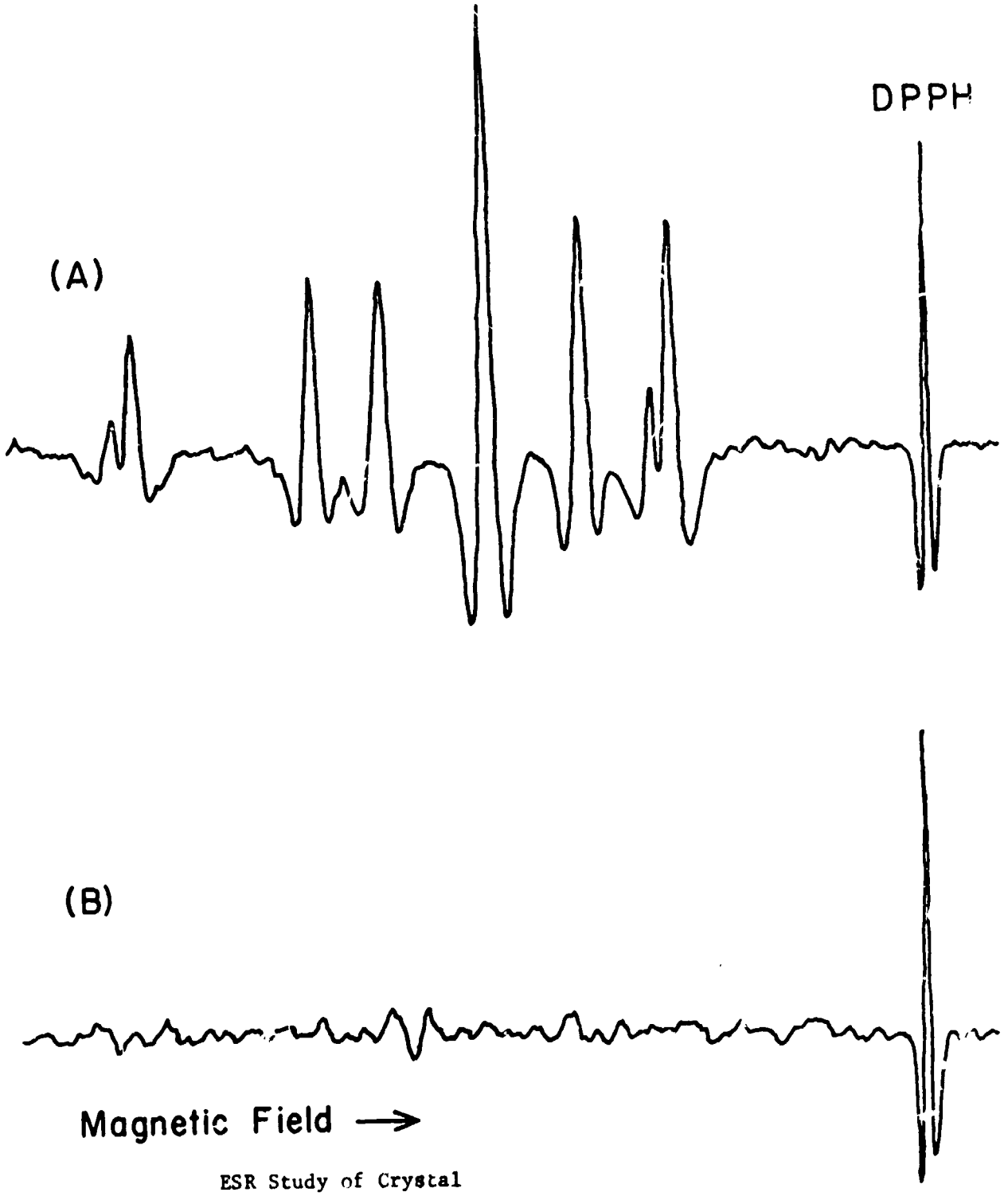

ESR Study of Crystal

(A) Region III

(B) Region I

Figure 20 shows the bath temperature against time during one of the growth experiments. The c-axis of the crystal was held horizontal during this growth experiment. After 80 hours of growth the crystal was removed from the solution and then examined. Figure 21 shows a sketch of the resulting crystal. Regions of growth are called A, B, and C, and correspond to periods I, II, and III in Fig. 20. That is, crystal growth in regions A and C are induced by the temperature drops in periods I and III, respectively, in Fig. 20. Growth in region B is the result of the aftereffect of growth in region A. Region A, which was obtained for a relatively high growth rate, was found to be heavily doped; while region B, which was obtained for a very slow rate, was found to be only slightly doped. Finally, region C, which was obtained for a moderate growth rate, was found to be doped, but the dopant concentration was less than 1/2 that of region A.

Thus it was concluded that there is a correlation between growth rate and concentration of metal ion dopant. Several other experiments similar to that given above supported our conclusion. Consequently we believe we have proven this correlation.

3.2-2 Doping in the Limit of Extremely Slow Growth Rates

It is important to determine whether or not doping occurs for a crystal grown at an extremely slow rate. An experiment was performed for this purpose. A solution at 32.4°C was cooled to 31.8°C over a period of three hours. It was then held at 31.8°C for 17 hours while the crystal continued to grow. For these conditions, the crystal is expected to grow as a result of the aftereffect of this slow cooling and hence the growth rate should be very low. This slow growth region of the resulting crystal showed no evidence of blue color and hence the doping concentration should be extremely small.

Figure 20. Cooling Curve for Experiment CuRS #7.

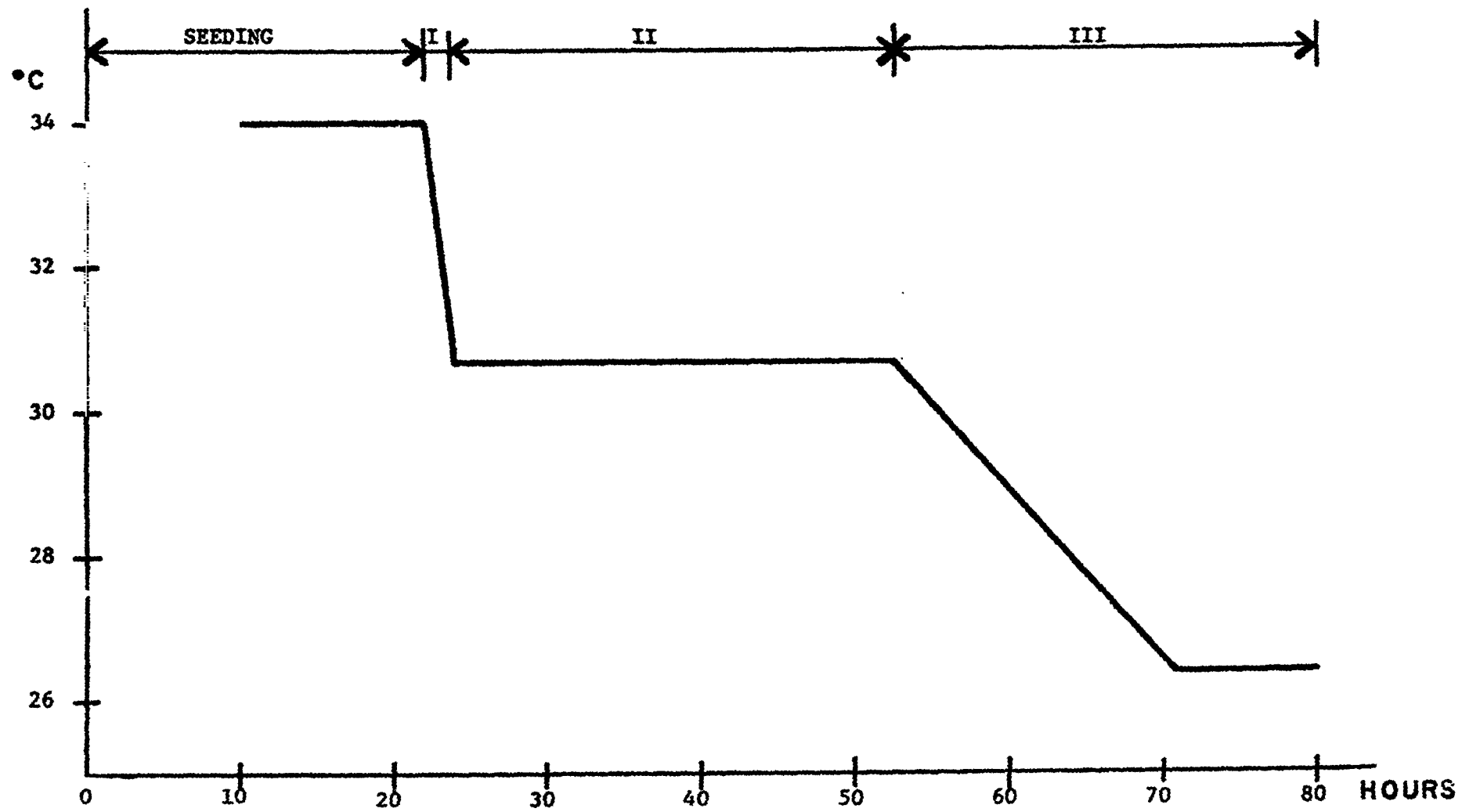

Cooling Curve

Figure 21. Crystal CuRS #7 in its Growth Vial.

The crystal regions A, B, and C correspond to the time periods I, II, and III in Fig. 20 respectively.

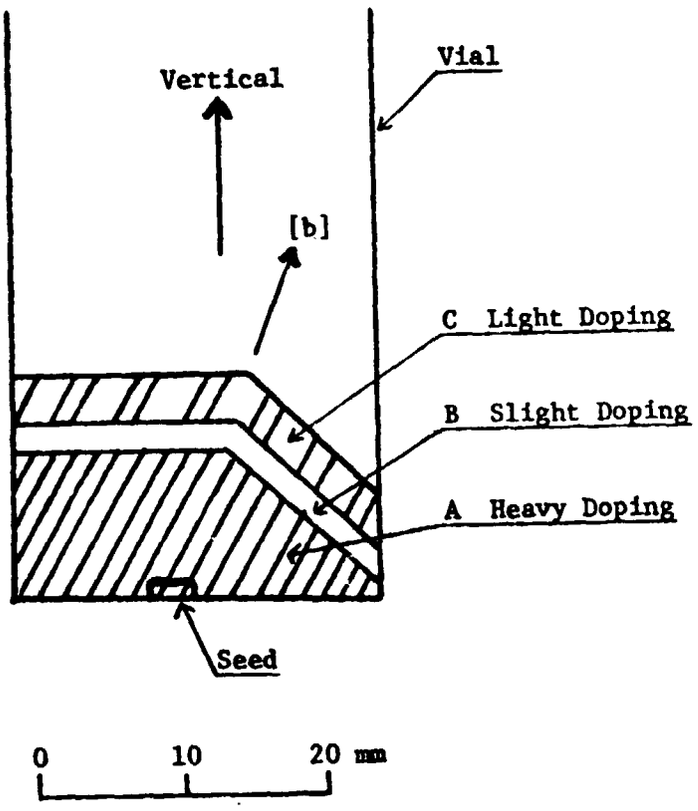
Vial
Vertical
[b]
C Light Doping
B Slight Doping
A Heavy Doping
Seed
0
10
20 mm

Previous investigations have shown that quality of a crystal is better for a slower growth rate. Consequently, the results in this section and the two preceding sections lead one to conclude that metal ion doping occurs at defects in the crystal and hence no doping should occur for a "perfect" crystal.

3.2-3 Control of the Dopant Concentration

In the previous investigations we proved that there is a correlation between growth rate and concentration of copper dopant in Rochelle salt crystals. Now we want to examine this correlation more carefully and determine whether the dopant concentration can be controlled.

A. Experimental - Solutions for doping concentration experiments were prepared by mixing the following materials at 60° - 70°C: 45 grams of water, 76.5 grams of Rochelle salt, and 0.45 gram of copper chloride (anhydrous). Further, by adding 0.3 gram of NaOH (anhydrous) the pH of the growing solution was adjusted to approximately 7.5. This solution was transferred while still warm to three identical vials. In each vial, a seed crystal was placed so as to grow with either the a, b, or c-crystal axis vertical. (Figure 22 shows the a, b, and c-crystal axes of a single crystal of Rochelle salt.) Then, the vial with the oriented seed and its growing solution was carefully lowered into the constant temperature bath.

Figure 23 shows the bath temperature versus time during one such growth experiment. After 70 hours of growth, the crystals were removed from their solutions and then examined. Figure 24a shows a photograph of the resulting crystals. (See Fig. 22 for identification of the crystal axes.) While the crystal on the right was growing, the a-axis was held vertical; similarly, the b-axis of the center crystal and the c-axis of the left crystal were vertical during the growth experiment.

Figure 22. Rochelle Salt Crystal Habit.

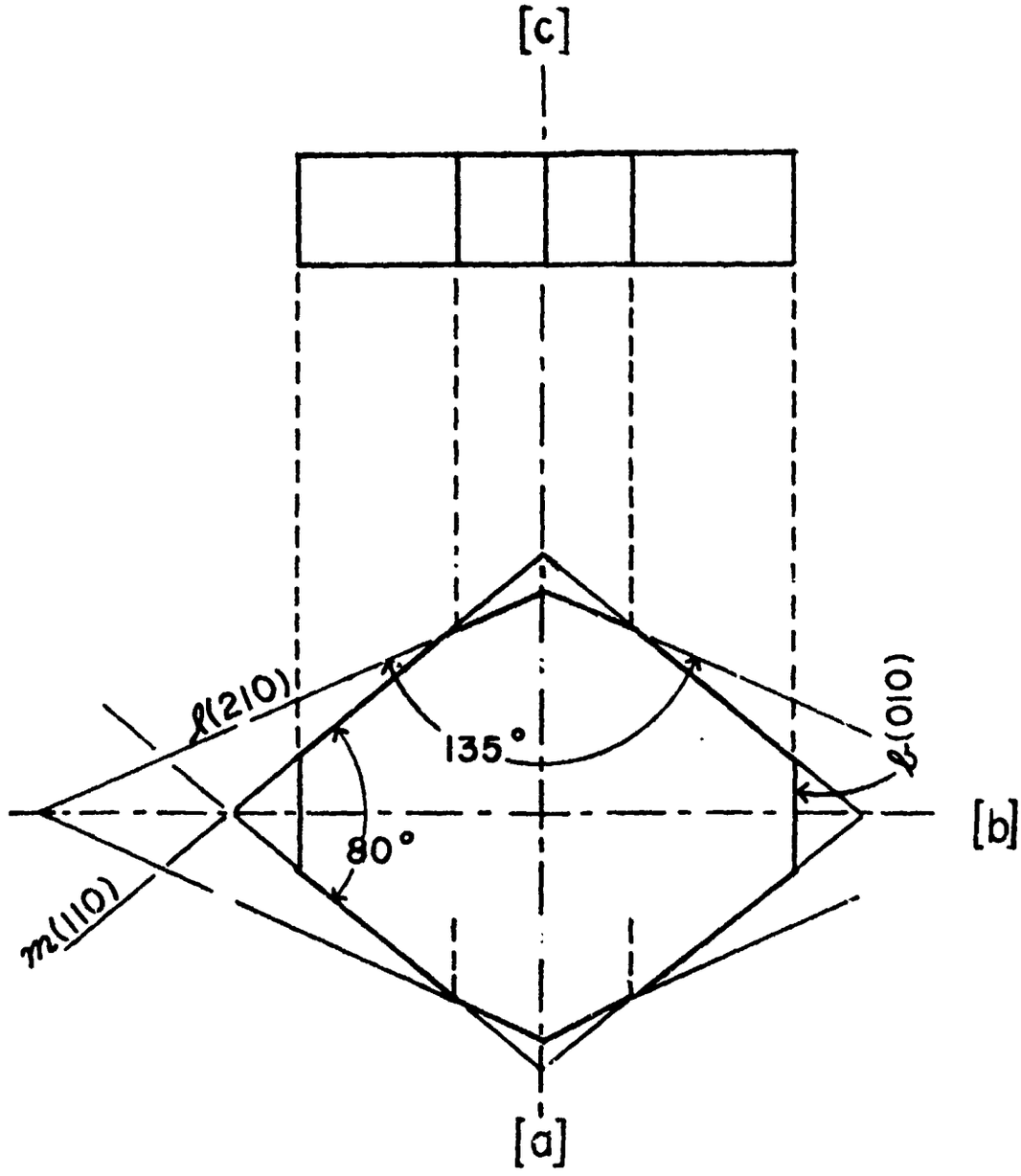
[c]
l(210)
135°
l(010)
[b]
80°
m(110)
[a]

Figure 23. Cooling Curve fo Experiment CuRS #23.

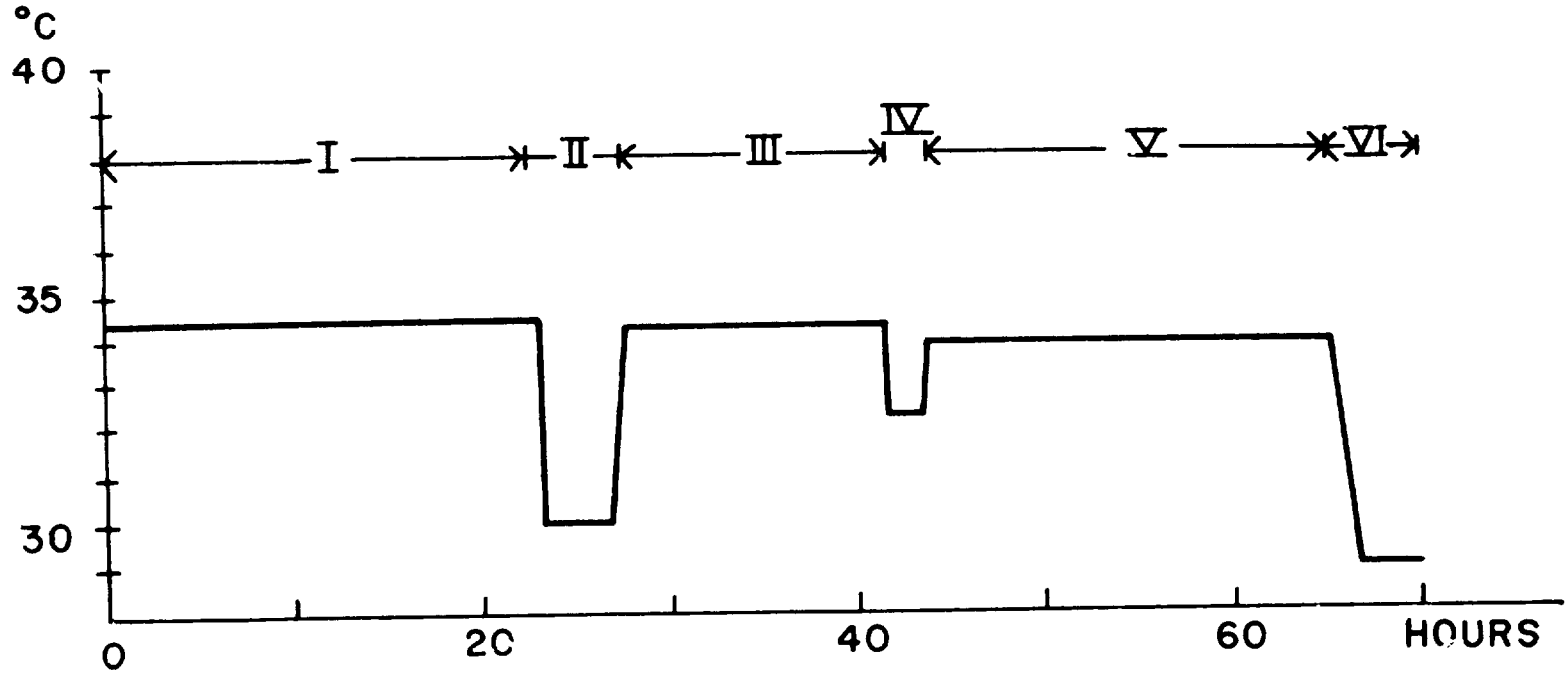
°C
40
35
30
I
II
III
IV
V
VI
0
20
40
60
HOURS

Figure 24a. Photograph of the Crystals Grown in Experiment CuRS #23. See Fig. 23 for the cooling curve. The c-axis of the crystal on the left was vertical during growth, while the b- and a-axes of the central and right crystal respectively were vertical while they grew.

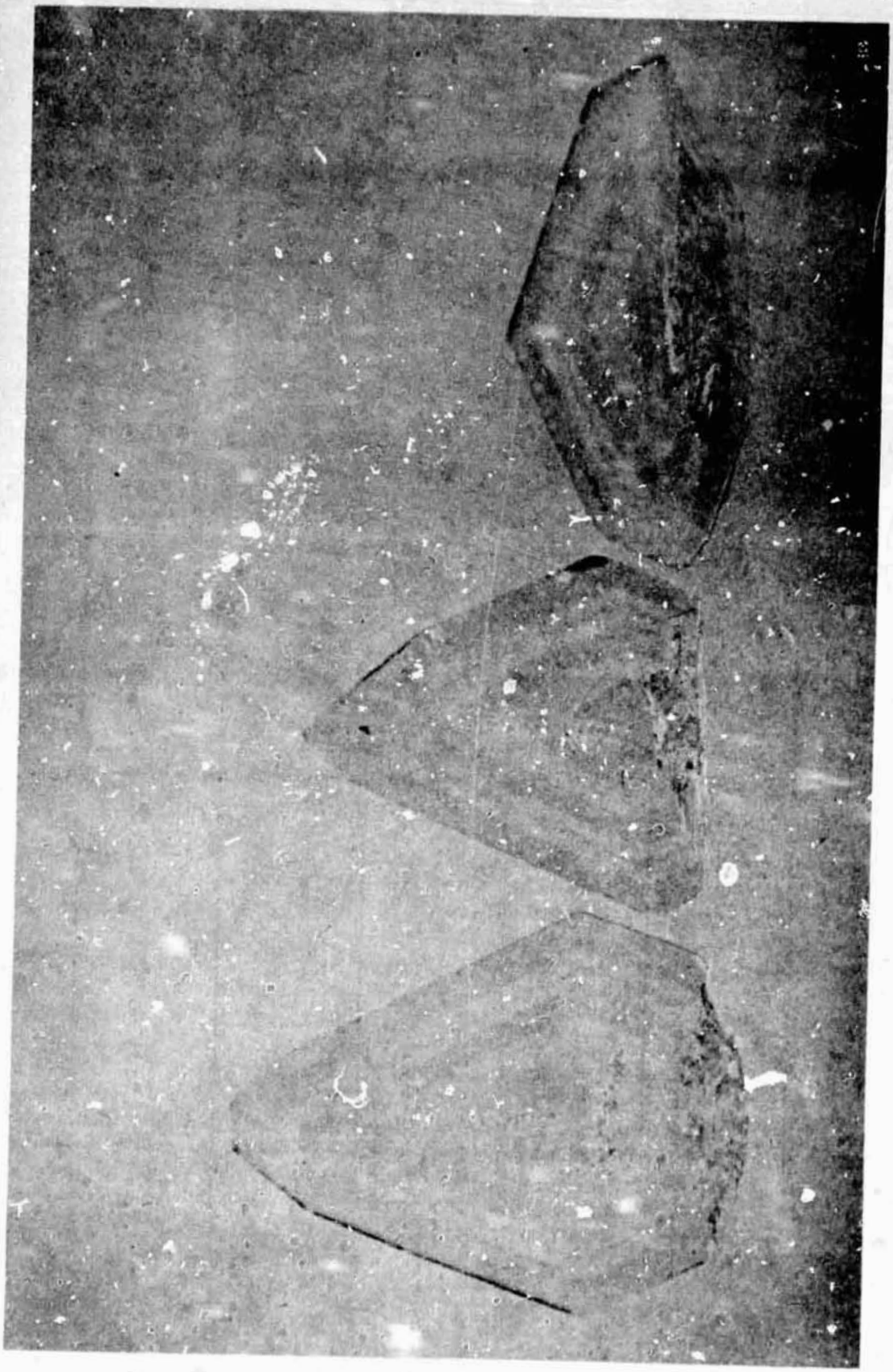

Figure 24b. Illustration of Figure 24a.

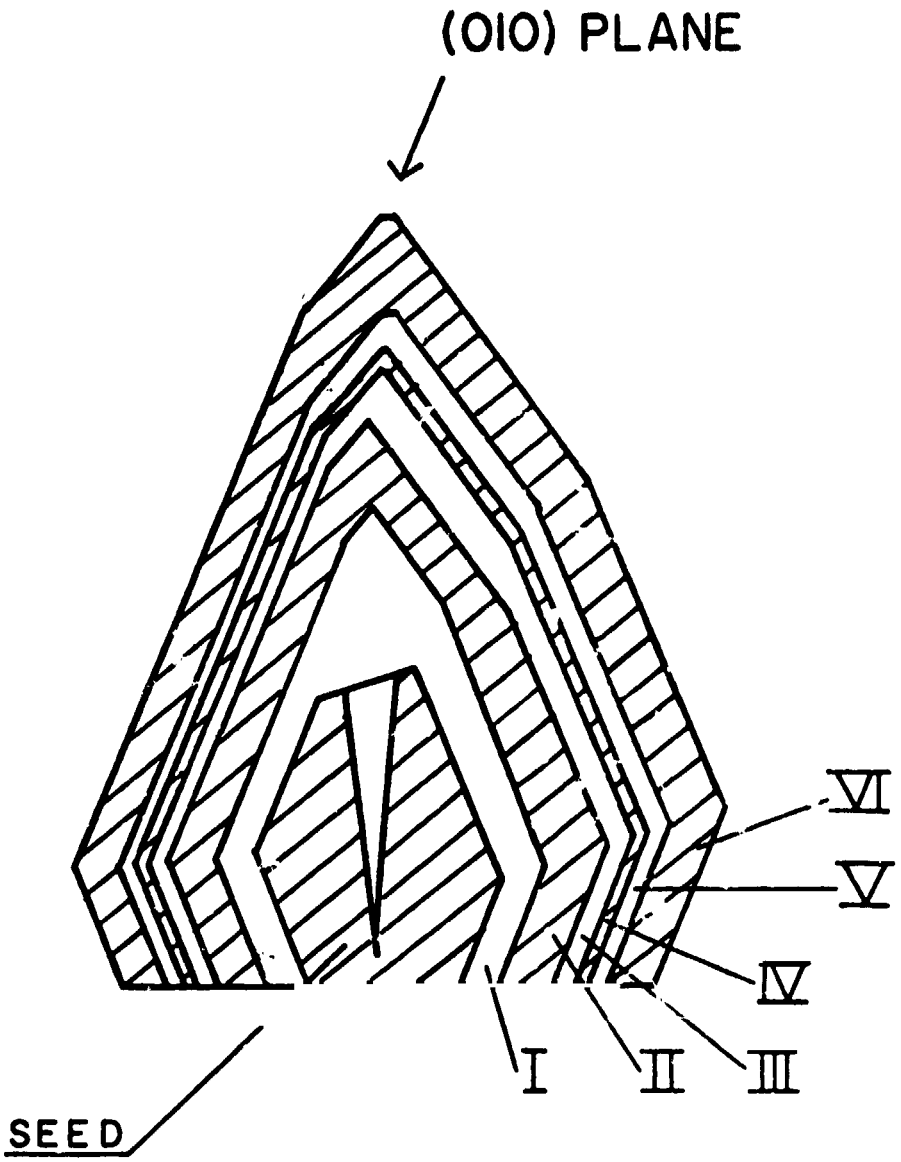
(010) PLANE
VI
V
IV
I
II
III
SEED

B. Results - Notice that all three crystals have similar growth patterns, that is, they all have similar alternating areas of dark and light shading. The dark areas are blue and are more heavily doped, while the light areas are practically colorless with no detectable doping. This growth pattern is further illustrated in Fig. 24b for the case of the crystal in the center. The growth layers I through VI are named in accordance with the growth periods shown in Fig. 23. For example, the layer II was formed by crystal growth during the growth period II. Table I lists the average thickness of each grown layer, growth time, and growth rate for these three crystals. We were able to adjust the growth rate by properly decreasing the bath temperature. This temperature decrease is also listed in Table I (see also Fig. 23).

Concentration of the copper dopant was determined as a function of growth rate by performing several semi-qualitative experiments. The results are given in Table II. The concentration values given here were determined by comparing the blue color of a sample crystal with that of a sample solution of the same thickness containing a known concentration of Cu^{++}. The relative concentration of copper dopant could also be roughly determined by comparing the intensity of blue color in crystals of the same thickness. Of course, it should be remembered that both these techniques can give only approximate values of the dopant concentration.

C. Conclusions - In conclusion, the experiments described above clearly demonstrate that the doping concentration can be controlled by controlling the growth rate.

Table I. Growth Rates for Experiment #23.

Layers	Thickness (mm)	Growth Time (Hours)	Growth Rate (mm/day)	Temperature decreases (°C)
I	1.2	22	1.3	0.4
II	1.4	3	11.2	3.8
III	0.5	20	0.6	0.4
IV	0.3	2	3.6	1.9
V	0.6	23	0.6	0.4
VI	1.7	4	10.2	4.9

Table II. GROWTH RATES AND DOPING CONCENTRATIONS (SEMI-QUANTITATIVE)

Growth Rates (mm/day)	$[Cu^{++}]$ (10^{-5} mole/cc)
16	6
3	3
1	<1

3.2-4 Conclusions

From all the preceding experiments we make the following conclusions;

(i) There is a correlation between growth rate and concentration of metal ion dopant.

(ii) Doping of copper ions in Rochelle salt crystals occur at defects in the crystals, and hence no doping should occur in the limit of extremely slow rates.

(iii) Doping concentration can be controlled by controlling the growth rate.

3.3 Effect of Convection on Crystal Properties - Further Studies

3.3-1 Evidence for the Effect of Convection on Dopant Concentration

The correlation between growth rate and dopant concentration suggests an association between convection and metal ion doping. In spite of intensive efforts, we have not been able to prove this association. We have several, indirect evidences suggesting this association, however. One such example is given in Fig. 25. This crystal was obtained by slow evaporation of a growing solution while the a-axis of the crystal was held vertical. The figure shows that the outermost regions along the horizontal c-axis are not doped, or doped only slightly.

It is remembered that effects of convection are greater along a vertical direction than along a horizontal direction. It is also noted that the c-axis is most sensitive to convection, that is, defects in a crystal most liekly appear along the c-axis; the a-axis is most stable against convection. Thus the result in Fig. 25 that shows no doping along the most sensitive c-axis can be explained only by assuming an association between convection and dopant concentration.

Figure 25. Slow Evaporation Experiment.

The crystal was grown by a slow evaporation technique with the a-axis held vertical.

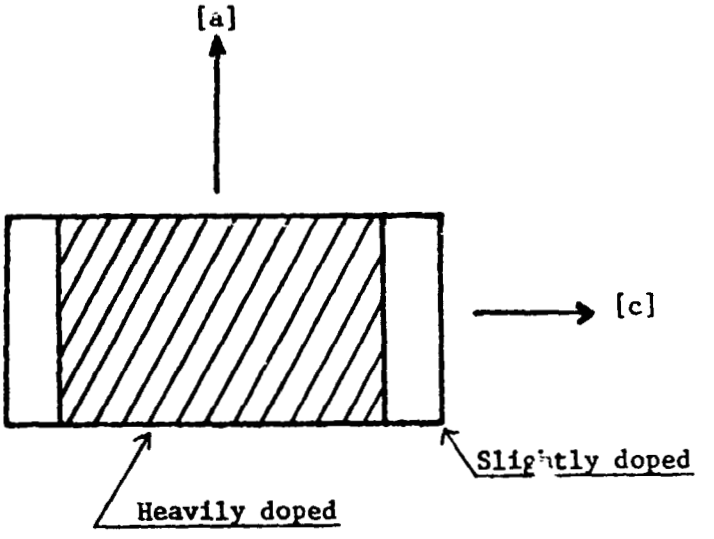

Slow Evaporation Experiment

It is noted that a slow evaporation experiment such as shown above should not be considered to be a controlled experiment. One can not claim that the association is proven until it is shown by slow cooling experiments for varying conditions.

If the association between convection and dopant concentration is proven, then the concept of space processing must be modified. So far we have assumed that the less the convection is, the better the resulting crystal will be. This is true for pure crystals. However, in some cases of doped crystals, apparently some convection is still needed to grow a uniformly doped crystal. Of course, one may expect that a convection suitable for such purposes can be produced under controlled gravity which can be achieved only in a spacecraft.

3.2-2 Effect of Convection on Crystal Habit

Crystallographers call the characteristic shape of a crystal its "habit". Figure 22 shows some of the crystal habits of Rochelle salt grown from a basic solution containing copper ions. The habit of a crystal, the relative sizes of its characteristic faces, is determined by the rates at which the different sorts of faces grow on it. Crystals of Rochelle salt grown from a basic solution in the presence of copper ions are, in general, thin plates in the ab-crystal plane with the c-axis perpendicular to the plane.

In Fig. 22 the (010) face is shown on the right side of the diagram; this small face is parallel to the a-crystal axis. The (010) face is also shown by the arrow at the top of the illustration of the crystal shown in Fig. 24b. Referring to Fig. 24a, it is noted that the (010) plane distinctly appears in the crystal on the left but is present only slightly in the

crystal at the center. This difference should be attributed to convection, since the only difference in growth conditions for these crystals is that the crystal axes were oriented differently in the gravitational field. The c-axis was vertical for the former and the b-axis was vertical for the latter. The shape of the third crystal on the right supports this conclusion. No (010) plane appears in this crystal whose a-axis was vertical during growth; Further, the (110) plane appears in the left and center crystals and is absent in the crystal on the right, the dominant plane being (210).

The above-mentioned result seems to suggest that convection might directly affect the dopant concentration along a given crystal direction. We cannot say we have proven the effect of convection on dopant concentration, although the results of several, uncontrolled experiments support the presence of this effect. One such example has already been given in Section 3.3-1.

3.3-3 Effect of Convection on Microscopic Defects

A. Experimental - Solutions for the growth experiment were prepared by mixing the following materials at 60° - 70°C: 45 grams of water, 76.5 grams of Rochelle salt, 0.45 gram of copper chloride (anhydrous) and 0.3 gram of NaOH (anhydrous). This solution was transferred while still warm to three identical vials. In each vial, a seed crystal was placed so as to grow with either the a, b, or c-crystal axis vertical. Then, the vial with its oriented seed and its growing solution was carefully lowered into the constant temperature bath. Figure 26 shows the bath temperature versus time for experiment CuRS #26. After about 80 hours of growth, the crystals were removed from their solutions and then examined. Figure 27 shows a

Figure 26. Cooling Curve for Experiment CuRS #26.

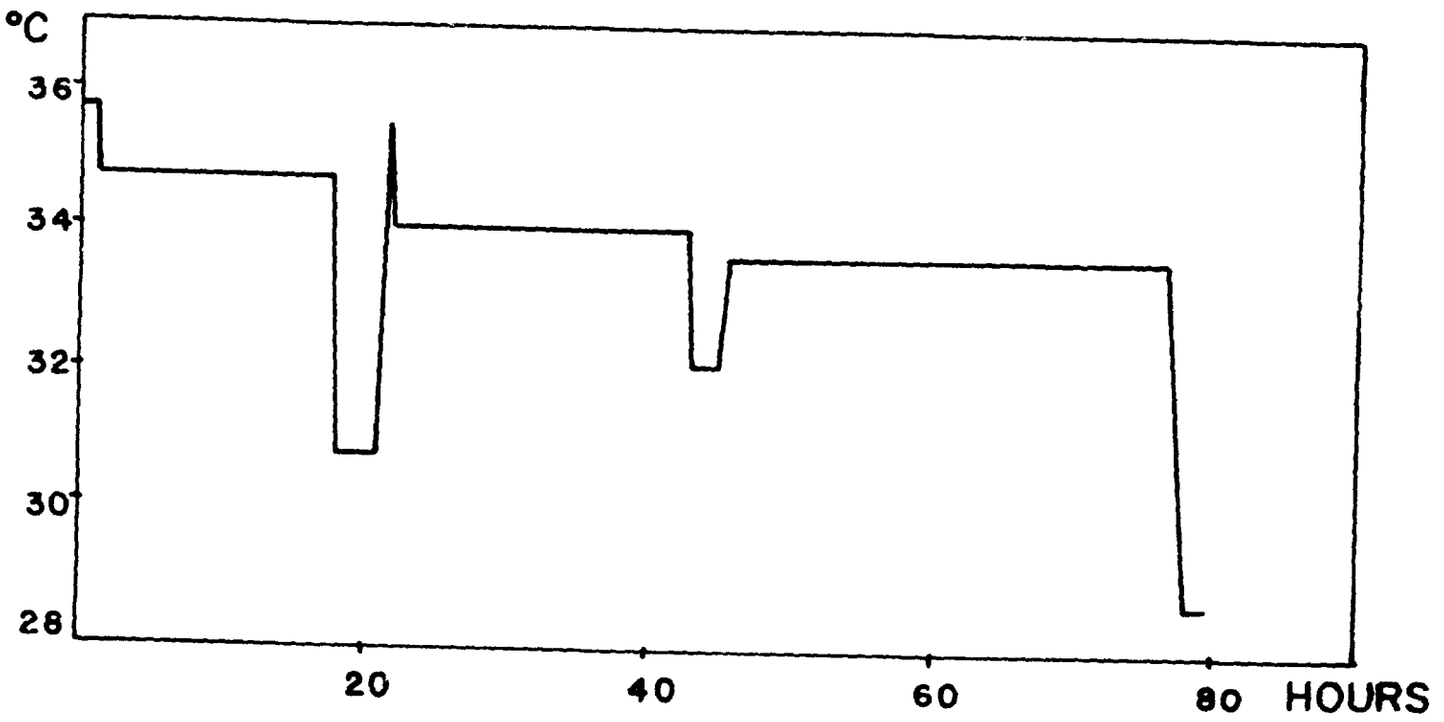
°C
36
34
32
30
28
20
40
60
80
HOURS

Figure 27. Photograph of Crystal CuRS #26.

See Fig. 26 for the cooling curve. This crystal was grown with the b-axis vertical. The three areas of dark coloring are the three regions of heaviest copper doping, and each grew during one of the three drops in temperature shown in Fig. 26. There are some defects visible in the outside dark area, near the edge of the crystal on the left side.

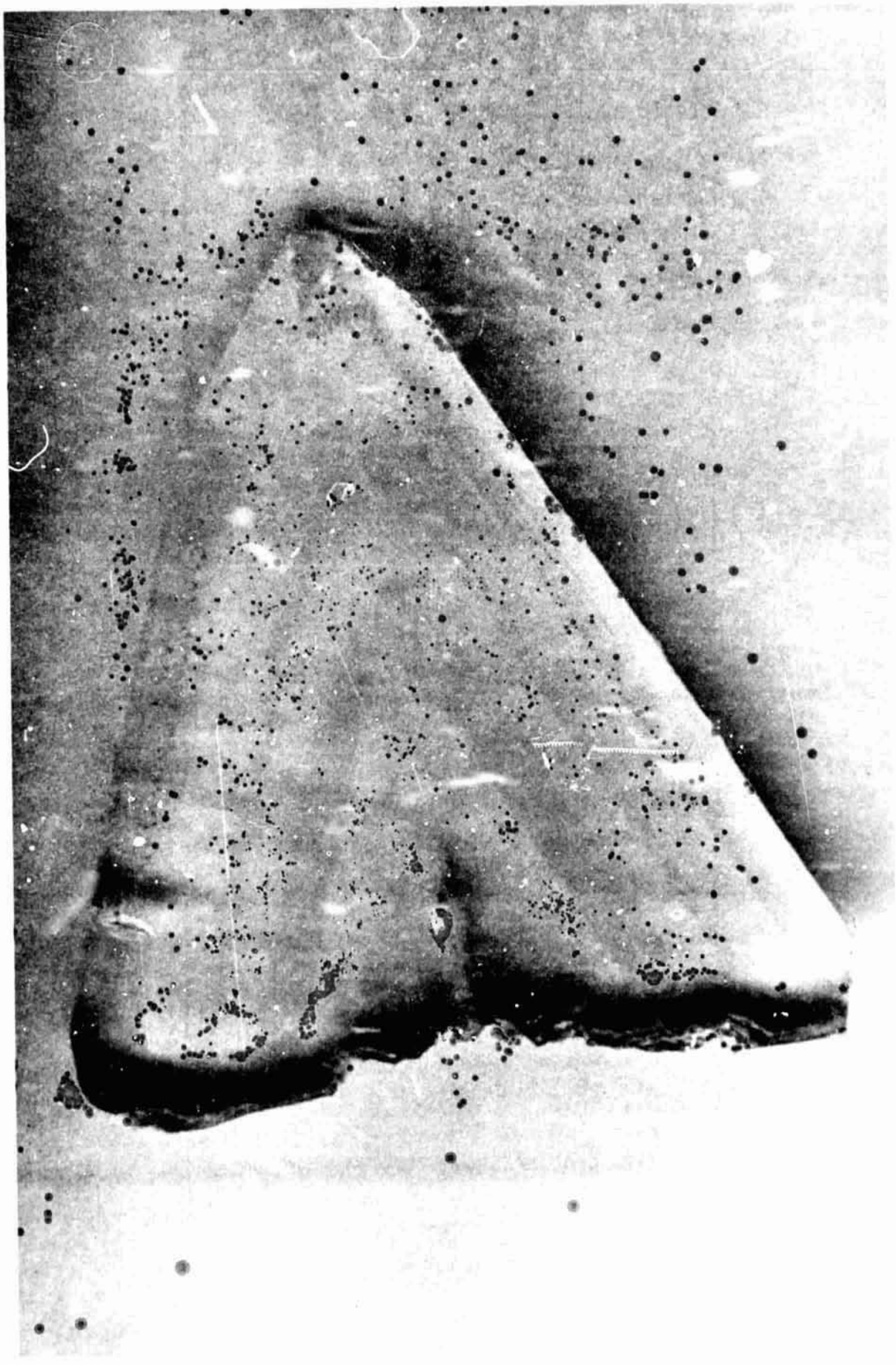

photograph of the crystal that grew with the b-crystal axis vertical. A section of the outside blue edge of the crystal, one from each side, is also shown after being enlarged 125 times (Figs. 28 and 29).

B. Results - The b-axis of the crystal shown in Fig. 27 was not precisely vertical during growth. The small tilt (5° or less) to one side was enough to produce stronger convection currents on the right side of the crystal compared to those on the left side. This difference in the realtive strengths of the currents at the right-hand growing surface as compared to the left was especially large during the growth of the outside blue layer. During the growth of this layer the temperature drop from the preceding steady-state condition was larger than for any of the previously grown layers (see Fig. 26) and so, whatever effect convection may have had would be strongest for this outside blue region. It should be remembered that the surfaces on both sides of the crystal are identical, the m (110) planes. If there is any difference between these two sides, the difference must arise from the effect of convection. From a visual inspection of the crystal in Fig. 27 there seems to be little difference in the right and left sides of the crystal. A microscopic examination revealed a significant difference, however. Figure 28 shows a small portion of the right side of the outside blue layer enlarged 125 times. Figure 29 shows a corresponding area from the left side magnified by the same amount. The defects from the right side, where convection was strongest, are two rows of tiny cavities, parallel to the edge of the crystal. These tiny cavities appear to be about 75% filled with solution.

Figure 28. Microscope View of Crystal CuRS #26.

Defects not visible to the naked eye could be seen after magnifying 125 times. Tiny cavities appeared to be arranged in two rows parallel to the edge of the crystal. Each cavity seemed to have a small amount of solution inside.

Figure 29. Microscopic View of Crystal CuRS #26.

A small area near the left edge of the crystal shown in Fig. 27. The barely visible defects have been enlarged 125 times and appear to be mostly empty cavities. Compared to the cavities shown in Fig. 28 at the right edge of this crystal, the cavities shown here on the left side are huge.

Figure 29 shows an area from the left side of the crystal where convection was relatively weak compared to the right side. After magnifying 125 times, we can see fairly large, mostly empty cavities. There are some areas which appear to contain trapped solution but most of the volume of each cavity is empty. The smooth bubble-like shape of these large cavities suggest that they may be filled with trapped air. This conclusion is further supported by the following fact: When a crystal with many empty cavities was dissolved, some small bubbles appeared on the surface of the solution.

To date we have grown three more crystals which show the same kind of defects as discussed above. That is, the side of the crystal with the stronger convection has tiny cavities which are about 70 - 80% filled with solution. The other side of the crystal, with less convection, had larger cavities which were only about 10 - 30% filled with solution.

3.3-4 Conclusions

From these preliminary results we conclude that one probable effect of convection is to trap solution in the tiny cavities formed in the area of rapid growth. Another possible effect is to prevent the formation of large empty cavities.

The present result that weak convection induces large, empty, microscopic cavities strongly suggests the possibility that crystals grown in a zero-gravitation environment would contain many such cavities. For this reason it is recommended that a careful study on the mechanism of production of these cavities be considered as one of the possible projects in the near future.

3.4 Application: Crystal Growth Under Vacuum - Preliminary Study

3.4-1 A New Technique as an Application of the Present Investigations

The fact that microscopic cavities arise from a trapped air bubble of microscopic size and the latter originates from dissolved air in the solution suggests a new technique of solution crystal growth: crystal growth under vacuum conditions. Since in this condition most of the dissolved air in a solution is removed, only a very small number of cavities should appear in the resulting crystal even in the case of a high rate of growth. Thus this technique should be useful for doping. It is noted that while doping concentration increases with increasing growth rate of a crystal, a high growth rate inevitably induces cavities from the dissolved air under atmospheric pressure. In the case of growth under vacuum conditions, however, one should be able to obtain a high doping concentration by growing the crystal at a high rate without inducing many cavities in the crystal. This was found to be the case.

3.4-2 L-Alanine Doped Triglycine Sulphate

One of the best candidates for this examination is L-alanine doped triglycine sulphate. It is known[9] that this crystal can be an extremely good infrared detector material, if a high doping is achieved and the doping concentration is controlled.

Figure 30 shows the apparatus used for this experiment. A solution which contains 11.4 grams of triglycine sulphate, 4 grams of L-alanine, and 20 grams of distilled water was introduced into the glassware and a seed crystal was added. The glassware was then transferred into a temperature bath at 40°C, and 2 grams more distilled water was added. Then the glassware was capped and connected to a vacuum system and the water in the

Figure 30. Vacuum Growth Apparatus.

Glass growth vials supported on a Plexiglas stand were used in the vacuum growth experiments. The inside of the vials could be brightly lit for observing convection currents in the growth solution. The Plexiglas stand had many holes drilled in the top and bottom support plates to allow rapid circulation of water in the temperature bath.

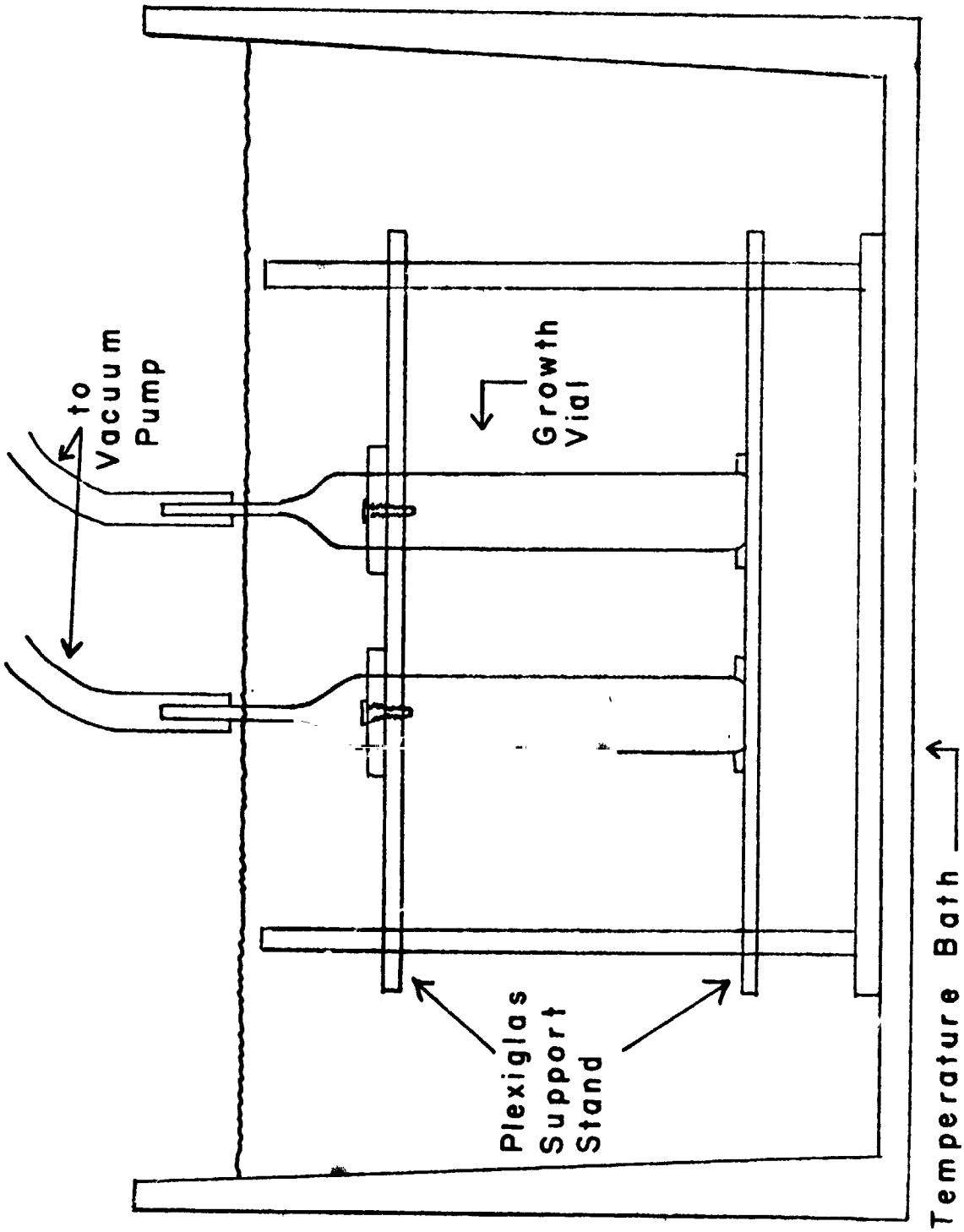
to Vacuum Pump
Growth Vial
Plexiglas Support Stand
Temperature Bath

solution was evaporated until the volume of the solution decreased by 2 cc. Afterwards the rubber tubing was clamped and the vacuum system was disconnected.

This process removed most of the dissolved air in the solution. Now the solution was ready for crystal growing. After six hours of a preliminary slow growth period, temperature of the bath was cooled as rapidly as possible by circulating cold water. Then the crystal started to grow at a rate as fast as 10 mm/day. After 20 hours of growth the crystal was removed and examined.

A microscopic examination was performed and it was found that the crystal contains only a small amount of cavities, both empty and solution-holding types, despite this high growth rate. An amino acid analysis by Dr. Hardman, Biochemistry Department of The University of Alabama, indicated that the crystal contained between 2% and 4% L-alanine. It is noted that the highest previously reported concentration is 2%.[10]

3.4-3 Conclusions

A new technique, crystal growth under vacuum, was established at least in principle. This technique, when applied to L-alanine doped triglycine sulphate, achieved doping of between 2% and 4% which should be compared to the highest reported value of 2%.

3.5 Preliminary Study on Suppression of Convection by an Inhomogeneous Magnetic Field

3.5-1 Significance of the Study

In the case of solution crystal growth, it has been shown that convection degrades quality of the resulting crystal,[8] as described already in this report. Of course, convection important for crystal growth can be most

effectively reduced in the zero-gravitation environment such as that which exists in a spacecraft. Because of the high cost of operation, however, use of a spacecraft for crystal growth, in particular that for industrial productions of crystals of practical values, can be permitted only when no other means has been shown to suppress convection effectively. Thus effort should be made to serach for a means which suppresses convection in the environment of the earth's surface. One such means is suppression by an inhomogeneous magnetic field. We do not claim that this technique suppresses convection over a large voluem of solution, even if this technique is shown to be effective. We have good supporting reasons, however, that this technique can work at least over a small volume, say a few cubic millimeters, without any sophistication in its application.

3.5-2 Principle

It is well known that an inhomogeneous magnetic field exerts the following force on a unit volume of any material:

$$f_m = \chi H \left(\frac{dH}{dx} \right) \tag{1}$$

where

χ = magnetic susceptibility,

H = magnetic field,

$\frac{dH}{dx}$ = magnetic field gradient (inhomogeneity) along the x direction.

The gravitational attraction per unit volume is given by

$$f_g = \rho g, \tag{2}$$

where

ρ = density,

g = gravitational acceleration.

Thus if

$$f_g = f_m,$$

the gravitational force is counterbalanced by the magnetic force, and hence convection in the material will be suppressed. This is the basic principle of the proposed technique.

If is important to note $\frac{dH}{dx}$, the magnetic field inhomogeneity, in Eq. (1). One sees that a uniform magnetic field for which $\frac{dH}{dx} = 0$ will not suppress convection. This is one of the possible reasons for the failure of magnetic suppression by Gato's group.[11] Before Gato's experiment, a European scientist claimed a successful suppression by a uniform magnetic field.[12] The result of Gato's experiment disagrees with this claim.

3.5-3 Supporting Evidence

A saturated solution of manganese chloride $MnCl_2$ has a relatively high χ because of a paramagnetic nature of the manganese ion and a high solubility of the chemical. Crystals can be grown easily from the saturated solution either by slow cooling or a slow evaporation method.

A small volume of this solution was introduced into a polyethylene sack, which was then sealed. It was demonstrated that the gravitational pull on the sack could be overcome by an attractive force at the edge of some large iron pole pieces where the magnetic field gradient was the greatest. The sack fell when the magnetic field decreased to 3000 gauss, which may be called the critical field for this condition. It is important to note that at an edge of the magnet pole piece $\frac{dH}{dx} \neq 0$. The magnetic field in the center region of a magnet is fairly uniform, and hence practically

$\frac{dH}{dx} = 0$. In this region, then f_m is zero as Eq. (1) predicts and there is no force to counterbalance gravitational attraction. This was found to be the case, even when a higher magnetic field was applied for the sack placed at the center region of the magnet.

3.5-4 Expected Magnetic Field

One may compute empirically the magnetic field required for the counterbalancing. For a given magnet, one may assume

$$\frac{dH}{dx} \propto H. \tag{3}$$

From Eqs. (1) - (3), for this assumption the required magnetic field is given by

$$H^2 \propto \frac{f}{x}\,, \tag{4}$$

or

$$H = H_m \sqrt{\left(\frac{\rho}{\rho_m}\right)\left(\frac{\chi_m}{\chi}\right)}\,, \tag{5}$$

where H_m, χ_m, and ρ_m are the required magnetic field, magnetic susceptibility, and density of a standard material. In the case of the presently used magnet, the $MnCl_2$ solution may be used as a standard material. Table III lists H for several materials for this magnet.

TABLE III. Examples of Required Magnetic Fields (H)

MATERIAL	$\chi(10^{-6})$	ρ	H (gauss)
Water	-0.7	1	18,000
Aluminum	0.6	2.7	32,000
Copper	-0.086	8.9	150,000
$MnCl_2$ solution	500.	2	3,000

Table III shows that the counterbalance can be achieved by a relatively low magnetic field even in the case of molten metal aluminum for this magnet system. It may be in practice difficult to counterbalance the sample in the case of molten copper metal.

The values in Table III support the soundness of the basic idea of this study.

It is noted that if convection in a given liquid is suppressed, convection in the vapor of the same material should be suppressed by a similar magnetic field, since the ratio $\frac{\rho}{\chi}$ in Eq. (5) does not change drastically from liquid to vapor.

3.5-5 Conclusions

This preliminary study has supported the feasibility of suppression of convection by an inhomogeneous magnetic field.

3.6 Other Studies

3.6-1 Nature of Convection Currents

The following investigations were intended to obtain further supporting facts for the conclusions given in the preceding report.[8]

In the previous investigation,[8] we showed the correlation between convection currents and crystal quality. We also showed that convection currents arise essentially from concentration gradients. However, we had not completely removed the possibility that temperature gradients in solution could cause or contribute to currents of this kind. Thus, at the beginning of this work period, experiments were done to see if a temperature gradient alone could induce convection in a growing solution.

A solution of 15.5 grams Rochelle salt dissolved in 25 cc water was used as the growth solution, and a small, high-quality seed of Rochelle salt was the growth center. As shown in Fig. 31, the temperature was raised and lowered around T_s, the saturation temperature for this system. At 38.3°C, which is 0.5° above T_s, no convection currents were visible; but at 37.3°C, 0.5°C below T_s, several currents could be seen. Lowering the temperature to 36.2° resulted in stronger currents. This result has often been seen before. Next the temperature was raised 38.3°, where there was no convection to 40.6° and allowed to stabilize. If it is true that lowering the temperature causes temperature gradients which give rise to convection currents, then convection should also be seen when the temperature falls from 40.6°C to 38.3°C.

Furthermore, as can be seen from Fig. 31 this 2.3°C drop in temperature did not start up the convection currents. As long as the temperature was above T_s, no convection currents were visible. Even a 3° drop in temperature could not make currents appear as long as the temperature was kept above T_s.

3.6-2 Ferroelectric Quality: S-Value

The effect of convection on ferroelectric quality has already been studied by observation of the S-value.[8] Recently, Dr. I. Suzuki informed us of an unpublished study performed in Japan on the ferroelectric quality distribution of a triglycine sulphate crystal. Although details are not available, these investigators seem to correlate the quality distribution with a factor other than convection. For this reason, an experiment was performed in order to confirm our previous conclusion.

Two crystals of pure Rochelle salt were grown under the same conditions, the c-axis being held vertical for one crystal and the a-axis for the other.

Figure 31. Convection Experiment.

Temperature versus time for a growing Rochelle salt crystal. The notation nc means no convection currents were visible during this time, and the small c means there were currents visible.

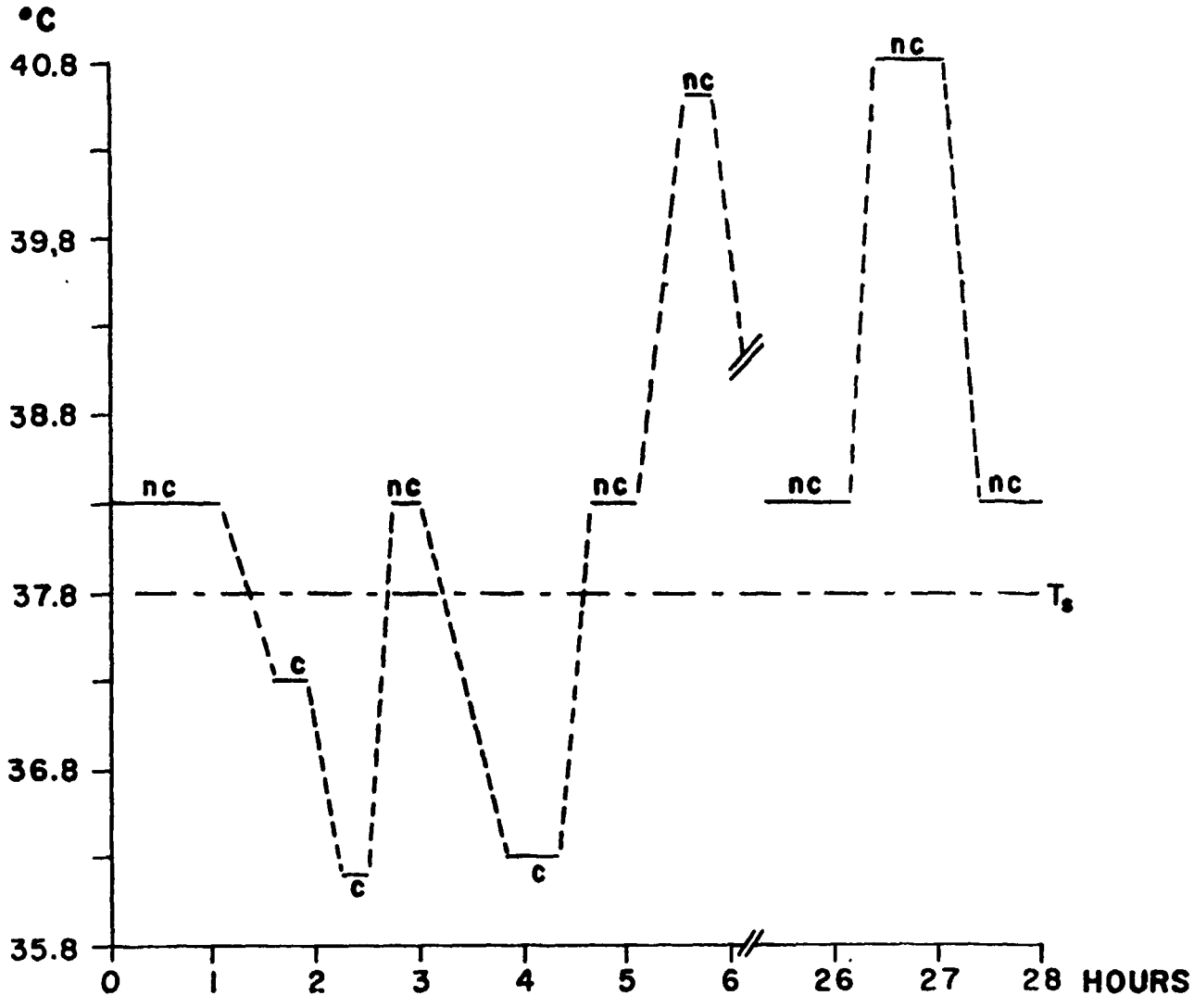

Convection Experiment

The bath temperature against time during the growth experiment is given in Fig. 32. The resulting crystals were sliced and ferroelectric hysteresis curves of each sliced piece were observed, and then the S-values were computed. Figure 33 summarizes the observed S-values. One finds that in both cases the S-value for the side-bottom piece is greater than that for the center-top piece: Compare 10.2 with 5.8 in the upper figure, and 5.0 with 4.0 in the lower figure. Thus the previous conclusion on the effect of convection is supported. One must note, however, that the difference in the S-value for the latter is much less than that for the former. This difference in the two cases should be attributed to the anisotropic nature of the crystal. That is, the S-value of a sample could possibly be a function of the direction along which the electric field was applied. Thus one may deduce the pure effect of convection by taking an average

$$1/2\ [(10.2 - 5.8) + (5.0 - 4.0)] = 2.7$$

for the present case. Similarly the pure anisotropic effect may be given by

$$1/2\ [(10.2 - 5.8) - (5.0 - 4.0)] = 1.7.$$

Thus the effect of convection seems greater than the anisotropic effect for the present growth condition. Of course, it is possible that the effect of anisotropy can be greater than the effect of convection depending on growth conditions. However, there is no doubt about the degradation effect of convection on ferroelectric quality.

3.6-3 Conclusions

The possibility that temperature gradients in a solution induce convection currents was excluded. Thus this result further supported one of the

Figure 32. Cooling Curve for Experiment AlTGS #3.

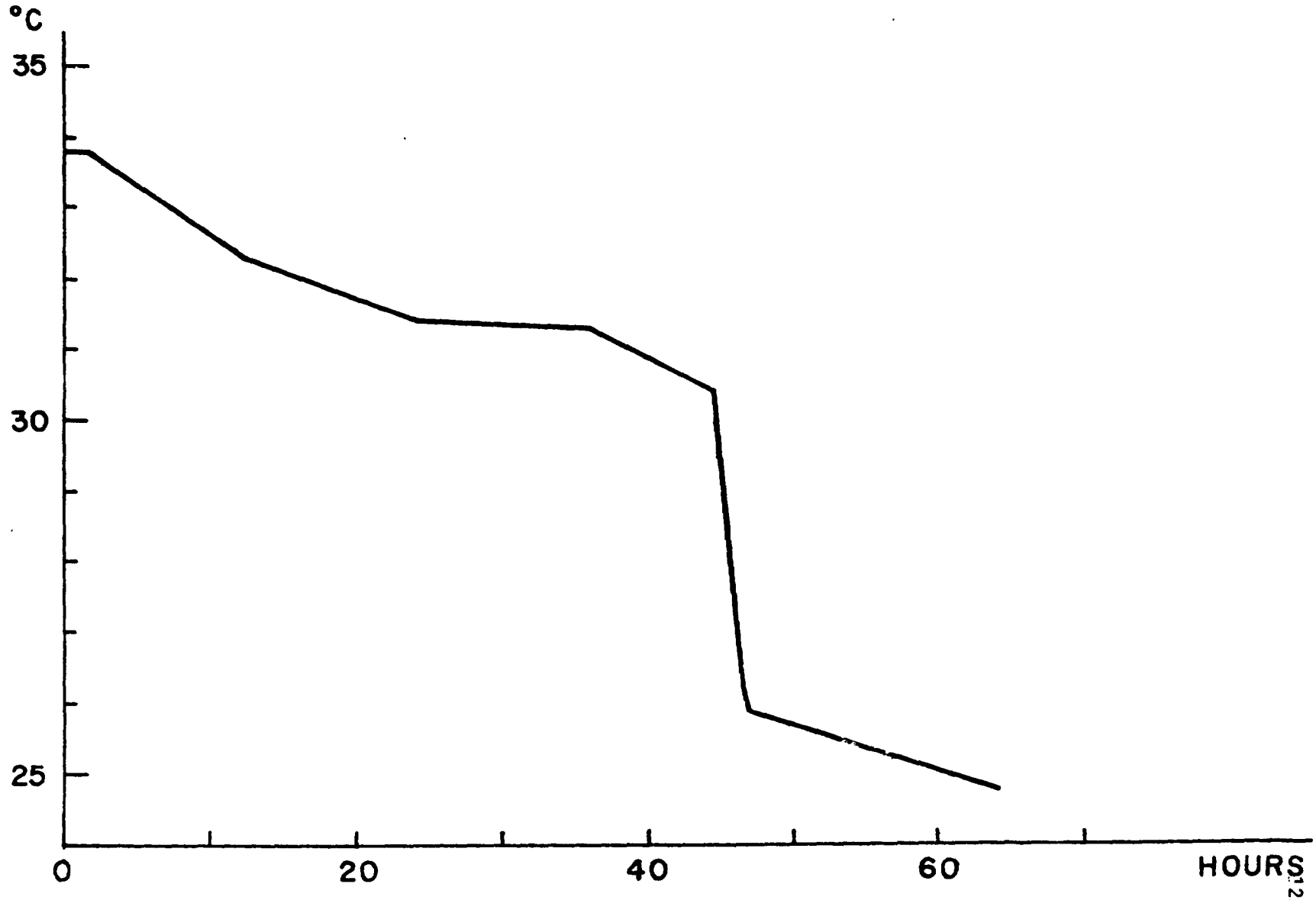

Cooling Curve

Figure 33. S-Values for Crystal AiTGS #3.

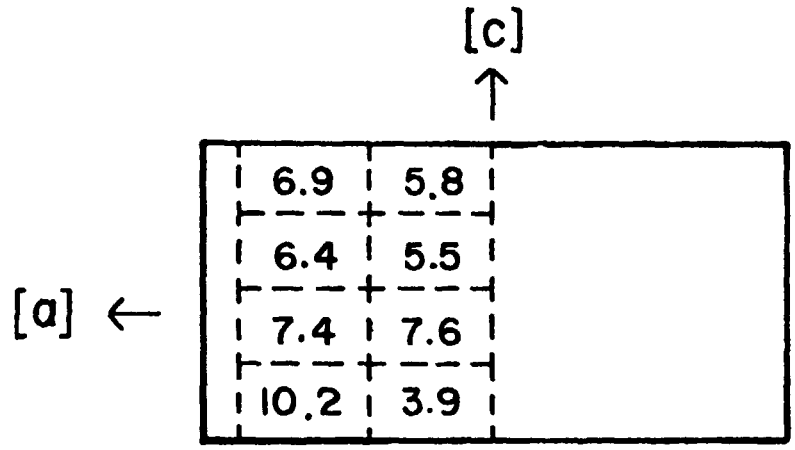
[c]
[a]
6.9
5.8
6.4
5.5
7.4
7.6
10.2
3.9

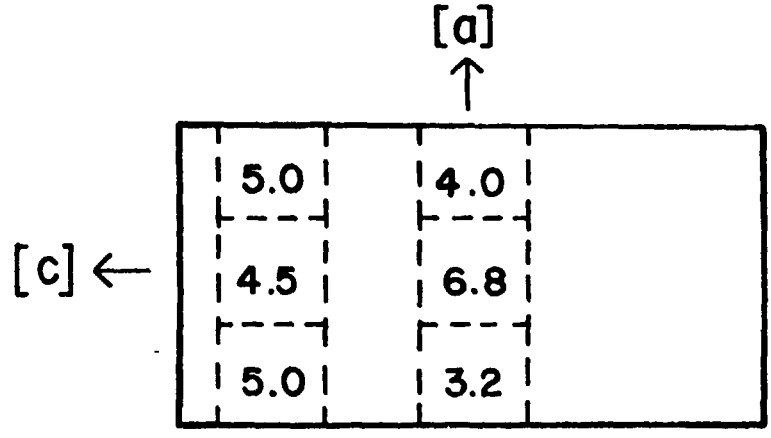
[a]
[c]
5.0
4.0
4.5
6.8
5.0
3.2

previous conclusions that the convection currents essentially arise from concentration gradients.

The effect of convection on ferroelectric quality was shown to be greater than the effect of crystal anisotropy on the quality. Thus this result also confirmed another previous conclusion that convection degrades ferroelectric quality.

3.7 Preparation for Flight Experiments

3.7-1 Preparation of Samples

The Rochelle salt chemical used was supplied by J. T. Baker Chemical Company. Large seed crystals were prepared for this experiment. Some of them were grown by a slow evaporation technique, and the others by a slow cooling technique. In the case of the slow evaporation technique, 100 grams of distilled water was added to 120 grams of Rochelle salt in a 500 cc beaker and the mixture was heated to about 70°C until the Rochelle salt dissolved completely, and then the beaker was removed from the heating device. After the solution cooled to room temperature, a small seed crystal was placed at the bottom of the beaker, and the crystal was allowed to grow at room temperature over a period of 3-7 days. In the case of the slow cooling technique, 100 grams of distilled water was added to 130 grams of Rochelle salt in a 500 cc beaker, and the mixture was heated to about 70°C, until the Rochelle salt dissolved completely. Then the beaker was transferred into a temperature bath at 38°C, and a seed crystal was placed at the bottom of the beaker. The crystal was allowed to grow by lowering the bath temperature slowly to room temperature over a period of about three days.

Granular Rochelle salt used for this experiment was prepared by the following method. 100 grams of distilled water was added to 200 grams of Rochelle salt, and the mixture was heated to 70°C for about 30 minutes until the Rochelle salt dissolved completely. Then the solution was allowed to cool to room temperature, and 24 hours afterwards the crystallized material was separated from the solution and dried over filter papers for 24 hours at room temperature.

The saturated solution used was prepared by the following method. 200 grams of distilled water was added to 240 grams of Rochelle salt, and the mixture was heated until the Rochelle salt dissolved completely. The resulting solution was cooled to room temperature before being used for the experiment.

3.7-2 Simulation Experiment

A three gallon metal can about 3/4 filled with water was heated on an electric hot plate. The power output of the hot plate was adjusted so that the temperature of the water in the metal can increased at a rate which is very similar to the rate for a Skylab heating-serving tray (see Fig. 34).

A seed crystal and granular Rochelle salt, their combined weight being 30 grams, were placed in a 500 cc beaker, and then some of the saturated solution of Rochelle salt which was prepared earlier was added until the total volume of the materials became 200 cc, that is, approximately the total volume of a Skylab food can. The beaker with this mixture of granular Rochelle salt, saturated solution and seed crystal was then placed in the above-mentioned metal can, and a simulation experiment was performed.

Figure 34 plots the temperature of the solution in the metal food can against time for one of the simulation experiments. It was shown that 40 minutes after the heater was turned on, the grar lar Rochelle salt dissolved completely, but a portion of the seed crystal remained undissolved (see Fig. 34).

Figure 34. Simulation of Skylab Heating Experiment.

The solid curve with the triangular points represents a temperature-time plot for the food product in a Skylab heating-serving tray. The solution mixture was 200 cc in volume and contained a seed Rochelle salt crystal of 5 grams and 25 grams of granular Rochelle salt solution saturated at 25°C. The vertical arrow indicates the time at which the granular Rochelle salt dissolved completely.

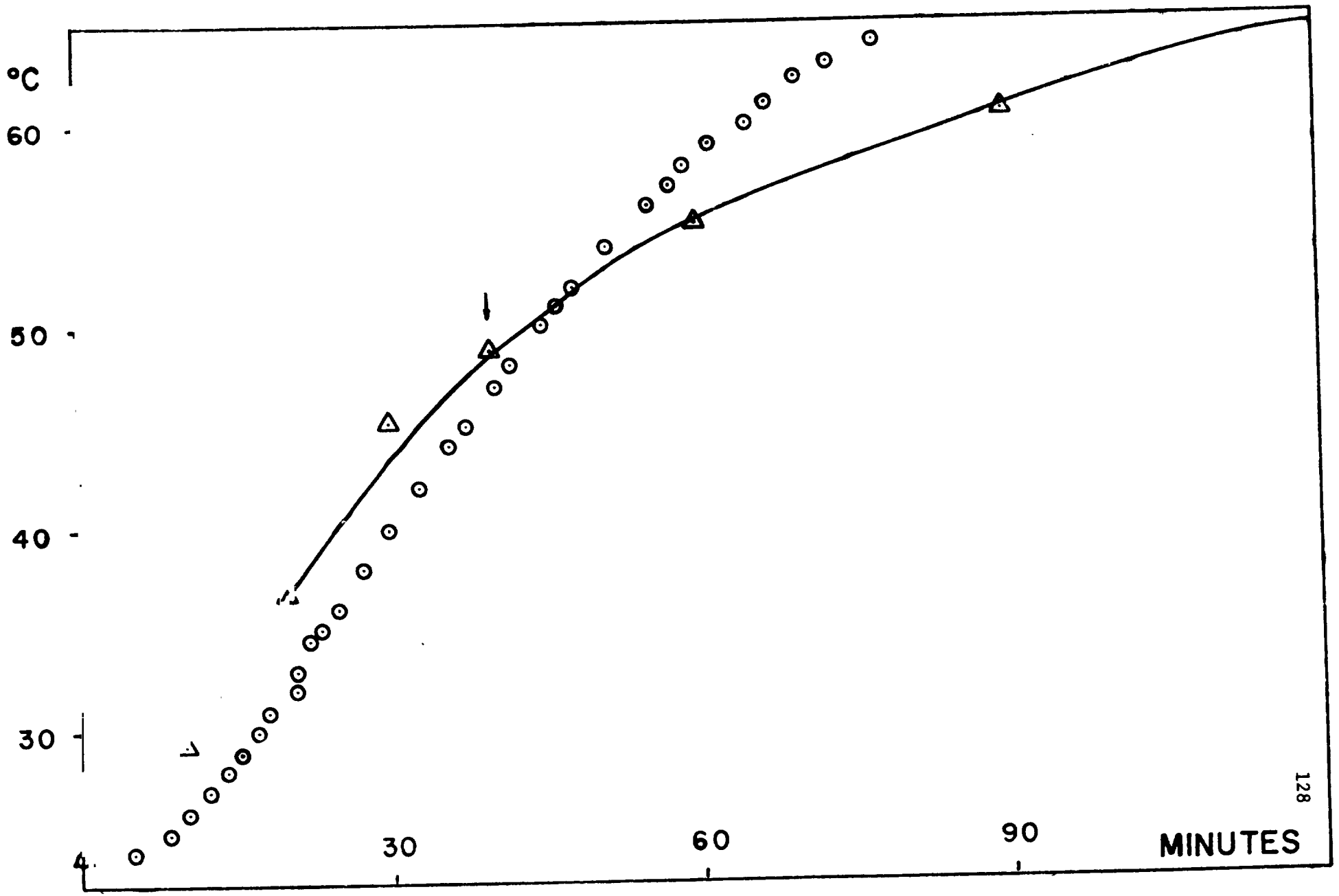
°C
60
50
40
30
30
60
90
MINUTES
128

This result was confirmed by several experiments. Thus it was suggested that the optimum heating time be 40 minutes.

The solution, when cooled to room temperature and allowed to precipitate for 48 hours, produced many small crystals of size 5 x 5 x 5 mm. Most of these crystals showed visible defects. Thus it will be interesting to determine if crystals grown in the zero-gravitation environment under similar conditions are greater than 5 x 5 x 5 mm, and if these crystals also have visible defects.

One important result was obtained accidentally. It was found that untreated powdered Rochelle salt was very difficult to dissolve even at 65°C: the powder remained undissolved even after three hours of heating, while an hour of heating at this temperature completely dissolved a large seed crystal. Thus it was important not to use untreated powder Rochelle salt for Skylab experiments.

3.8 Summary and Conclusions

An investigation was performed to identify the factor which determines the dopant concentration of a crystal. The factor was found to be the growth rate: The concentration of the doping copper ion in Rochelle salt increased with increasing rate of crystal growth, while no doping occurred in the limit of an extremely slow growth rate.

A microscopic study was performed in order to gain an insight into the nature of the degradation effect of convection. It was found that in general a crystal has many microscopic defects, even though the crystal appears perfect to the unaided eye. It was also found that these microscopic defects can be classified into two groups: relatively large empty cavities and

relatively small cavities containing solution. Moreover it was found that convection increases the relative number of the solution-holding cavities compared to the empty cavities in a crystal. It is expected that the solution in the cavities absorbs electromagnetic energy and hence increases the AC conductivity of the crystal. Thus this result suggested the nature of the degradation of ferroelectric quality by convection. Finally some evidence indicated that the cavities, both empty and solution-holding ones, originate from dissolved air in the solution.

The above-mentioned results suggested a useful technique of crystal growth in solutions. A solution under vacuum should contain only a very small amount of dissolved air, if not be completely free of it. Thus the concentration of both types of cavities in the resulting crystal would be very low, even for a high rate of growth. Accordingly one should be able to achieve high doping under vacuum by increasing the growth rate to such an extent that many cavities would be produced if grown under atmospheric pressure. This was found to be the case. In a study of L-alanine-doped triglycine sulphate grown under vacuum conditions, doping concentrations of between 2 and 4% were achieved consistently. Moreover the doping concentration was easily controlled by controlling the growth rate. It is noted that the highest previously reported dopant concentration is about 2%.[10,13]

Recently pyroelectric infrared detectors using triglycine sulphate have begun to offer advantages over some of the older detectors such as thermopiles, bolometers, and Golay cells.[9] For example, these detectors effectively perform over a wide range of electromagnetic radiations from visible to millimeter wavelength. One of the serious disadvantages of these detectors is

the life time is relatively short. Very recently, British workers have shown that doping with L-alanine can help this problem. Thus, development of the crystal growth technique has become very important in order to obtain a high dopant concentration consistently. The technique of crystal growth under vacuum developed during the current project has shown to be useful for this purpose, as already described. It is noted that one of the most important aims of the current project was, if possible, to apply the obtained results to improve qualities of crystals with scientific and industrial significance.

Preliminary work on suppression of convection by an inhomogeneous magnetic field was also done during the current project. Finally, some investigations were conducted in order to further support the previous conclusions:[8] convection degrades ferroelectric quality.

Section 4. Skylab Experiment - Preparation, Observation and Analysis (Third and Fourth Years' Work)

4.1 Introduction

4.1-1 Aim of Study

This project was intended to study growth from solutions as one of the programs for "Space Processing Applications". The work during the previous contract periods has shown that strong convection in the growth solution produces defects in the resulting crystal.[8] The essential nature of these defects was clarified and several factors which affect crystal quality were identified.[14]

The most important result of the current project was the study of the crystal grown on Skylab-4 using the techniques of analysis developed in the previous contract periods.

The current investigation was concerned mostly with analysis of the Rochelle salt crystal returned from Skylab-4. This crystal was grown in a near zero-gravity environment, and offered the first opportunity to experimentally examine the effect that the absence of gravity would have on solution crystal growth.

Concurrent with this investigation, an attempt was made to further understand the basic mechanisms of solution crystal growth. Techniques for observing the growth process, in particular convection currents around the growing crystal, were investigated. In order to understand what is happening at the surface of a growing crystal, it is necessary to be able to observe the changing surface of the crystal and the solution flow in the vicinity very accurately.

Another aim of the investigation is to continue to search for ways to improve the quality of crystals grown from solutions, both in zero-gravity environments and in ground-based experiments.

In order to meet the aims of this investigation, the following studies were made: The crystal returned from Skylab-4 was carefully but thoroughly examined using all the techniques developed in the first two years of this contract period. The techniques developed earlier for inducing high doping concentrations in solution grown crystals were applied to the case of triglycine sulpnate doped with L-alanine. Studies of convection currents in the growth solution were made with the help of a new illumination technique. Theoretical studies of the shape of ferroelectric hysteresis curves and the degrading effect that defects in the crystal would have were also made.

4.1-2 Scope of Work

The analysis of the crystal returned from Skylab-4 was accomplished with the techniques developed in earlier reporting periods.[14] The nature of the defects present and their degrading effect on ferroelectric hysteresis was studied. Ways of improving crystal quality in future zero-gravity experiments were suggested.

Techniques for increasing both crystal quality and the amount of L-alanine dopant in crystals of triglycine sulphate were investigated. The results of previous investigations were successfully applied to this system which could make a potentially excellent infrared detector.

Theoretical studies of the shape of observed ferroelectric hysteresis curves were made. It was attempted to quantitatively describe the degrading effect that microscopic voids, one common type of defect, have on ferroelectric hysteresis.

The continuing effort to understand the basic chanisms of solution crystal growth has resulted in a greatly improved method of observing convection currents in the growth solution; laser illumination of the growth cell makes it much easier to see the flow of solution in the vicinity of a growing crystal.

4.2 Growth of Rochelle Salt on Skylab-4

The effects of convection on crystal growth have been actively studied by many workers, especially for the case of metal crystals.[15] Some effort has also been made by our group at UAT to understand the effect of convection in solution crystal growth.[8] Our group has found that convection degrades the quality of the resulting crystal. Thus we suggested that if a crystal were grown from solution placed in a zero-gravity environment the quality of the resulting crystal should be extermely high. For this reason a crystal of Rochelle salt was actually grown on Skylab-4 and the quality of the recovered crystal was investigated. The code number of this experiment is TV-105, and Astronaut Col. Pogue performed it. Rochelle salt was a particularly interesting research material because of its ferrelectricity.[16]

4.2-1 Ground-based Preparation

Details of the ground-based preparations are given elsewhere.[14] The Rochelle salt chemical used was supplied by J. T. Baker Chemical Company.

The large seed crystals for this experiment were grown by slow cooling techniques. Granular Rochelle salt used for this experiment was prepared by slowly cooling a saturated solution and afterwards was dried over filter papers. The solution used for the experiment was saturated at 25°C.

A seed crystal and granular Rochelle salt, their combined weight being 30 grams, were placed in a Skylab food can and filled with saturated solution. This food can was heated under conditions similar to those found in a Skylab food tray. It was determined that 40 minutes after the heater was turned on, the granular Rochelle salt dissolved completely, but a portion of the seed crystal remained undissolved. Thus it was suggested that the optimum heating time was 40 minutes.

The material actually supplied for the flight experiment is as follows:

seed	21.6 grams
granular Rochelle salt	8.4 grams
Sum	30.0 grams,

and some Rochelle salt solution saturated at 25°C.

4.2-2 Summary of the Flight Experiment

The sealed food can with Rochelle salt mixture supplied was heated to about 65°C for about 40 minutes in one of the units of the food tray, then slowly cooled to ambient cabin temperatures. We estimate the cooling process took 5-10 hours, and the initial growth period was about 48 hours. After approximately 30 more days of growth time the can was opened and the resulting solid material was recovered.

The following list of materials was returned to the PI at UAT:

1. Film Serial SL4-520, Title-Skylab-4
   DAY004, TV-105
2. TV-105 Color Prints
   SL4-14604894 through 4896 and
   SL-148-5018 through 5020

3. 35 mm slides, H-02547-H

4. Voice record MC1706, MC1787-1, and MC1787-2

5. Rochelle salt crystal and wipes used to dry it after recovery.

The 16 mm film clip shows Col. Pogue beginning to heat the food can containing Rochelle salt and saturated solution. The color prints and the 35 mm slides show the food can during the experiment and the Rochelle salt crystal that was recovered.

4.2-3 Observations

A. Recovered Crystal - The recovered solid consists of three relatively large crystals whose weights are

the largest, Skylab I	8.73 grams
medium, Skylab II	2.82 grams
the smallest, Skylab III	0.52 grams.

In addition, 16 small crystals each of which is 2 mm on a side or less were obtained. Thus, the total weight is about 12 grams which is less than the expected weight of 30 grams. One possible explanation for this small amount of recovered product is that because of the lack of convection currents the dissolved Rochelle salt molecules reached the surface of the growing crystal very slowly, since the only transport process was diffusion. Thus, even after 30 days of growth time, the solution was still supersaturated. Supporting evidence for this explanation is the "slush" or "ice cream salt" the astronaut reported when he opened the food can to recover the crystal. This shows that the solution was still supersaturated when it was opened. We prefer this explanation to the following two explanations previously given in the Quick-look Report; that is, considerably high cabin temperature, and

accidental cooling of the Rochelle salt solution during transportation. Later evidence showed both these explanations to be improbable.

The crystal originally precipitated in the cabin is believed to be one single crystal, as was confirmed by photographs taken on board which became available to the PI after the Quick-look Report was submitted. Figure 35 shows the three crystals Skylab I-III assembled into one large crystal. Thus, most of the other small crystals, if not all of them, probably appeared when the big crystal was broken. The breaking of the large crystal probably occurred during re-entry or splash-down of the module.

The crystal grown on board Skylab-4 is actually a collection of at least five single crystals (see Fig. 36 and Fig. 37). One very unusual thing about this collection of crystals is that the a, b, and c crystal axes of all the component crystals are parallel or very nearly parallel to each other. The crystal axes are identified in Fig. 37A and 37B.

B. Macroscopic and Microscopic Defects - Most of the crystal has many defects and is not good optically, but some parts of the crystal are almost completely free of defects and appear extremely good optically.

Figure 38 shows microscope photographs of Skylab II and an earth-grown crystal for comparison. One can see that the cavities in the Skylab II crystal are highly regular compared to those in the earth-grown crystal. A typical length for a cavity in the Skylab II crystal was found to be 4 mm. The cavities shown in Fig. 38 have their long axes in the direction of the c-crystal axis. Almost all the defects in the crystals returned from Skylab-4 are small-diameter tubes elongated in this way. Such an extremely small diameter-to-length ratio is rarely found for cavities in earth-grown crystals.

Figure 35. Photograph of the TV 105 Crystal.

The upper photograph shows the three largest crystals of TV-105. The lower photograph shows the same crystals assembled into one body.

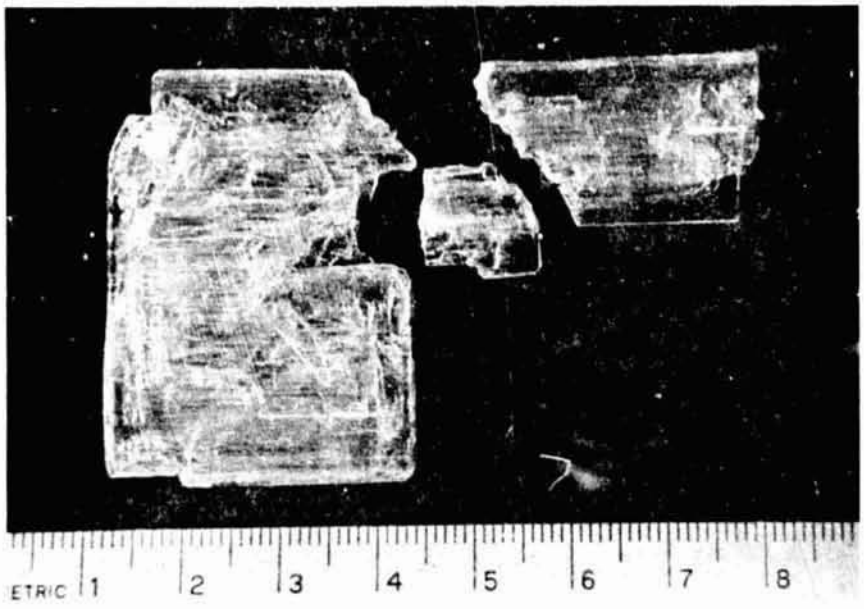

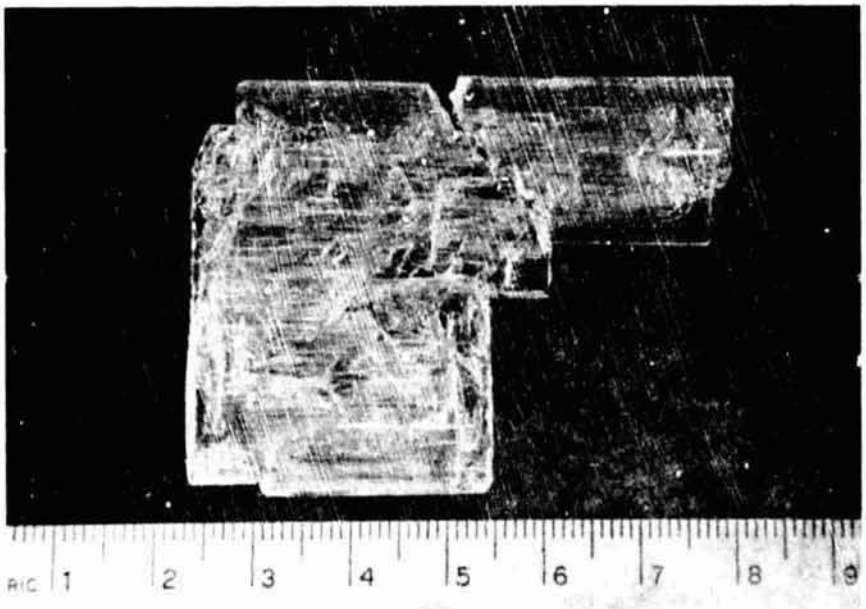

Figure 36. Photograph of the Second Largest Crystal, Skylab II. The c-axis, which is the fastest growth direction, is approximately perpendicular to the photograph plane.

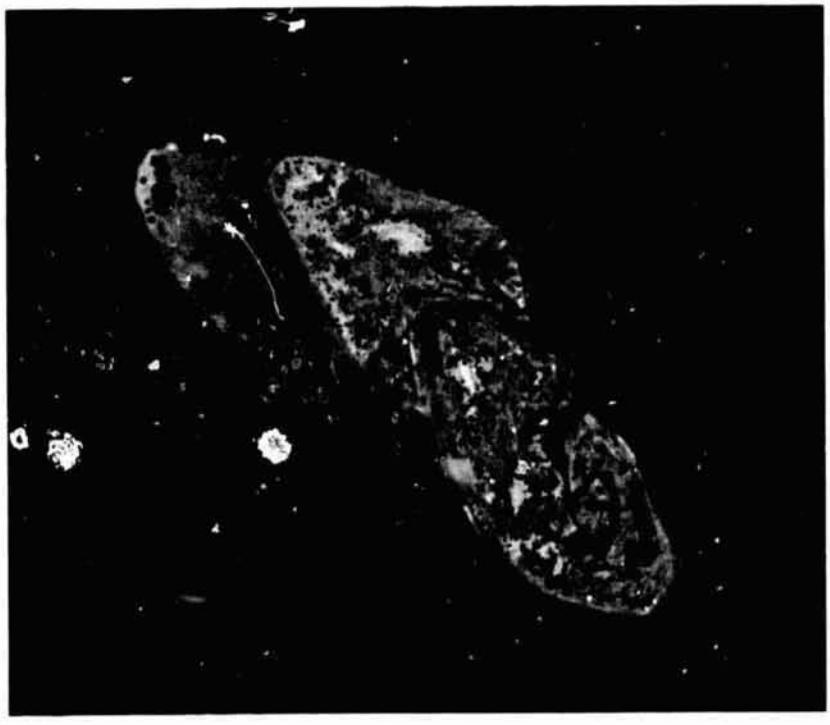

Figure 37. Illustrations of the Photographs.

(A) for the lower photograph in Fig. 35. (B) for the photograph in Fig. 36. Both illustrations show that the crystal consists of several single crystals; the crystal axes are also shown.

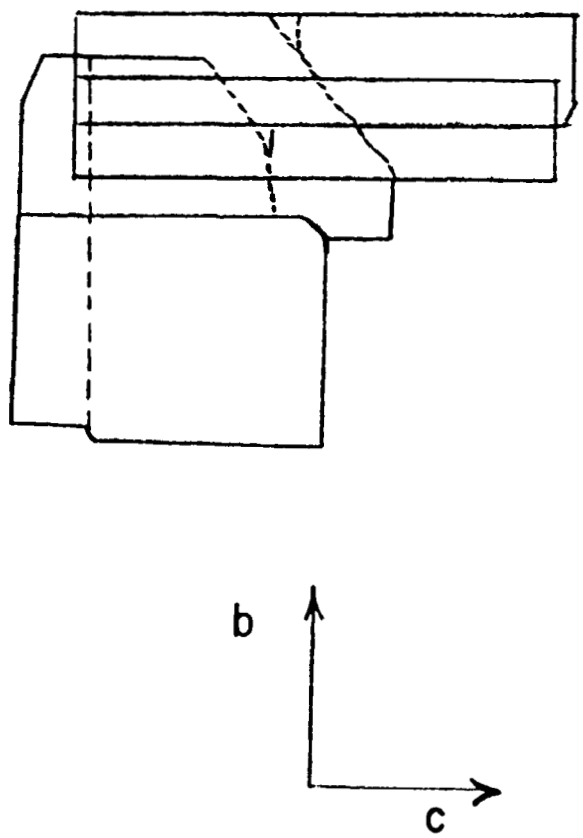

Figure 37 (A)

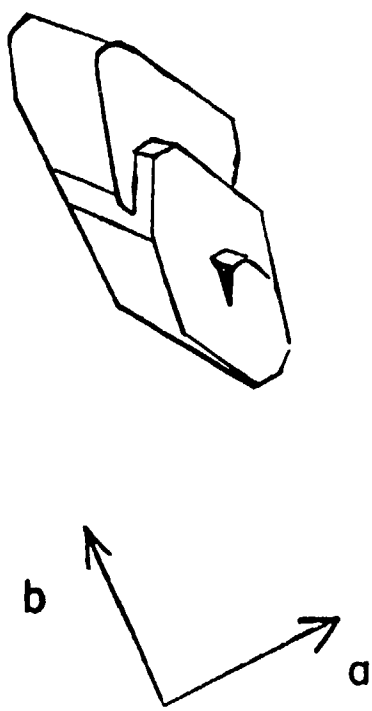

Figure 37 (B)

Figure 38. Microscope Photographs.

The lower photograph is from the Skylab II crystal. The upper one is from an earth-grown crystal. The magnification is approximately 125.

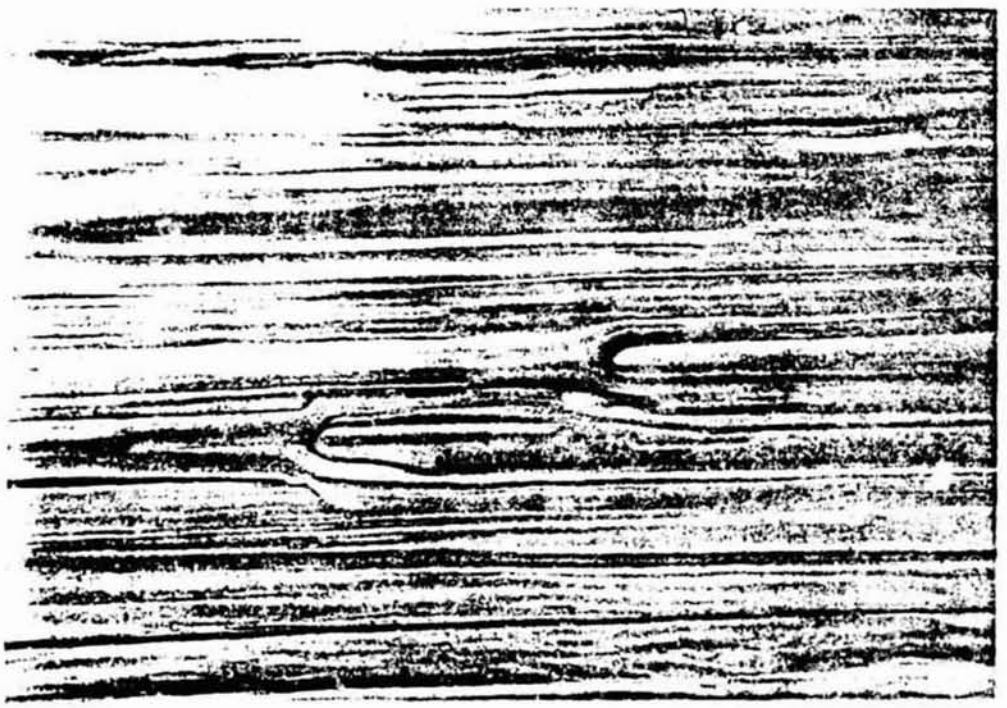

C. S-value for the Bulk Crystal - The crystal returned from Skylab-4 was found to be mechanically very fragile. Thus it was concluded that slicing it by any currently available technique would probably ruin this precious crystal. For this reason we attempted to observe the preliminary hysteresis curve of this sample without slicing it.

Several sets of electrodes were constructed and tested on earth-grown crystals of the same size and the most satisfactory results were obtained from the system shown in Fig. 39. Because of the high voltages necessary for this thickness (0.5 cm) of crystal, some of the circuit parameters in the original capacitance bridge were also changed (see section 2.1-3).

The hysteresis curve for TV-105 is given in the lower photograph of Fig. 40. The hysteresis curve for an earth-grown crystal of about the same size and thickness is shown in the upper photograph of Fig. 40, for comparison. The S-value was calculated from these curves to be 2.69 for the earth-grown crystal and 1.36 for the Skylab crystal.

The S-value, which has been defined previously,[8] is one factor which characterizes ferroelectric quality. High S-values usually indicate uniform domain structure and hence better ferroelectric qualities. The low S-value observed for the Skylab crystal seems to indicate "poor" ferroelectric quality. However, we believe that this conclusion is premature for the following reason; we used the bulk crystal for the hysteresis measurement and it has many empty microscopic cavities as is shown in Fig. 38. It is probable that even if the domain structure were uniform, the presence of many microscopic cavities would lower the S-value, as will be explained in part 4.5 of this report.

Figure 39. System for Hysteresis Observation.

The crystal is held in place on the thermometer bulb with modeling clay. The wire electrodes are attached to the crystal surface by conductive silver paint.

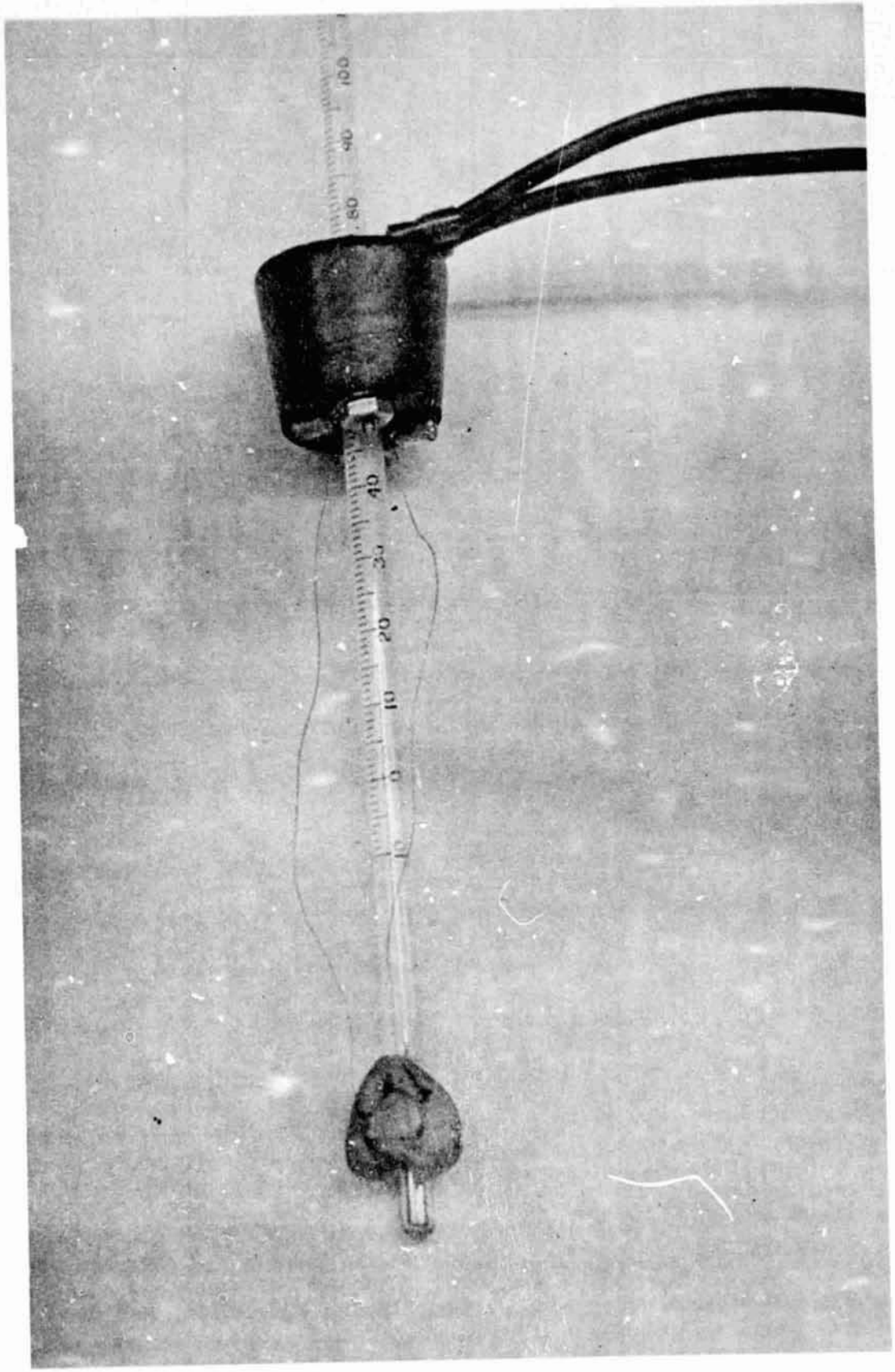

Figure 40. Hysteresis Curves.

The upper curve is from a large good-quality earth-grown crystal. The lower one is from Skylab Crystal II.

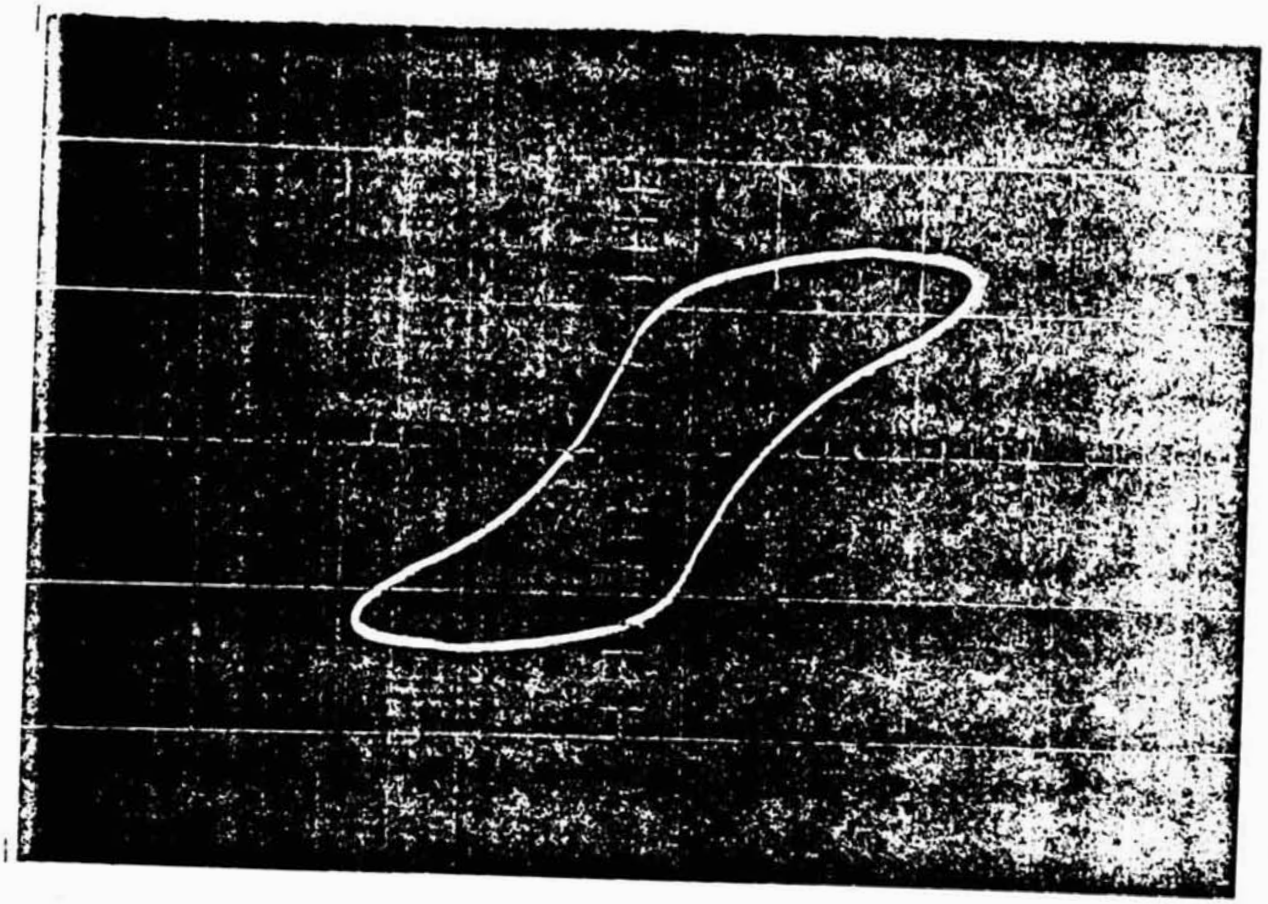

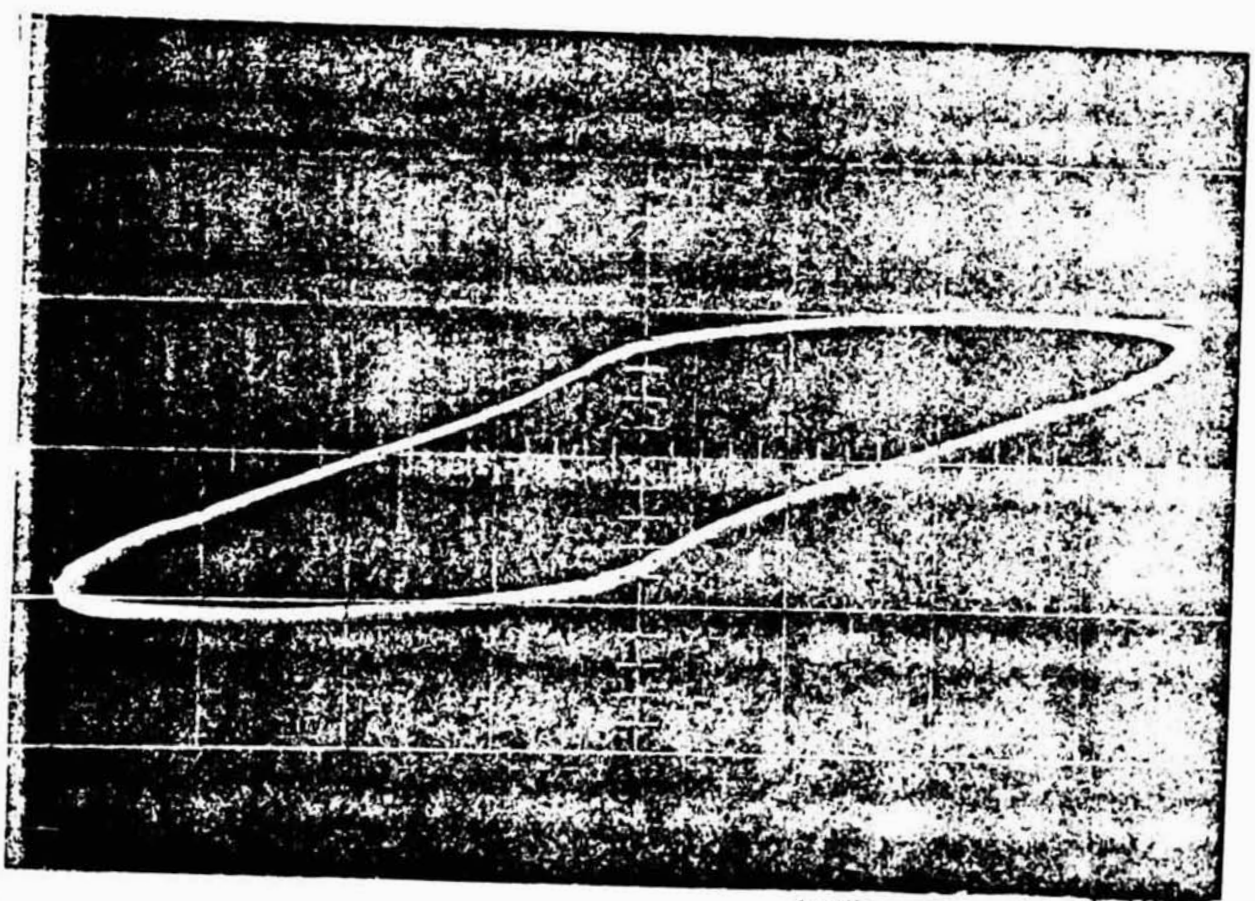

D. S-value for a Chip - The apparatus used for measuring the S-value of the Skylab bulk crystal is given in part C of this section. A small chip from Skylab Crystal I was also used to measure the hysteresis of a part of the crystal. The chip was broken from the larger crystal sometime before it was returned to our lab. The orientation of its a axis, which must be determined in order to observe the hysteresis curve of the sample, was apparent from the way the chip fit back into the large crystal.

The hysteresis curve for the chip is shown in Fig. 41. The S-value calculated from this curve is 2.44. This number is larger than 1.36 which is the S-value reported for the bulk Skylab sample. Microscopic examination of the chip showed there were fewer cavities per unit volume than in the bulk sample. This is in agreement with our previous result that the S-value of a sample containing many cavities would appear to be low, even if the quality of the sample is excellent.

E. Hysteresis from a Sliced Sample - Since the crystal recovered from Skylab-4 was so fragile, it was necessary to develop special slicing techniques in order to get a sample whose ferroelectric hysteresis curve can be measured. Many techniques were investigated using fragile earth-grown crystals and it was decided that the most efficient method was to use a water-impreganted cotton string to cut the crystal. Experience showed that some sort of control over the cutting rate was also necessary.

It was decided to modify an already existing commerical crystal saw to use our wet-string cutting technique. Control over the cutting rate was provided by a small motor on the end of the cutting arm. A photograph of the modified wet-string crystal saw is shown in Fig. 42. With this technique

Figure 41. Ferroelectric Hysteresis from the Skylab Crystal.

Hysteresis curve of a small chip broken from Skylab Crystal I. The S-value calculated from this curve is 2.46.

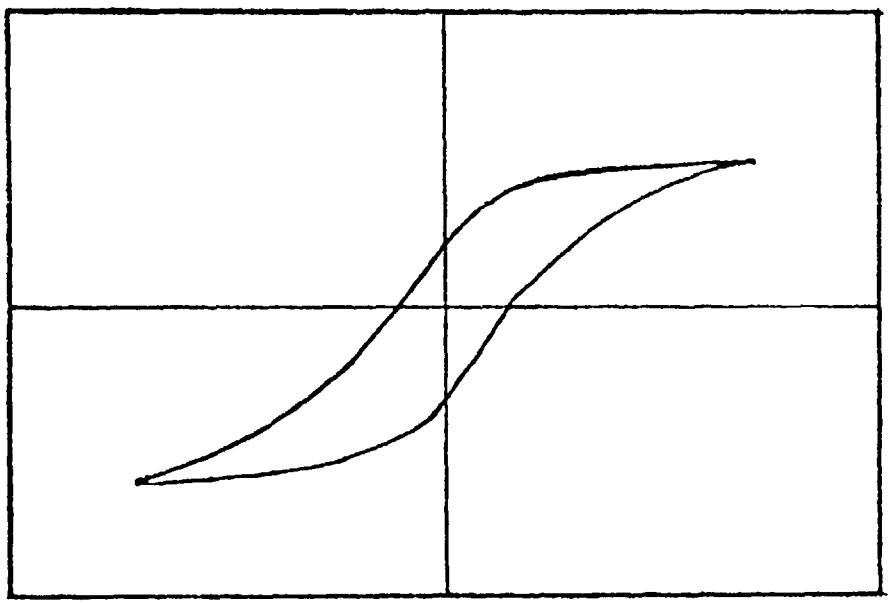

Figure 42. Photograph of the Modified Crystal Saw.

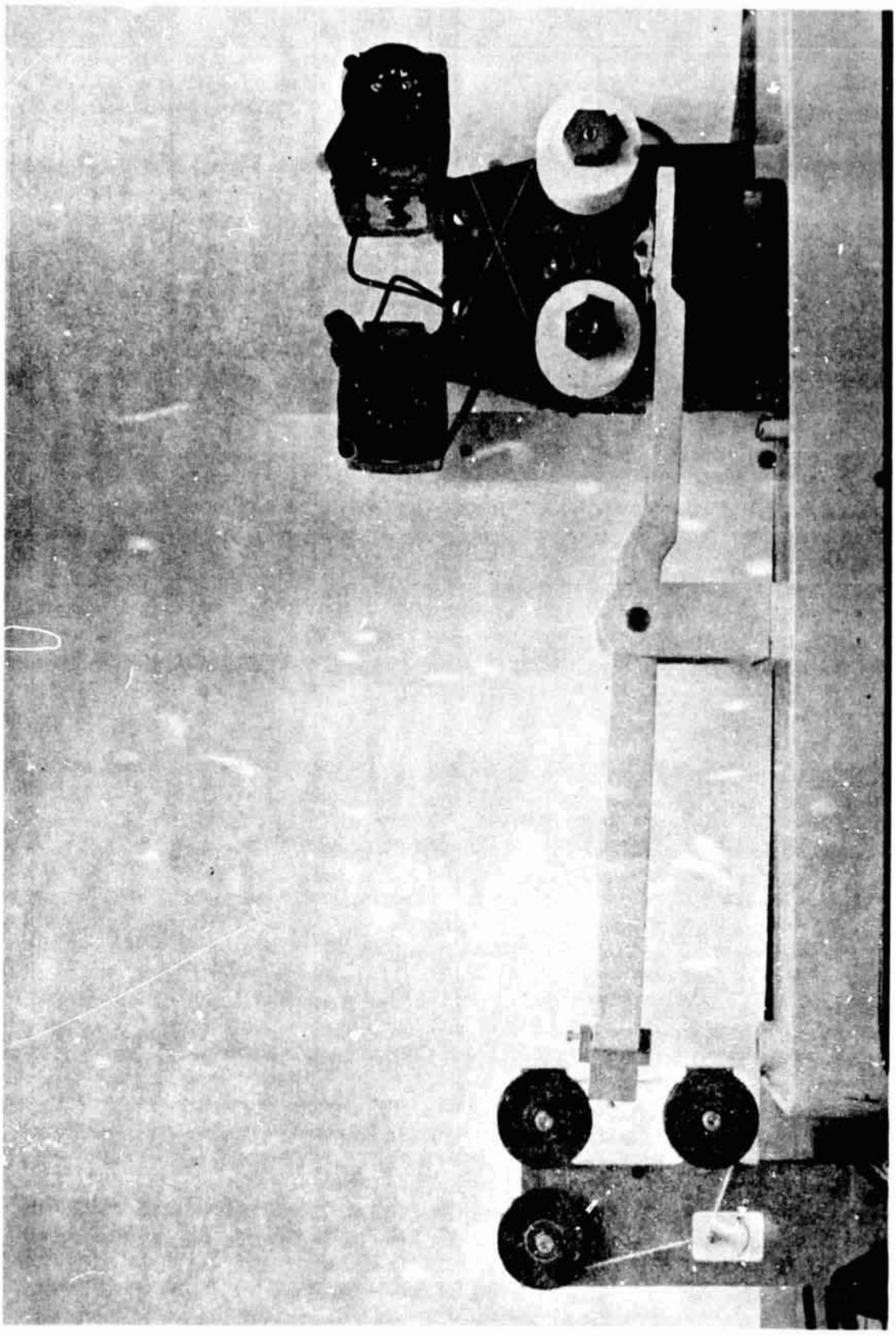

it was possible to safely cut slices as thin as 0.5 mm with a kerf loss of about 0.5 mm. The optimum cutting rate for a very fragile crystal of Rochelle salt was about 0.5 cm/hr. Rubber cement was used to attach the crystal to the glass plate on the cutting arm.

We decided to take advantage of the way in which Skylab Crystal II had grown to cut our first slice from the Skylab crystal; that is, there was a natural projection on the end whose crystal axes could easily be determined. Figure 43 shows Skylab Crystal II immediately after the first cut was made. Figure 44 shows the slice resulting from the first cut and the arrangement of the defects present.

In order to observe the ferroelectric hysteresis curve of the slice shown in Fig. 44, it must be cut again in such a way that electrodes may be placed approximately perpendicular to the a crystal axis. Because of the way certain defects in the slice were arranged it was decided to make the second cut about 20° from the a-perpendicular direction. This procedure was first tried on several earth-grown Rochelle salt crystals, and did not significantly degrade the resulting hysteresis curve. Figure 45 shows the direction of the second cut.

The final cutting resulted in a 1 mm thick sample for hysteresis osbervation. The results of the measurement are shown in Fig. 46. S-values of this sample are compared to the other measurements we have made on this crystal in Table IV.

Figure 43. Skylab Crystal II.

Skylab Crystal II is shown attached to the glass plate for cutting. The cut from the wet string is visible on the right side of the crystal near the end. The slice resulting from this first cut is about 1.5 mm thick.

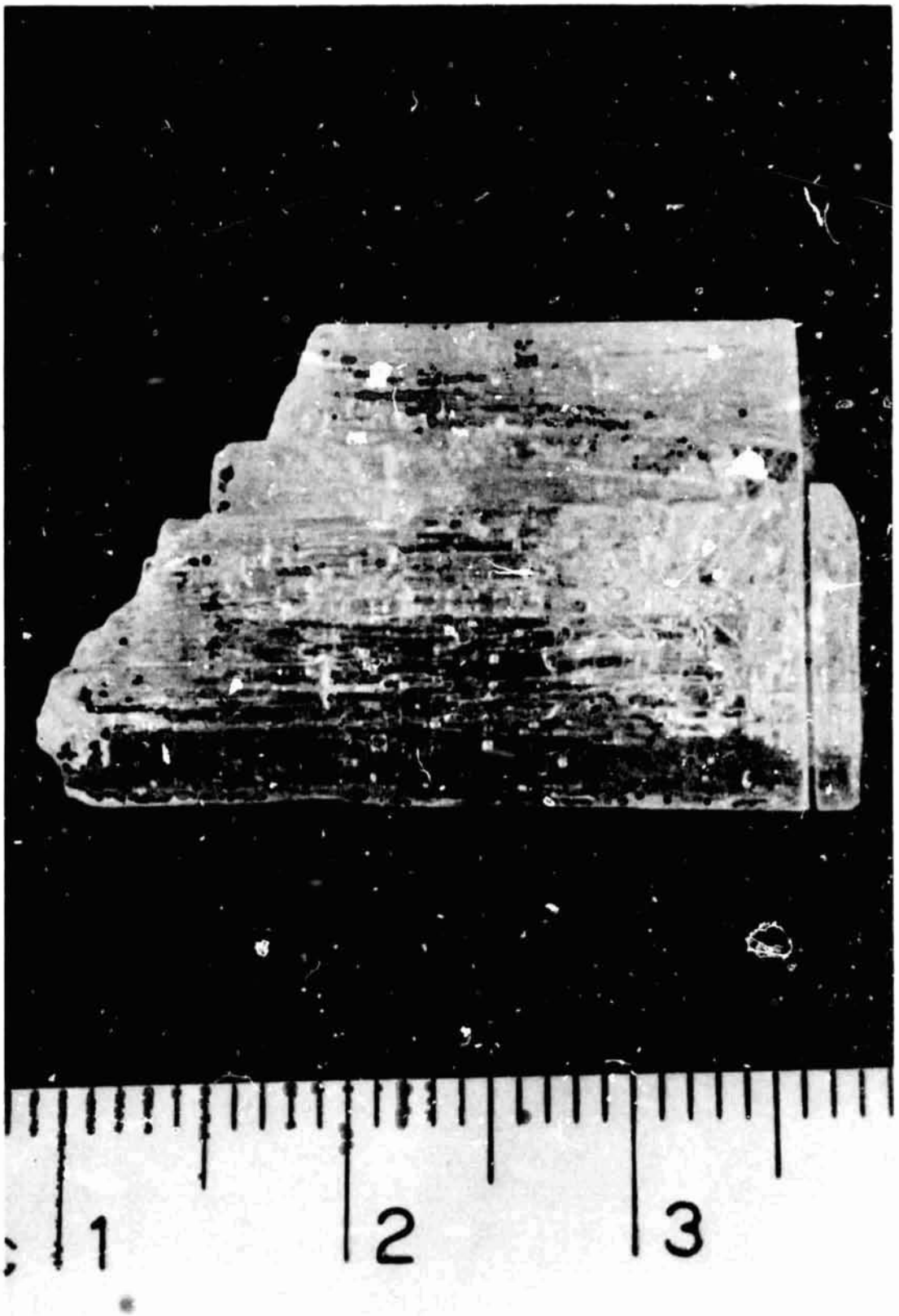

Figure 44. Slice from Skylab Crystal II.

Cross section of the slice resulting from the first cut. The arrangement of defects made it necessary to make the second cut near one edge (see Fig. 45). In this way a fairly good sample was obtained for hysteresis observation.

Figure 45. Slice from Skylab Crystal II for Hysteresis Measurement.

The slice in Fig. 44 was cut in the direction shown in order to get a slice for hysteresis measurement. Usually Rochelle salt crystals are sliced perpendicular to the a crystal axis, but in this case defects in the crystal would not permit slicing in that direction.

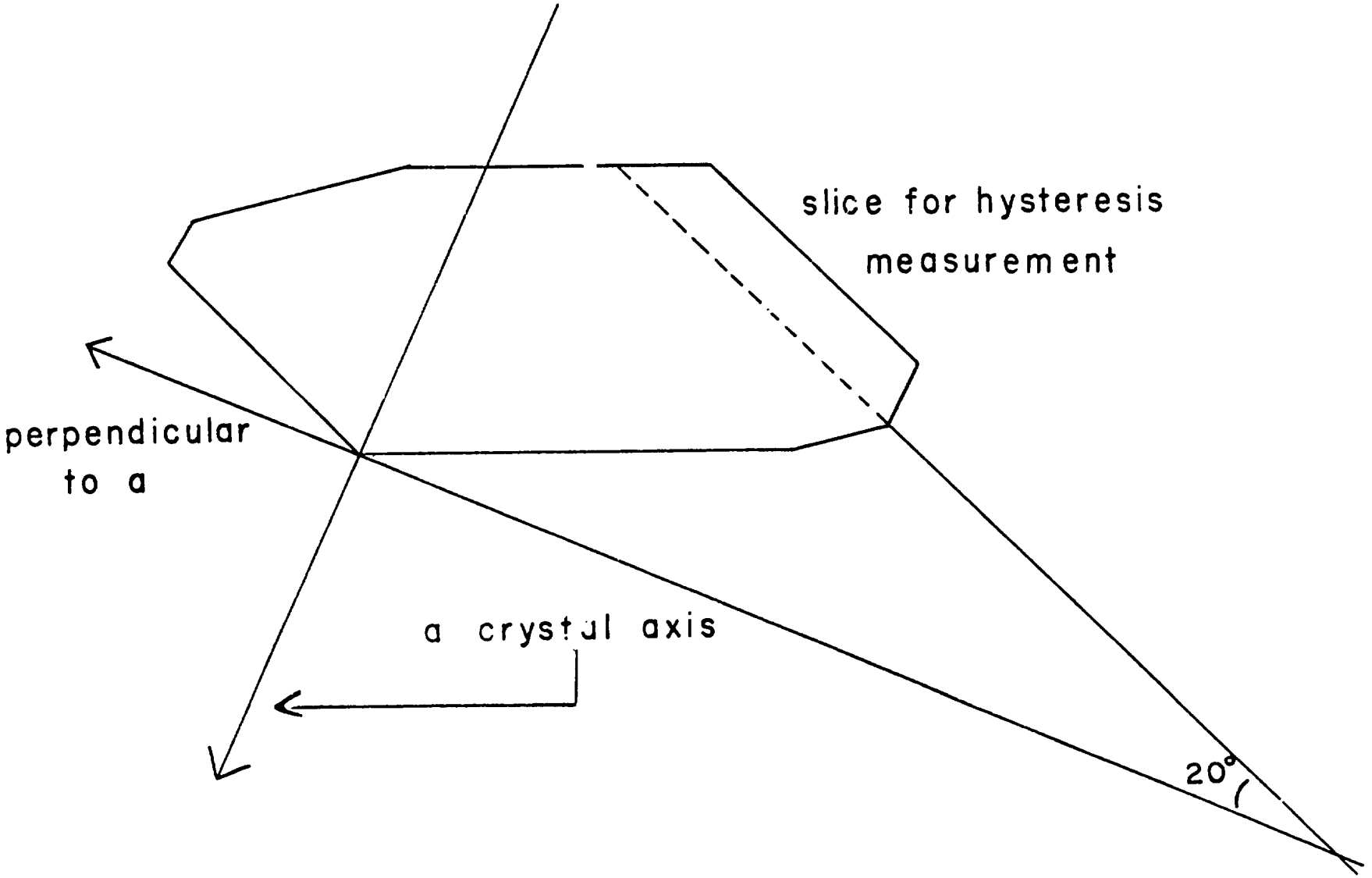
slice for hysteresis
measurement
perpendicular
to a
a crystal axis
20°

Figure 46. Ferroelectric Hysteresis Curve of the Slice from Skylab Crystal II.

The sample shown in Fig. 38 was painted with silver conducting paint and cooled to 5°C. The hysteresis curve was recorded and the S-value calculated to be 4.05.

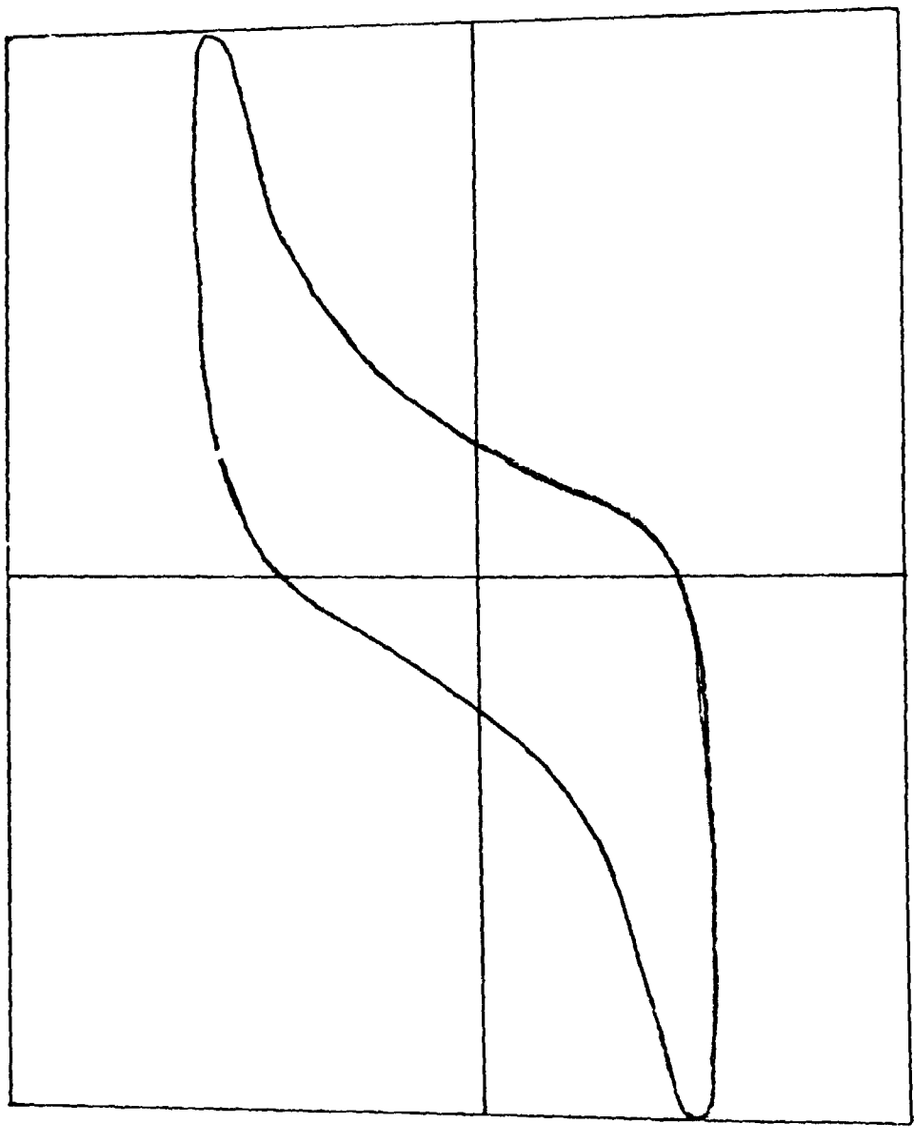

Table IV. S-Values From Skylab Crystal II.

Skylab Crystal II	S-value
Bulk sample	1.36
Small chip	2.44
Sliced sample	4.05

4.3 Growth Study of L-Alanine Doped Triglycine Sulphate

4.3-1 Introduction

Infrared detectors are important in many applications, including those for the space program; for example, missile launch detectors, infrared telescopes, "Explorer"-type satellite heat detectors, and weapons guidance systems.[17] Recently British workers[13,17,18] have discovered that L-alanine doped triglycine sulphate (TGS) has potentially excellent qualities as a detector material. However, the highly doped material has not yet been produced. Moreover, the dopant concentration of the product is not uniform, that is, the dopant concentration differs from one product to another.

In the case of copper dopant in Rochelle salt crystals we can control the dopant concentration by controlling the growth rate. Also we have shown that high dopant concentrations can be achieved with high growth rates.[14] This result should be applied to the case of L-alanine doped triglycine sulphate (TGS) in order to grow a highly doped crystal. It was also shown, however, that high growth rates induced microscopic cavities which degrade the electrical and optical properties of the resulting crystals.[14] To avoid this problem we suggested a technique in which the crystal is grown under vacuum conditions (see part 3.4-1 of this report). This technique was actually applied during the present contract period.

4.3-2 Experimental Technique

The new technique is based on the following facts:

Our past investigations have shown that microscopic cavities in crystals grown from solutions often arise from trapped air bubbles of microscopic size.[14] The fact that these microscopic air bubbles most probably originate

from dissolved air in the growth solution has suggested a new technique of solution crystal growth; crystal growth under vacuum conditions. Under these conditions most of the dissolved air in the growth solution is removed by reducing the pressure on the solution from 15 psi (normal atmospheric pressure) to less than 1 psi. Thus only a small number of cavities should appear in the resulting crystal even for the case of high growth rates. This technique should be useful for doping. While doping concentration increases with increasing growth rate of the crystal, high growth rates inevitably induce cavities from the air dissolved in solution under atmospheric pressure. In the case of growth under vacuum conditions, however, it should be possible to obtain high doping concentrations by growing the crystal at a high rate without inducing many cavities in the crystal. This technique was applied to growth of TGS crystals in the present project.

4.3-3 Results and Analysis

The experimental apparatus used for this experiment is the same as that reported in a previous work (see part 3.4-1 of this report). A solution containing 11.4 grams of TGS, 4 grams of L-alanine, and 20 cc of distilled water was introduced into the glassware and a seed crystal was added. The glassware was then capped, connected to a vacuum system, and the water in solution was evaporated until its volume decreased by 5 cc. Afterwards the rubber tubing was clamped and the vacuum system disconnected.

This procedure removed most of the dissolved air in solution. Now the solution was ready for crystal growth. After several hours of preliminary slow growth, the temperature of the bath was cooled rapidly by circulating cold water. Then the crystal started to grow as fast as 10 mm/day. After

several more hours of this fast growth the crystal was removed and examined. Fig. 47 shows the time vs. temperature curve for one such experiment.

A microscopic examination was performed and showed that the number of microscopic cavities, both empty and solution-holding, was relatively small despite the high growth rate. An amino acid analysis was performed with the help of a Beckman 119 Amino Acid Analyzer. The results are shown in Fig. 48. The alanine peak is weak, but definitely visible. Analysis of the intensities indicated that the crystal contained L-alanine in concentrations between 2% and 4%. The highest previously reported concentration is 2%.[13] It is also noted that this vacuum growth technique makes it possible to obtain higher doping concentrations consistently.

A preliminary hysteresis study of the doped crystals was also performed. The hysteresis curve of crystal AlTGS #14 is compared to an undoped TGS sample in Fig. 49. The hysteresis loop of the undoped sample is centered around the origin, as expected for a material with no internal polarizing field. The alanine-doped crystal still shows a hysteresis loop, but the presence of the L-alanine in the doped crystal sets up an internal polarizing field. The hysteresis loop is centered on this internal polarizing field rather than on the origin as is the case for pure TGS. The biasing voltage for the doped sample in Fig. 49 was about 3480 volts/cm. The sample was about 1 mm thick.

The results of this preliminary analysis are difficult to compare to other works.[10] Probably a reasonable comparison can be made by measuring L/d, the ratio of the biasing field to the width of the hysteresis loop (see Fig. 50). We found 1.1 for L/d from the result reported by Lock,[10] while the analysis of our hysteresis curves gives values of 2.0 for this number.

Figure 47. Time vs. Temperature Profile.

Typical cooling curve for growing TGS crystals doped with L-alanine.

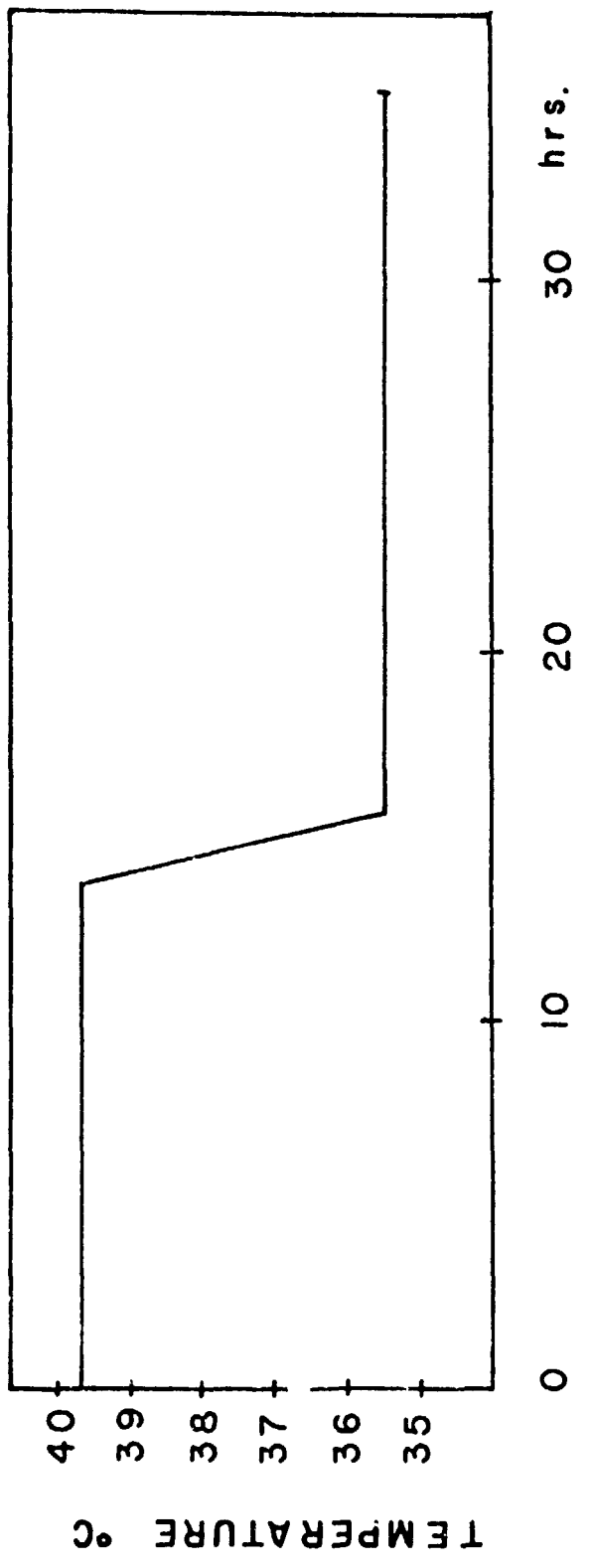

FIGURE47 TIME vs. TEMPERATURE

Figure 48. Amino Acid Spectrum.

The amino acid analysis of the L-alanine doped TGS crystal grown in experiment AlTGS #14 is shown in the figure. The glycine peak strength in this spectrum is shown off scale so that the smaller alanine peak on the right is visible. Analysis of the intensities of these curves indicated that the TGS crystal had an L-alanine doping concentration of 2% or more.

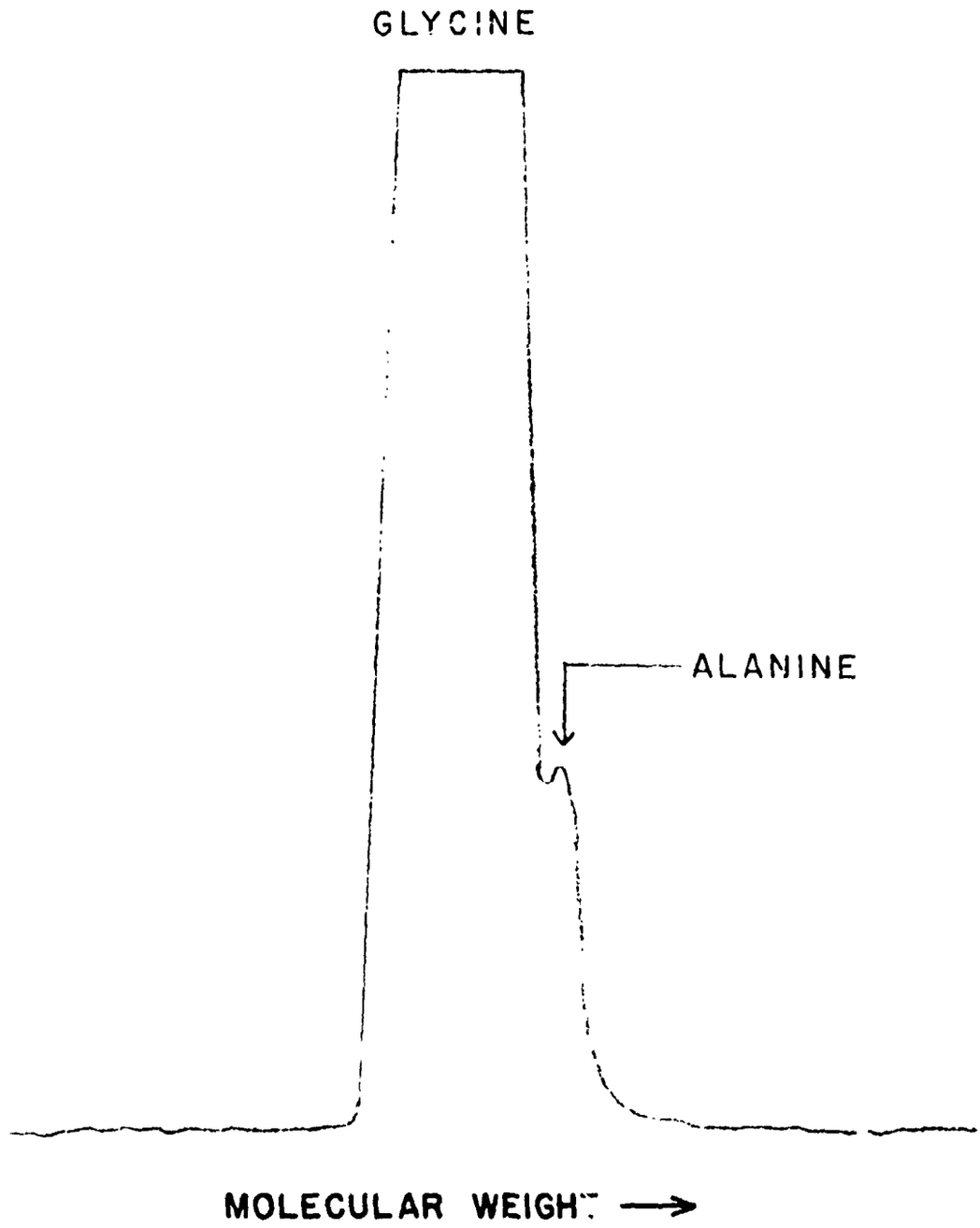
GLYCINE
ALANINE
MOLECULAR WEIGHT →

Figure 49. Hysteresis Study.

The top curve is a .al hysteresis loop of a pure TGS crystal about 1 mm thick. The loop is centered on the origin or zero volts. The bottom curve is the hysteresis loop of a 1 mm slice of crystal AlTGS #14. The loop is centered around 3480 volts.

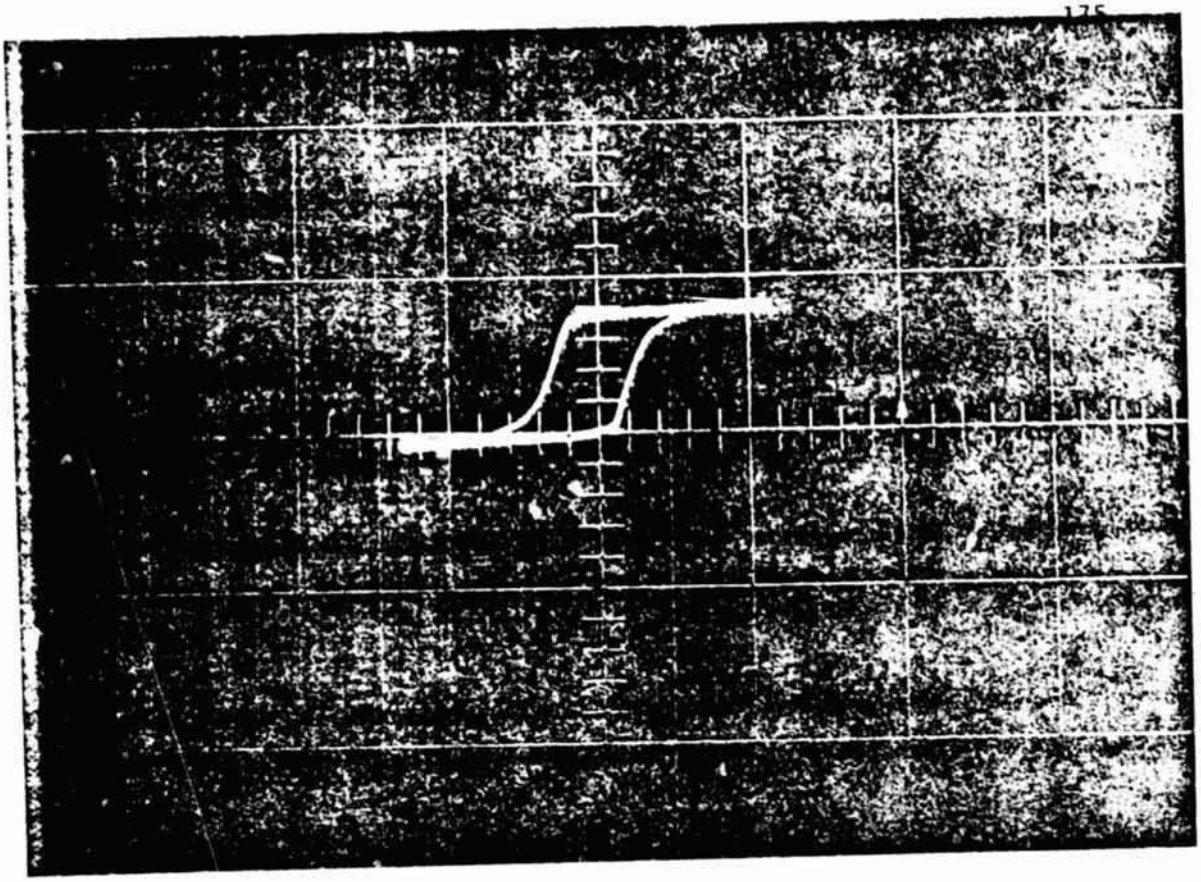

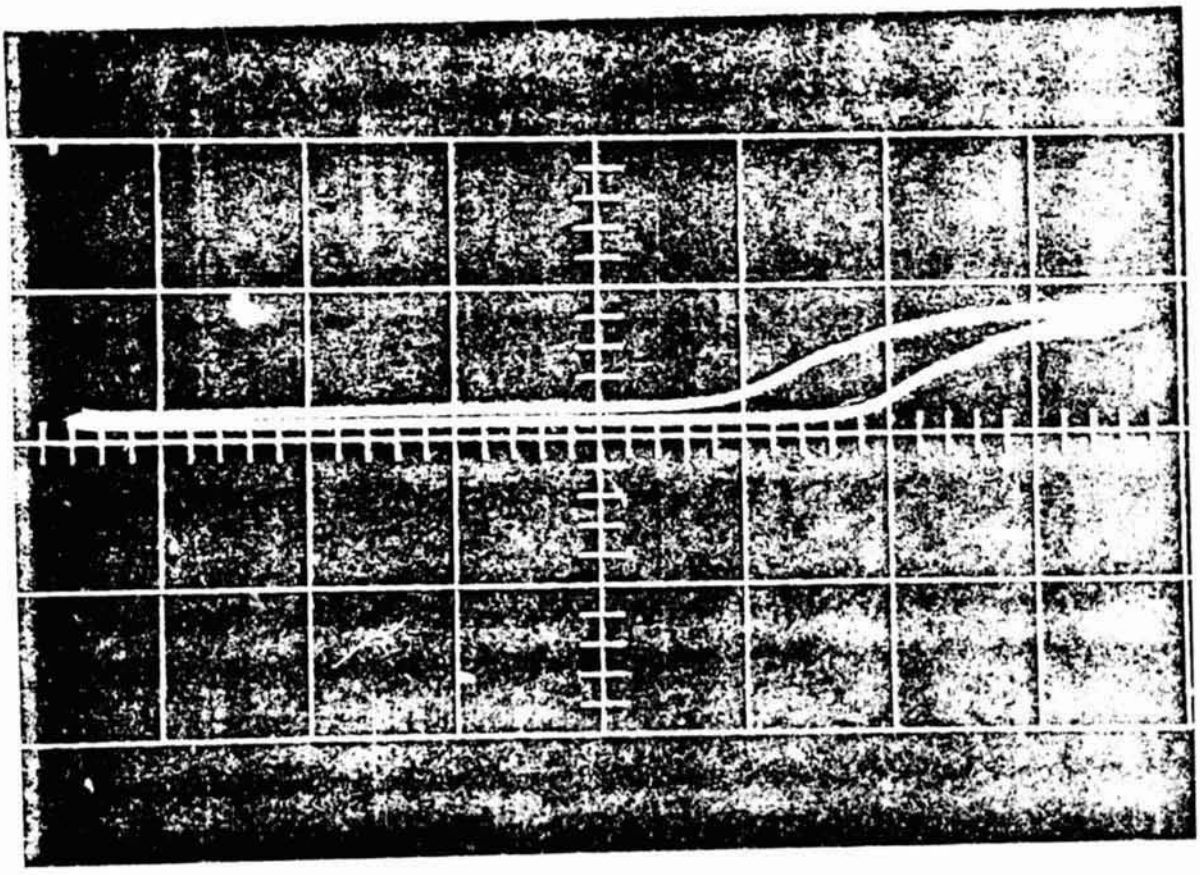

Figure 50. L/d.

The quantity L/d, the ratio of the internal biasing field to the width of the hysteresis loop is defined. This number can be compared to the results of hysteresis studies done by other workers.[16]

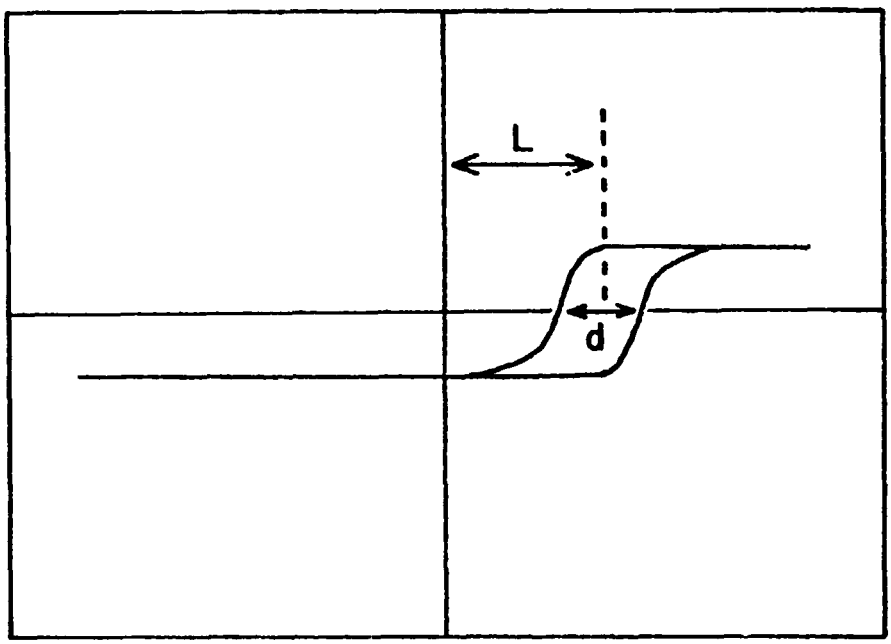
L
d

4.3-4 Conclusions

The preliminary results lead us to conclude that the new technique allows us to grow TGS with consistently high concentrations of L-alanine dopant.

4.4 Laser Illuminated Study of Convection Currents

4.4-1 Introduction

Our experience has shown that the difficulty in accurately observing convection currents during solution crystal growth is mainly due to poor illumination. That is, it is very hard to light up the growth solution in such a way as to make the convection currents visible. It is even more difficult to supply proper lighting for photographing convection currents, and photographs are the most practical and convenient way to make a permanent record of a crystal's growth. For these reasons, we have attempted to improve our ability to make convection currents visible, both to the unaided eye, and for purposes of photographic measurements.

4.4-2 Description of the Experiment

The equipment for these preliminary studies was as follows: one Helium-Neon Laser (from Spectra Physics), 0.5 mW minimum and 1.0 mW maximum output, beam diameter 0.88 mm; one diverging lens, focal length -8 mm; one slit, 1.2 cm wide; one projector screen; and a temperature bath with stand, crystal growth vial and heating and cooling equipment which has been described before.[14] A diagram of the equipment is shown in Fig. 51.

The parallel beam from the laser goes through the first lens and becomes slightly divergent. The wide slit then is adjusted so that a beam of light

Figure 51. Diagram of the Laser Illumination Apparatus.

A laser beam passes through the diverging lens and falls on the slit. This beam of light enters the temperature bath where it is focused by the crystal vial. The light emerging from the vial leaves the temperature bath and falls on the projection screen. Photographs were taken of the image of the growing crystal and surrounding solution that is formed on the screen.

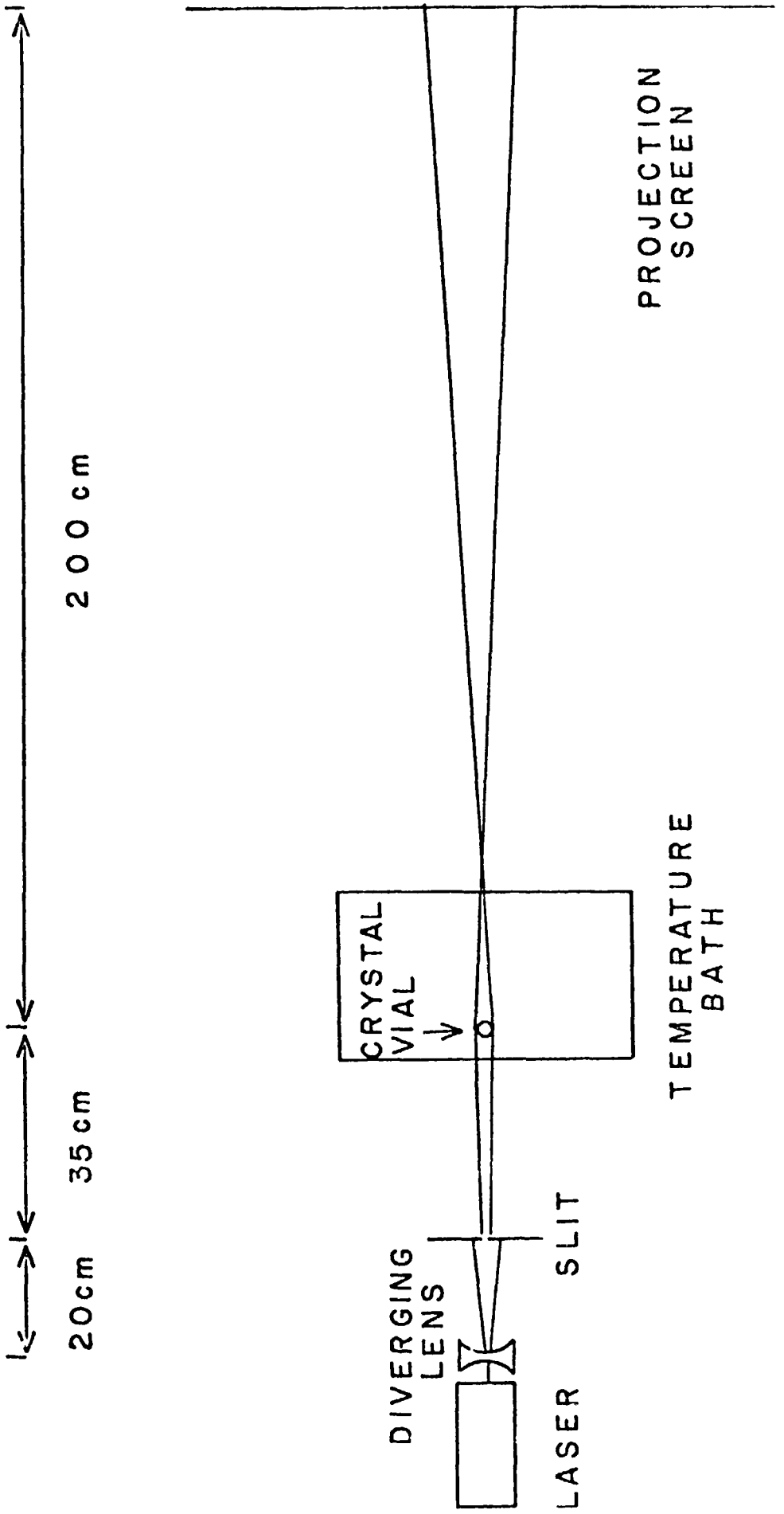
200 cm
35 cm
20cm
PROJECTION SCREEN
CRYSTAL VIAL
TEMPERATURE BATH
DIVERGING LENS
SLIT
LASER

approximately the same diameter as the vial is allowed to shine into the temperature bath. The cylindrical crystal growth vial, filled with solution, acts like a converging lens and brings the beam to a focus just outside the temperature bath. This image is allowed to fall on a screen two meters away. Since the crystal in the growth vial blocks the path of the laser beam, the shape of the crystal appears as a shadow in the image formed by this system. The string that was used to support the crystal also appears as a shadow.

Small changes in the density of the solution near the crystal due to its growth or dissolution will cause a change in the index of refraction in this neighborhood. For this reason, a small region of the growth solution which has fewer Rochelle salt molecules will refract light differently than the surrounding more dense solution. Since convection currents are often regions of the growth solution that have been depleted of dissolved material by the crystal's growth, they should refract the laser beam differently than the richer, more dense regions of the growth solution. This effect should make them visible as either lighter or darker regions against a gray background surrounding the growing crystal.

The procedure for these experiments was as follows:

About 20 cc of a Rochelle salt solution saturated at room temperature was heated to dissolve five more grams of Rochelle salt. This warm solution was transferred to a temperature bath at room temperature and a seed crystal on a string was lowered into the cooler. Photographs were taken while the seed crystal and solution cooled to saturattion temperature and began to grow. The results are shown in Fig. 52.

Figure 52. Photographs of a Rochelle Salt Crystal and Growth Solution.

(A) Crystal Dissolving

(B) Saturation Conditions

(C) Beginning Growth

(D) Steady-State Growth

The oblong horizontal shadow is the Rochelle salt crystal, and the vertical shadow is the supporting string.

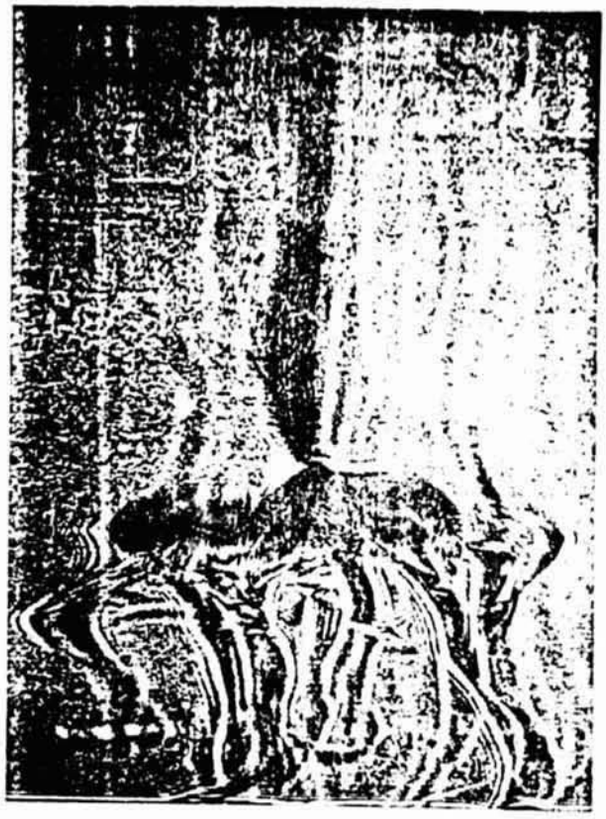

(A)

(B)

(C)

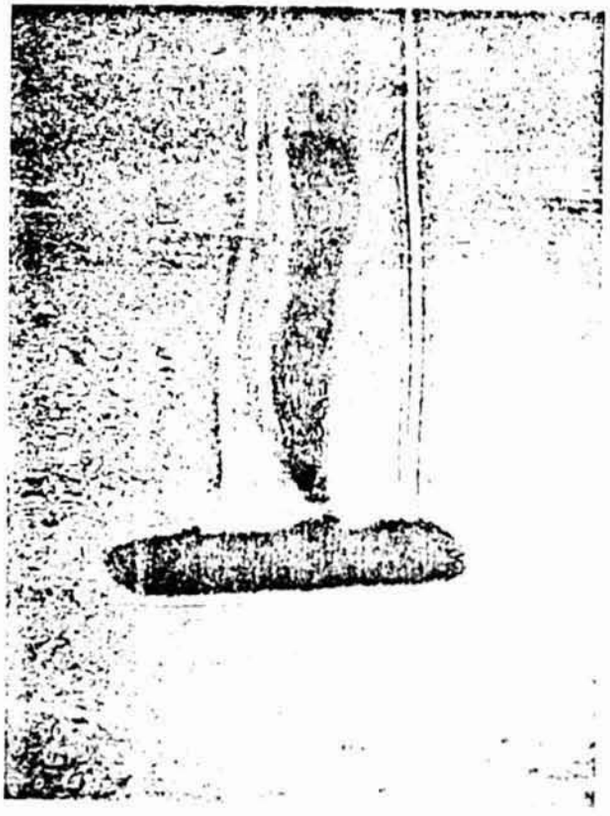

(D)

4.4-3 Results

Figure 52 (A) shows the crystal shortly after it was lowered into the warm growth solution. The seed is dissolving, making the solution nearby richer in dissolved Rochelle salt. Being heavier than the surrounding solution, these regions of solution close to the crystal tend to fall under the influence of gravity. These downward-moving convection currents can be seen as darker areas in the solution below the shadow of the crystal in Fig. 52 (A). About two minutes later the solution had cooled several degrees and the vigorous downward-moving convection currents had almost stopped. Figure 52 (B) shows a picture taken at this time when the system is close to saturation conditions. There are few remaining downward currents and the beginnings of other motion at the top surface of the crystal is visible here. These small movements in the solution at the top of the crystal grew in size and then began to lift away from the crystal surface. Figure 52 (C) shows two of these upward-going convection currents shortly after they were formed. These convection currents are lighter than the surrounding solution because the crystal is now growing and depleting the dissolved Rochelle salt material in the region around it. This depleted region is thus lighter and tends to rise up and away from the growing crystal.

If these currents are allowed to continue undisturbed they will become almost straight lines going from the crystal to the top of the growth solution. Figure 52 (D) shows our system after about five minutes of steady growth. The two straight bright areas are the convection currents present in this steady-state growth condition. These currents continued until saturation was reached and then disappeared. In principle it is possible to observe

convection currents such as shown in Fig. 52 with very simple optical arrangements and the unaided eye, but in practice only very strong convection currents in limited areas of the growth solution could be detected. As Fig. 52 shows our technique of laser illumination greatly improves the sensitivity of observation by enhancing the contrast and widening the region of observation to include the entire growth solution.

4.5 Theory of the Ferroelectric Hysteresis Curve

4.5-1 Introduction

Measurement of the ferroelectric hysteresis curves for samples of solution-grown Rochelle salt is one convenient way to assign a quantitative measure to a crystal's "quality". The S-value, defined in a previous work,[14] is a number with which we may compare the quality of two crystals, at least with respect to their response to an applied electric field. This quantitative measure of crystal excellence is thus a way one may also compare the success of different techniques for solution crystal growth. That is, we may measure the ferroelectric hysteresis curves of Rochelle salt crystals grown under different conditions and compare their quality by comparing their S-values. It should be remembered, however, that S-value comparisons are only one measure of a crystal's excellence. Other measurements, such as the number and character of microscopic defects per unit volume, electrical conductivity, and amount of dopant present may be more valuable in some cases. In general the definition of crystal quality depends very much on the particular use that the crystal of interest may have.

Because ferroelectric hysteresis measurements are one common way of comparing crystal quality, it would be convenient to have some theory which directly relates the shape of the ferroelectric hysteresis curve to some observable parameter of the crystal or to some influence during its growth. For this reason we have developed the following theory which predicts the shape of a crystal's hysteresis curve as a function of the number of defects or voids per unit volume.

4.5-2 Theory and Calculations

Let us being by considering the simple case of two parallel plate capacitors such as those shown in Fig. 53; both have the same plate area A and the same plate spacing d. One is completely filled with a dielectric material whose dielectric constant is κ, while the other is filled with the same material but has a gap in the center. We would like to calculate the electric field inside the dielectric of the partially filled capacitor and compare it to the field in the completely filled case. For purposes of calculation let us divide the partially filled capacitor into three capacitors, each having 1/3 the spacing of the completely filled capacitor. Referring to Fig. 54, we will calculate the value of the electric field E_1 ($=E_3$). The capacitance of the filled capacitor is given by

$$C_o = \frac{\kappa \varepsilon_o A}{d} .$$

For the capacitance of the three series capacitors, we have

$$C_1 = \frac{\kappa \varepsilon_o A}{d/3} = 3 C_o ,$$

Figure 53. Illustration of a Capacitor with a Gap.

Two identical capacitors, one completely filled with a dielectric and the other having a gap in the dielectric material.

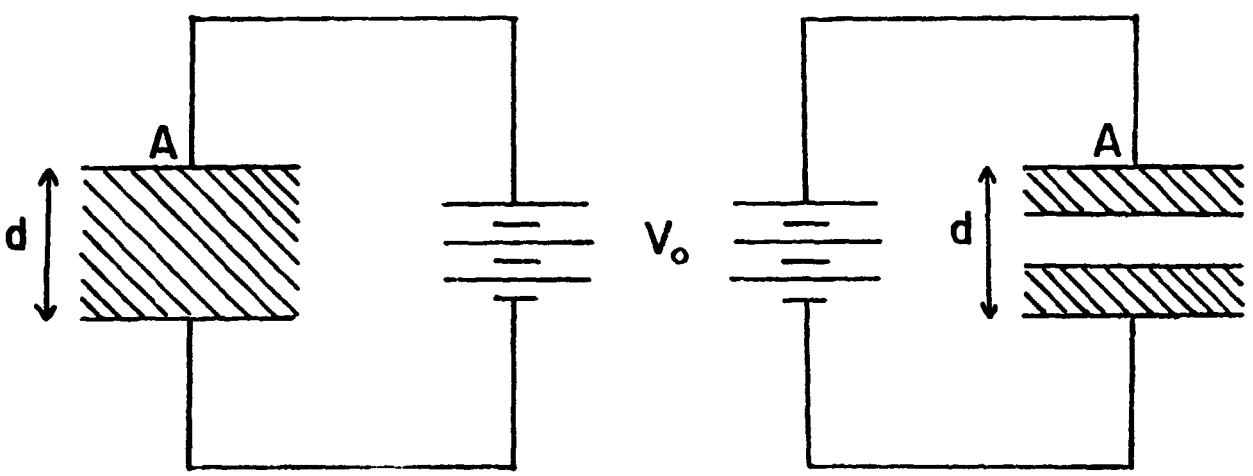

C3

Figure 54. Details of the Circuit in Fig. 53.

The circuit shown in this figure is identical to that shown in Fig. 53, but the details of the partially filled capacitor are given more clearly.

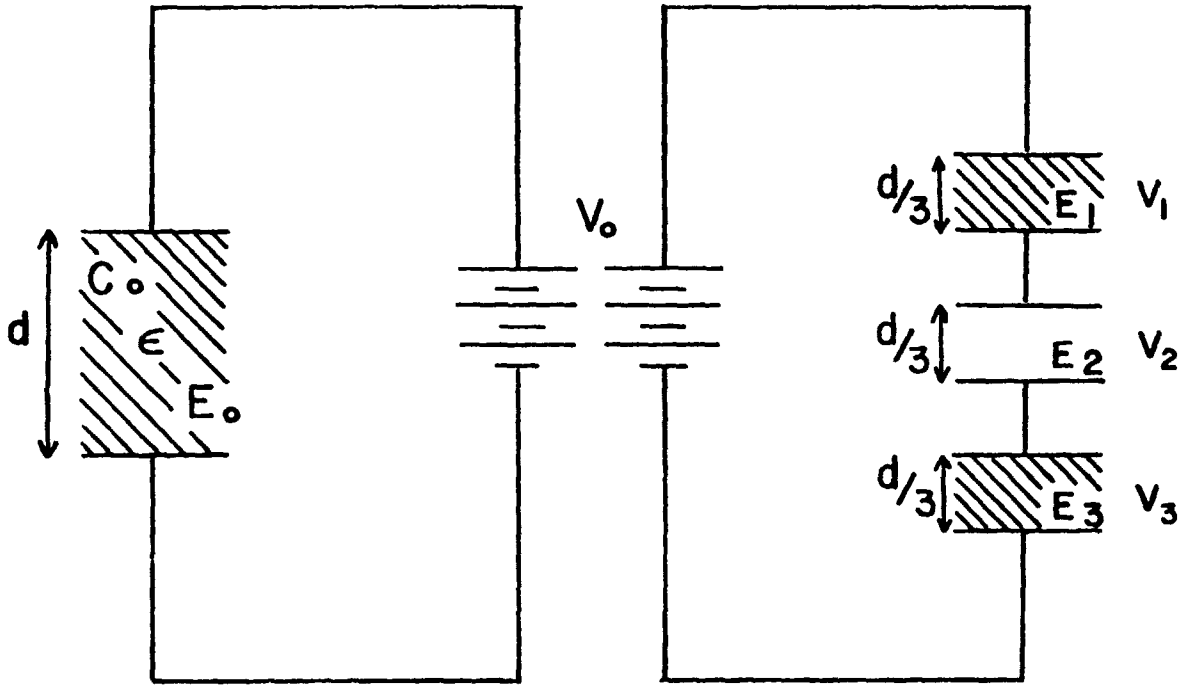
d
C₀
ε
E₀
V₀
d/3
E₁
V₁
d/3
E₂
V₂
d/3
E₃
V₃

$$C_2 = \frac{\varepsilon_o A}{d/3} = \left(\frac{3}{\kappa}\right) C_o,$$

$$C_3 = \frac{\kappa \varepsilon_o A}{d/3} = 3 C_o.$$

Thus, for the total capacitance, we have

$$\frac{1}{C_{Total}} = \frac{1}{C_1} + \frac{1}{C_2} + \frac{1}{C_3} = \frac{1}{3C_o} + \frac{\kappa}{3C_o} + \frac{1}{3C_o} = \frac{2 + \kappa}{3 C_o}$$

Consequently,

$$\frac{V_1}{V_0} = \frac{C_{Total}}{C_1} = \frac{1}{2 + \kappa}$$

or

$$V_1 = \frac{V_o}{2 + \kappa} .$$

Thus

$$E_1 = \frac{V_1}{d/3} = \frac{3}{2 + \kappa} \left(\frac{V_o}{d}\right).$$

Since the electric field in the filled capacitor is given by

$$E_0 = \frac{V_0}{d} ,$$

then we have

$$E_1 = \frac{3}{2 + \kappa} \ E_0.$$

We can see that if κ is large, E_1 can be very much smaller than E_0.

Now let us extend our model to include the case of many layers of empty spaces in the crystal. We may divide the bulk crystal into thin vertical

strips as is shown in Fig. 55. Defects in the bulk crystal are the origin of the empty spaces, d_j, in each vertical strip. One can easily show that the electric field in the crystalline material part of the strip, E_p, is related to the applied electric field E (= v/d) from the voltage source by

$$E = E_p [1 + (k - 1)\Delta] \tag{1}$$

where k is the dielectric constand and Δ is defined by

$$\Delta = \frac{\sum_j d_j}{d} \quad . \tag{2}$$

The quantity Δ is the ratio of the thickness of the empty layers to the thickness of the whole sample.

It is of interest to note that in the equation relating E_p and E, E_p is independent of the distribution of the empty layers and depends only on their combined thickness. We may apply this result to the case of a large sample of Rochelle salt between two parallel capacitor plates. For a given applied voltage, the region of the crystal with more defects, hence more empty spaces, experiences a lower average electric field. Therefore, higher applied fields are needed to switch the polarization of the sample. Also, a region with fewer cavity defects would require relatively low voltage for switching. This demonstrates that the S-value would appear low if the sample contains many cavities.

In any real crystal, the number of defects within a given volume may be very large for low-quality samples or very small in very good crystals. Within a single crystal, also, some regions may have many defects while others are almost defect-free. Thus, the value of Δ may differ from one

Figure 55. A Sample Crystal in a Parallel Plate Capacitor.

(A) The bulk sample

(B) A vertical component piece

(A)

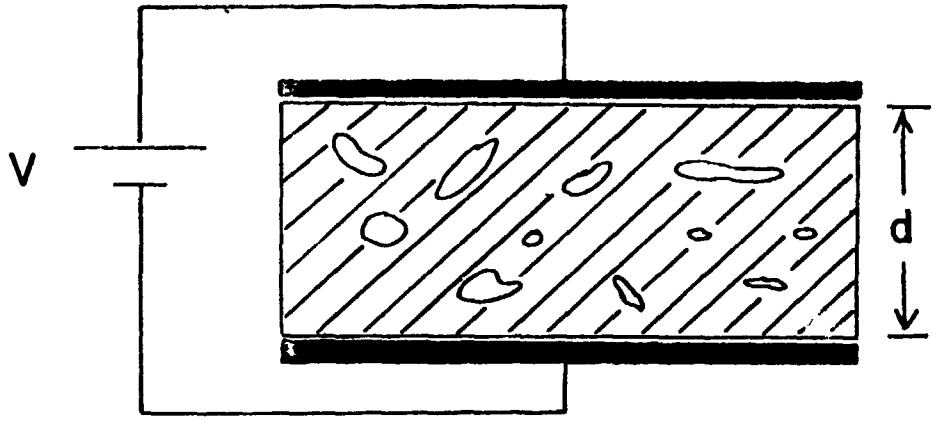

(B)

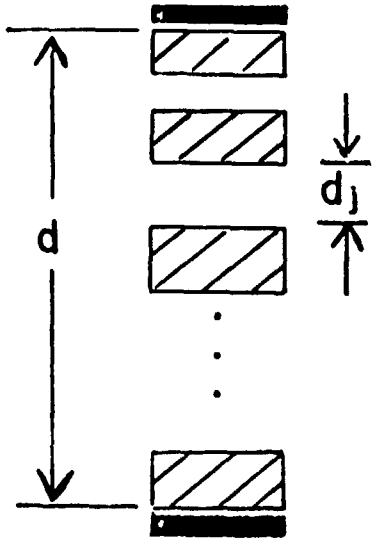

Figure 56. Cavity Distribution Curve.

(A) For a typical crystal.

(B) For a perfect crystal.

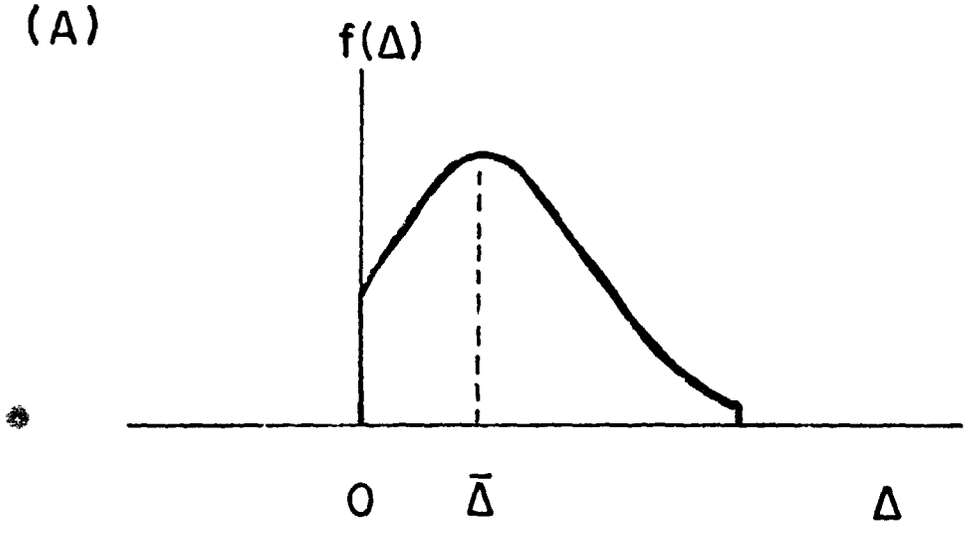
(A)
f(Δ)
0
Δ̄
Δ

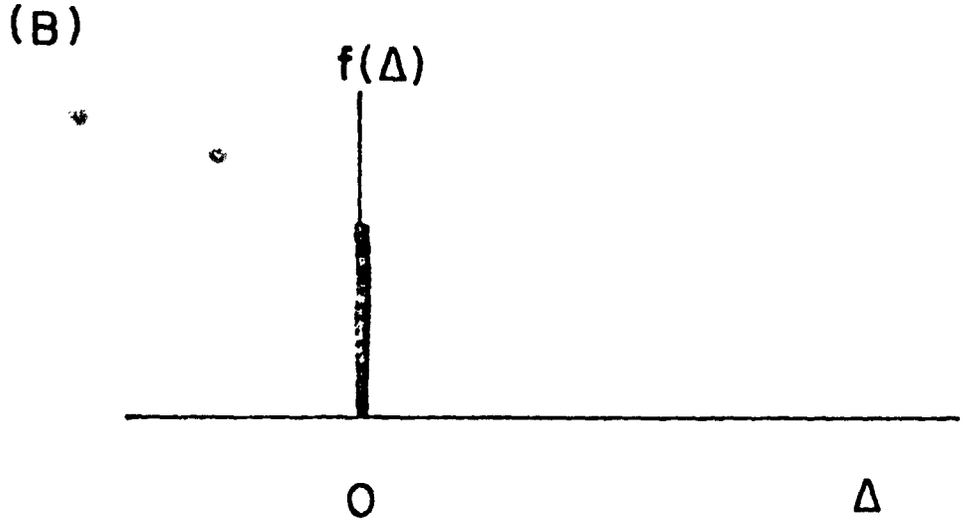
(B)
f(Δ)
0
Δ

Figure 57. Theoretical Hysteresis Curves for b = 1 and k = 200.

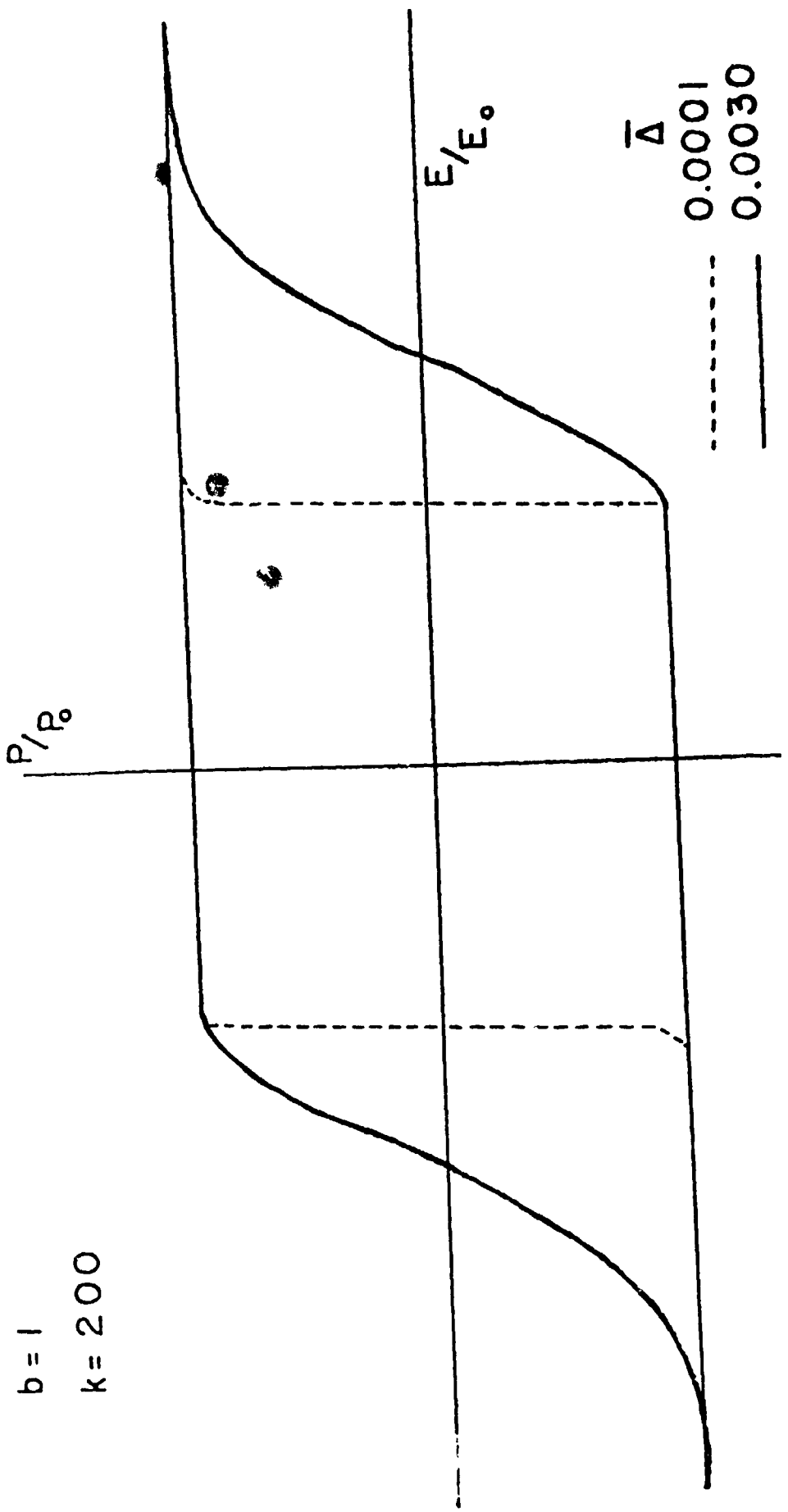
E/E₀
P/P₀
Δ̄
0.0001
0.0030
b=1
k=200

vertical strip to another in the same crystal. For simplicity, we will describe the arrangement of defects as a Gaussian distribution function $f(\Delta)$

$$f(\Delta) = \frac{\exp\left[-\alpha^2 (\Delta - \bar{\Delta})^2\right]}{\int_0^1 \exp\left[-\alpha^2 (\Delta - \bar{\Delta})\right] d\Delta} \quad \text{for } 0 \leq \Delta \leq 1 \tag{3}$$

and $f(\Delta) = 0$ for $\Delta < 0$ or $\Delta > 1$, where $\bar{\Delta}$ is the average Δ over the crystal.

An example of $f(\Delta)$ is given in Fig. 56A. If the crystal were perfect, $f(\Delta)$ should be a delta function such as that shown in Fig. 56B. This condition requires that

$$\alpha = \frac{1}{b\bar{\Delta}} \tag{4}$$

where b is a constant parameter. As $\bar{\Delta} \to 0$, the distribution function approaches a delta function.

Now, as E increases, E_p increases, and at E_p = critical field (E_p^o), the molecular dipole switches from, for example, the (-) direction to the (+) direction. According to Eq. (1), in a component sheet whose Δ is relatively small, this switching occurs for a relatively low applied field E. If the component sheet has a large Δ, a relatively high E is required for switching. With this assumption, polarization of the crystal may be given by

$$P = 2P_o\left[\int_{-\infty}^{\Delta} f(\Delta)\, d\Delta - 1/2\right]. \tag{5}$$

On converting the variable Δ to E with the aid of Eq. 1, one obtains a hysteresis curve

$$P = 2P_o\left[\int_{-\infty}^{E} f_{\bar{\Delta},b}(E)\, dE - 1/2\right], \tag{6}$$

where P_o is the maximum polarization of the crystal and the -1/2 term in the parenthesis is added in order to make P = 0 for E = 0.

Examples of the hysteresis curves obtained with the use of Eq. (6) are given in Fig. 57. In this figure, P/P_o is plotted against E/E_p^o, in the case for b = 1 and k = 200 (dielectric constant of Rochelle salt at 5°C), for $\bar{A} = 0.0030$ and $\bar{A} = 0.0001$. One can see that these curves reproduce the observed ferroelectric hysteresis curves, at least semiquantitatively.

4.6 Summary and Conclusions

The crystal of Rochelle salt grown on board Skylab-4 has the following unique features: (i) the typical cavity is a long tube extending in the direction of the c-crystal axis; the average length being 4 mm compared to 0.1 mm that is the average size in the case of typical earth-grown crystals; (ii) the crystal consists of several single crystals, the corresponding axes of which are parallel to each other. This second result suggests the presence of an orientation-dependent long-range force whose effective distance is possibly as large as a few millimeters. Further characterization of the Skylab crystal include measurements on microscopic defects and ferroelectric hysteresis curves.

The application of our new growth technique, growth from solutions under vacuum conditions, has resulted in crystals of TGS with consistently high L-alanine doping concentrations. The observation of convection currents during solution crystal growth has been improved by a new method of illumination. A Helium-Neon laser beam was used as a source with a Schlieren type observation technique.

A theory for the shape of the ferroelectric hysteresis curve was formulated. It was found that the shape of a hysteresis curve is sensitive

to the concentration of cavities in the crystal. For example, when a high cavity concentration was assumed, the resulting hysteresis curve was similar in shape to that observed for a poor-quality crystal.

Section 5. Other Studies

5.1 Growth in Zero Gravity - Sounding Rocket Flights

5.1-1 Introduction and Background

During the present work period we tried to determine if the few minutes of zero-gravity growth time available on sounding rocket flights could provide an opportunity to perform a useful solution crystal growth experiment. We want to determine if the L-alanine dopant concentration in solution-grown polycrystalline samples of triglycine sulphate (TGS) could be drastically increased if the samples were prepared in a zero-gravity environment. For this purpose, apparatus for growing polycrystals of TGS doped with L-alanine (or other material) in a zero-gravity environment was designed and built. Ground-based experiments which simulated the time course of a sounding rocket flight were performed. Crystals were recovered from these experiments whose size permitted analysis of quality and dopant concentration. We have concluded from these preliminary experiments that sounding rocket flights would be useful for performing doping studies of polycrystalline samples grown in a zero-gravity environment.

In addition, we are continuing to improve the cutting, drilling, and polsihing techniques for examination of the Skylab crystal.

The Skylab-4 growth experiment with Rochelle salt has definitely shown that growth characteristics of a crystal grown in a near-zero gravity environment drastically differ from those of earth-grown crystals. Thus, further growth studies in zero-gravity conditions are needed. The sounding rocket program can provide opportunities for more zero-gravity experiments.

The zero-gravity phase of the rocket's flight lasts only a few minutes. In spite of the short time, however, we believe it is worthwhile to examine the feasibility of using sounding rockets for zero-gravity solution growth experiments for the following reasons:

In the case of moderate rates of solution crystal growth, it has been found that the doping rate increases with increasing rate of crystal growth.[14] When the growth rate is very high, however, the dopant concentration is rather low and many inclusions and cavities appear in the resulting crystal. These facts lead one to speculate: If a crystal is grown at a very high rate in a zero-gravity environment, would the dopant concentration be very much higher than what one can achieve in a one-gravity environment? L-Alanine doped triglycine sulphate is a potentially excellent infrared-detector material, if a highly doped crystal could be obtained. Thus, further investigation is needed to determine if use of a zero-gravity environment drastically improves the doping concentration in general and for this application in particular.

It would be desirable to be able to perform a controlled solution crystal growth experiment such as that already done on Skylab-4. However, the Shuttle/Spacelab programs, which offer opportunities for such long-time zero-gravity growth experiments, are not available to us in the immediate future. Therefore, we have decided to investigate the feasibility of performing experiments during the few minutes of zero-gravity time available during sounding rocket flights. The sounding rocket program is primarily intended to develop experimental techniques and accumulate operational experience in preparation for longer zero-gravity experiments on Shuttle/Spacelab.

5.1-2 Description of the Flight Experiment

The time course of a typical sounding rocket flight is shown in Fig. 58(A). After ignition at t = 0, the rocket accelerates for 32 sec. Approximately one minute after ignition, the vehicle reaches altitudes above 250,000 ft where aerodynamic forces are no longer important. At this point, the payload section is separated from the rocket motor and vehicle rotation rates are reduced to no more than 0.2 degree/sec in all rotational degrees of freedom. At these rotation rates, centripetal accelerations will be less than 10^{-5}g at all points in the payload; stabilization to this level will be completed within 75 to 80 seconds after ignition. Following stabilization, several minutes of weightlessness will be available for data gathering. During this phase of its flight the payload follows a ballistic trajectory and is essentially in free fall.

The payload will typically begin its re-entry into the atmosphere between 5 and 8 minutes after liftoff. A drogue parachute is deployed at 20,000 ft altitude, followed after 12 seconds, by the main parachute, and each event can produce shock loads up to 5g in any direction. The payload ordinarily lands about 15 minutes after liftoff at velocities between 30 and 40 ft/sec, and is usually returned to the launch site by helicopter.

Figure 59(B) shows the time course of a typical solution crystal growth experiment performed in our ground-based laboratory. Details of these experiments will be given in part 5.1-3. The sequence of events is chosen to imitate things that would happen to a solution crystal growth payload during a sounding rocket flight. For example, between ignition and t = 90 seconds the solution is kept warm and under low pressure to remove trapped air; but

Figure 58. Sounding Rocket Flight

The upper drawing shows a typical sounding rocket flight as a function of time. The zero-gravity phase of the flight lasts about 4 minutes.

The lower drawing is a representation of a simulation crystal growth experiment performed in our ground-based laboratory. Crystal growth is typically completed in 60 seconds.

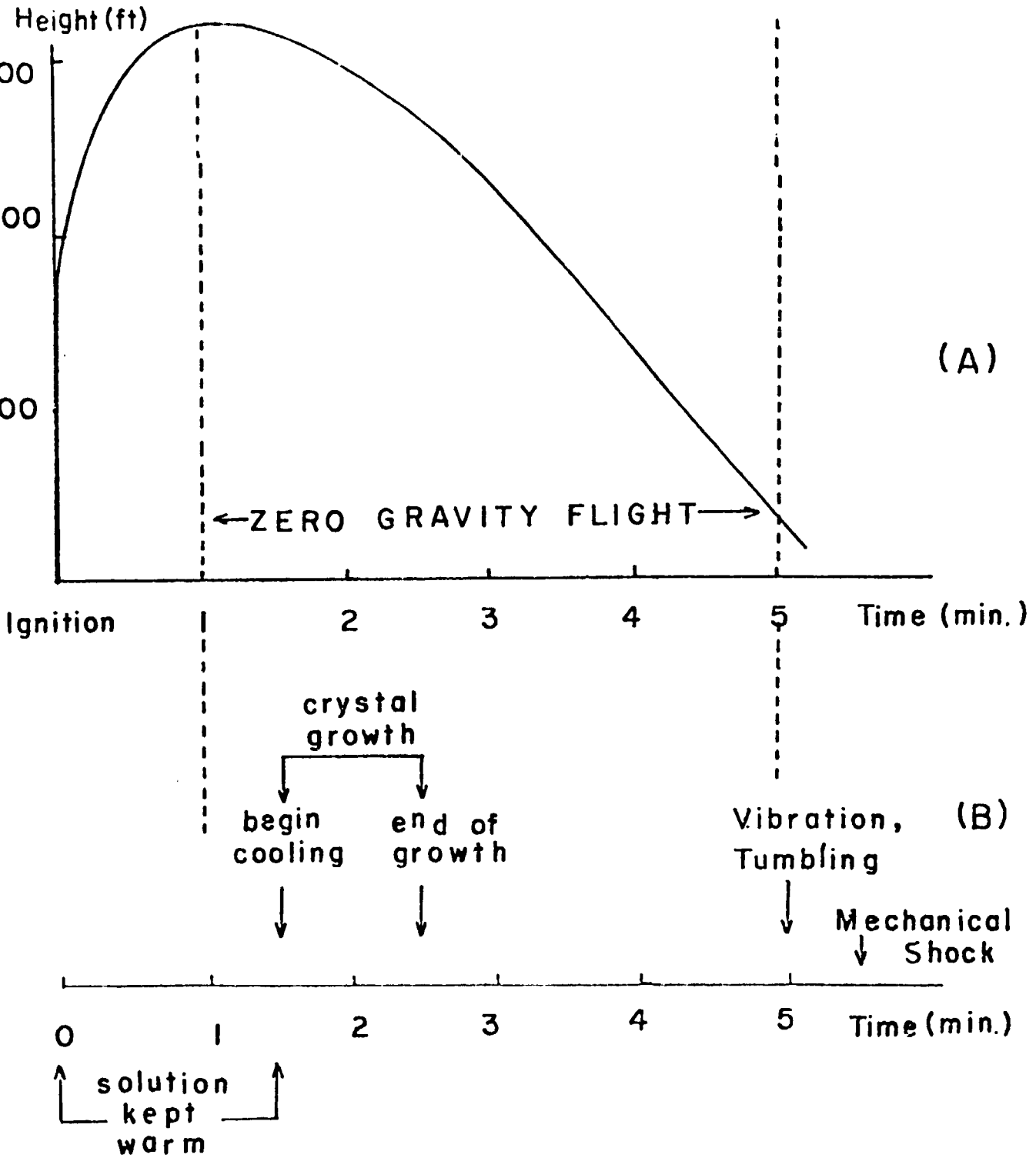
Height (ft)
9 00,000
6 00,000
3 00,000
(A)
←ZERO GRAVITY FLIGHT→
Ignition
2
3
4
5
Time (min.)
crystal growth
begin cooling
end of growth
Vibration, Tumbling
(B)
Mechanical Shock
0
1
2
3
4
5
Time (min.)
solution kept warm

crystals are not allowed to grow while the motor is accelerating the payload. The solution is then cooled very rapidly when the sounding rocket reaches the zero-gravity phase of its flight, and crystals grow very quickly from the supersaturated solution. At re-entry, the payload would receive a considerable mechanical shock, so we apply a large mechanical shock to our ground-based system. We wish no crystals to grow as a result of this shock, because we are interested only in crystals grown during the zero-gravity phase of the experiment. Thus we must choose a suitable initial concentration and temperature change for the growth process so that it will automatically stop before the shocks occur.

5.1-3 Ground-Based Experiments

Table V summarizes the results of several simulation crystal growth experiments performed in our ground-based laboratory. A small volume of growth solution was placed in a 20 cc growth cell. At t = 0, a vacuum pump was switched on and allowed to evacuate the cell to about 1 psi in about 5 seconds. This rapid evaporation cooled the growth solution below its saturation temperature and precipitate was formed. The material that was produced was allowed to grow for various lengths of time. The pumping was stopped at some point and the solution was observed to see when all growth or precipitation stopped. In most cases, the entire time of growth was only 60 seconds. The growth cells were sometimes given a mechanical shock to see if new crystalline material could be produced.

After about 5 minutes the material formed during the experiment was recovered and examined for size and quality. Typical crystals ranged from 50 - 100 μ in size although larger ones were frequently found. By choosing a suitable initial concentration and temperature change the growth process can be made to terminate at any desired time after the solution is cooled.

Table V. Simulation Experiments

Small amounts of triglycine sulphate (TGS) solution with $CuCl_2$ or L-alanine dopant were placed in a growth cell. Rapid cooling was performed by pumping on the solution. In most cases crystals or precipitate were formed within about 20 seconds after pumping began and growth was completed after one minute. The crystalline product was examined under a low-power microscope for size and quality.

Material	Saturation Temperature	Volume of Solution	Time of Crystal Appearance	Time to End of Growth	Time to End of Pumping	Time to Solution Separation	Size of Recovered Crystals	Comments
TGS + 5% $CuCl_2$	23°C	1.5cc	20 sec	60 sec		10 min	0.03mm	Mechanical shock produced no crystals from recovered growth solution.
TGS + 5% $CuCl_2$	40°C	1.5cc	3 min	4 min	3 min	8 min	0.5mm	Reculting polycrystals had very faint blue color; high copper doping.
TGS + 5% $CuCl_2$	23°C	1.5cc	30 sec	90 sec	60 sec	5 min	0.03mm	
TGS + 5% $CuCl_2$	23°C	1.5cc	0-20sec	90 sec	2 min		0.1mm	
TGS + 5% $CuCl_2$	23°C	1.1cc	0-20sec	90 sec	2 min		0.1mm	
TGS + 10% L-al.	30°C	1.5cc	20 sec	80 sec	100sec	6 min	0.1mm	Boiling occured.
TGS + 10% L-al.	30°C	1.5cc	0-20sec	80 sec	60 sec	6 min	0.1mm	
TGS + 10% L-al.	30°C	1.5cc	50 sec	100 sec	60 sec	6 min	0.2mm	Good crystals formed.
TGS + 10% L-al.	23°C	1.5cc	60 sec	120 sec	30 sec	30 min	0.05mm	Boiling happened; 1 day later remaining solution had produced no more crystals at room temperature
TGS + 10% L-al.	23°C	1.8cc	60 sec	120 sec	45 sec	30 min	0.05mm	After 1 day at room temperature remaining solution had produced no more crystals
TGS + 10% L-al.	23°C	1.0cc	90 sec	160 sec	1 min	10 min	0.1mm	
TGS + 10% L-al.	23°C	1.5cc	20 sec	90 sec	1 min	10 min	0.15mm	
R.S. + 10% $CuCl_2$	23°C	1.5cc	no crystals formed		90 sec			Boiling occured.

The results of these preliminary experiments have clearly demonstrated that it is possible to grow polycrystals large enough to be analyzed during the zero-gravity phase of a sounding rocket flight.

Since we have shown that useful crystals can be grown in a zero-gravity environment during a sounding rocket flight, it was necessary to build a device that could serve as the growth cell on the payload. Because there is an excellent vacuum available during the zero-gravity part of the flight, it was decided to use fast evaporation to rapidly cool the growth solution.

Figure 59 shows a cross-sectional view of our prototype. The growth cell is thermally insulated by a stainless-steel vacuum jacket to protect the contents from environmental temperature fluctuations. Figure 60 shows a photograph of our growth cell without the stainless steel jacket. To initiate growth, one first evacuates the chamber immediately above the growth cell. The current in the solenoid is then switched on to open the valve which causes the pressure inside the growth cell to drop suddenly. The valve is allowed to remain open until the desired amount of solution has evaporated (about 30 seconds). The current is switched off and the valve is closed due to the attraction between the permanent magnet and the solenoid core. The crystal growth continues without further intervention. Growth terminates automatically when a saturation condition exists at the new temperature and pressure.

We propose the following procedure for using the device described in the preceding paragraphs during a sounding rocket experiment. The apparatus of Fig. 59 should be mounted in the payload stage in such a way that the average acceleration during powered flight will be directed along the vial

Figure 59. Cross Sectional View of Vacuum Evaporation Crystal Growth Cell.

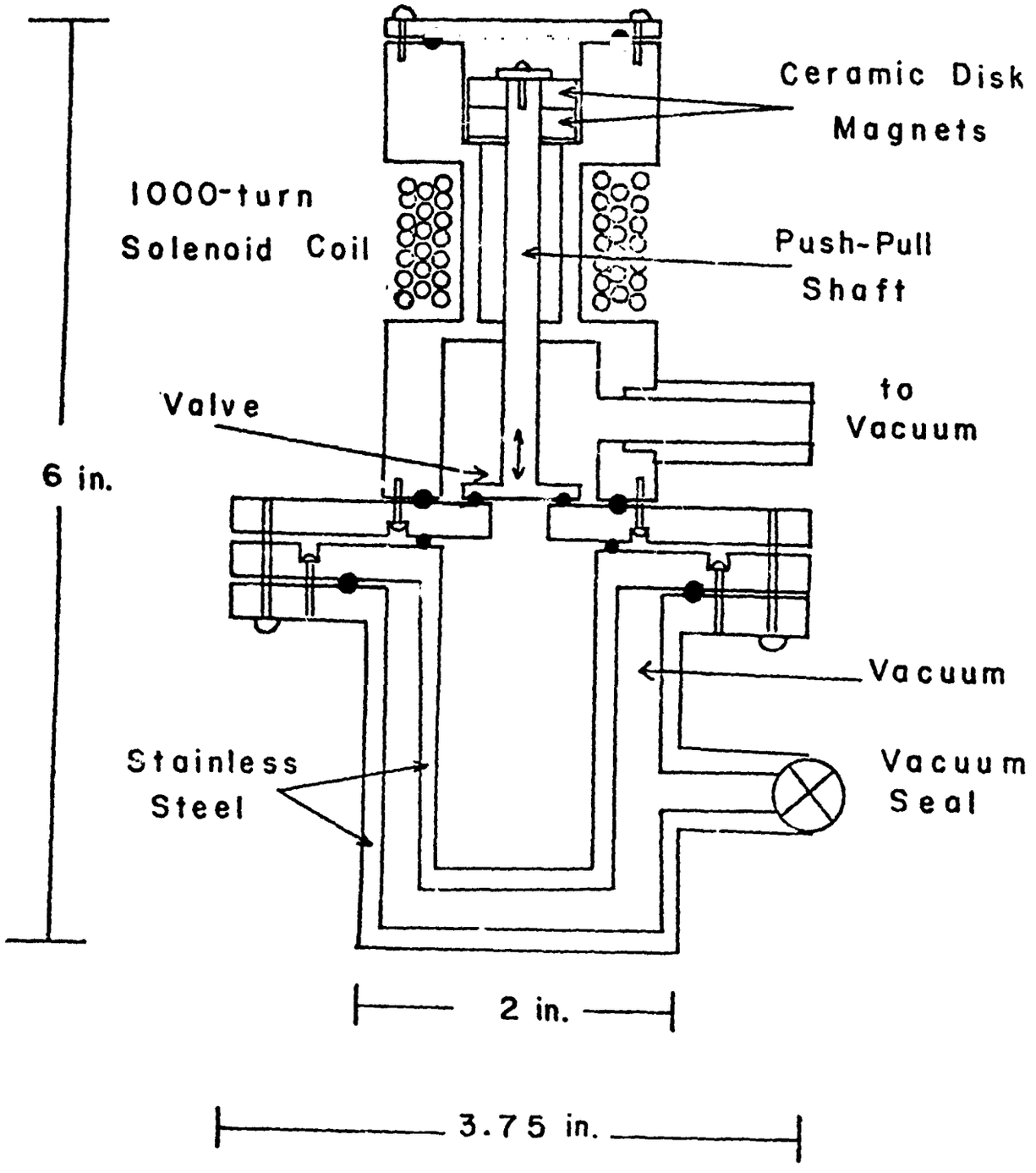
Ceramic Disk
Magnets
1000-turn
Solenoid Coil
Push-Pull
Shaft
to
Vacuum
Valve
6 in.
Vacuum
Stainless
Steel
Vacuum
Seal
2 in.
3.75 in.

Figure 60. Photograph of Growth Cell.

The photograph shows our prototype solution crystal growth cell without its stainless steel jacket. The cell is made of Plexiglas so that growth can be easily observed.

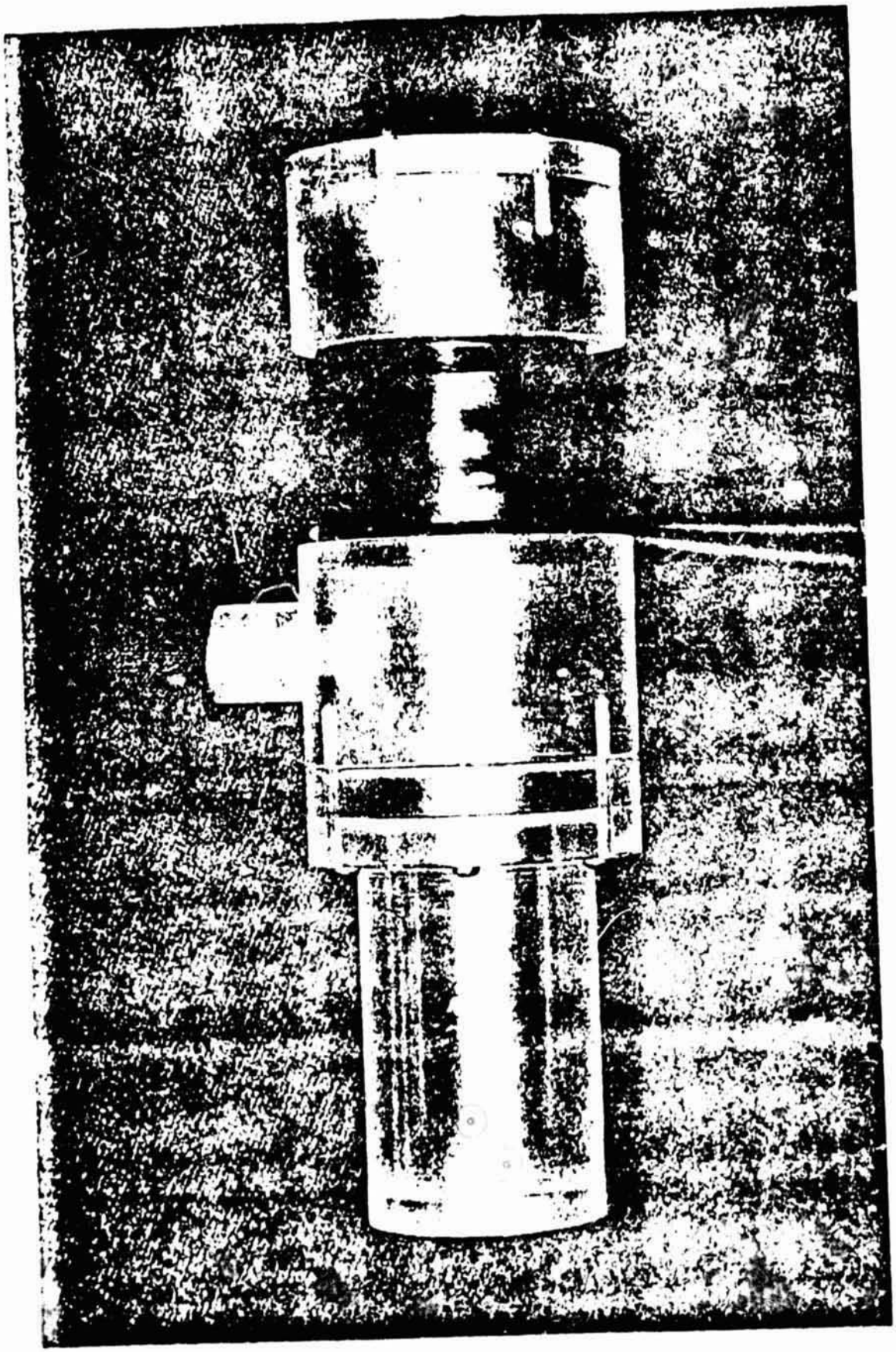

axis, away from the valve. Thus, the growth solution will be confined to the end of the apparatus opposite the valve and will experience minimum stirring accelerations. The growth solution should be transferred to the vial at about 25°C, and the vacuum jacket sealed in place. This will thermally insulate the solution while the rocket begins its flight. When the payload begins the zero-gravity phase of the flight, the valve should be opened. Ground-based simulation experiments show that 1.2 amps switched through the 1000-turn solenoid coil will quickly and reliably operate the valve. After about 3 seconds, enough water will have evaporated from the solution to insure that the temperature of the solution will drop and crystals will begin to grow. At this point the valve should be closed by switching off the current. Crystal growth may then continue in the closed vial until saturation conditions are reached. By a proper choice of initial concentrations, the growth may be stopped while the solution is still in zero-gravicy surroundings. The stainless-steel vacuum jacket will maintain the lower temperature resulting from the sudden evaporation for the rest of the flight. This insures against higher solution temperatures dissolving crystals grown in the zero-gravity phase or much lower temperatures precipitating material from the solution which was not grown under zero-gravity conditions.

The largest dimensions of our prototype are 6 inches by 3.75 inches. Its weight, subject to flight safety standards that may later be imposed by NASA, is less than one pound, including the growth solution. Any combination of amp-turns that equals 1200 or more is enough to reliably operate the valve. The resistance of our solenoid coil was about 10 ohms, thus our power requirements were 14.4 watts. Coils with different amp-turns could require less power.

Safe internal temperatures could be maintained by the stainless-steel vacuum jacket for as long as one hour to allow time for recovery of the precipitated material. If ambient temperature is excessively warm, special precautions may have to be taken to insure that the crystalline product does not re-dissolve in the remaining solution.

The most important information that will be obtained from the zero-gravity sounding rocket experiment is the amount of dopant present in the recovered crystalline product. Amino-acid analysis may be used in the case of L-alanine doped into crystals of TGS, while ESR (Electron Spin Resonance) techniques can measure the copper ion concentration in triglycine sulphate crystals doped with $CuCl_2$. Both these techniques are likely to be successful with very small amounts of powder-like crystalline material.

If larger crystals (1 cubic millimeter or more in volume) are produced in the experiment, analysis of microscopic defects will be performed. These microscopic defects will be compared to defects in crystals grown under one-gravity conditions and to those found in other crystals grown in zero-gravity surroundings.[19]

If it is possible to perform a preliminary experiment, the information gained could be used to improve the apparatus for the next growth experiment. Thus, it would be desirable to perform more than one solution growth experiment.

5.2 Crystal Defects

In some regions of the Skylab crystal and in several earth-grown crystals, we have observed the type of microscopic defect shown in Fig. 61. These defects

Figure 61. An Example of One Type of Defect.

The photograph shows an example of a type of defect found in the Skylab crystal and in many earth-grown crystals. The drawing below shows the structure of the dark sphere with its bright ring and central bright spot for clarity.

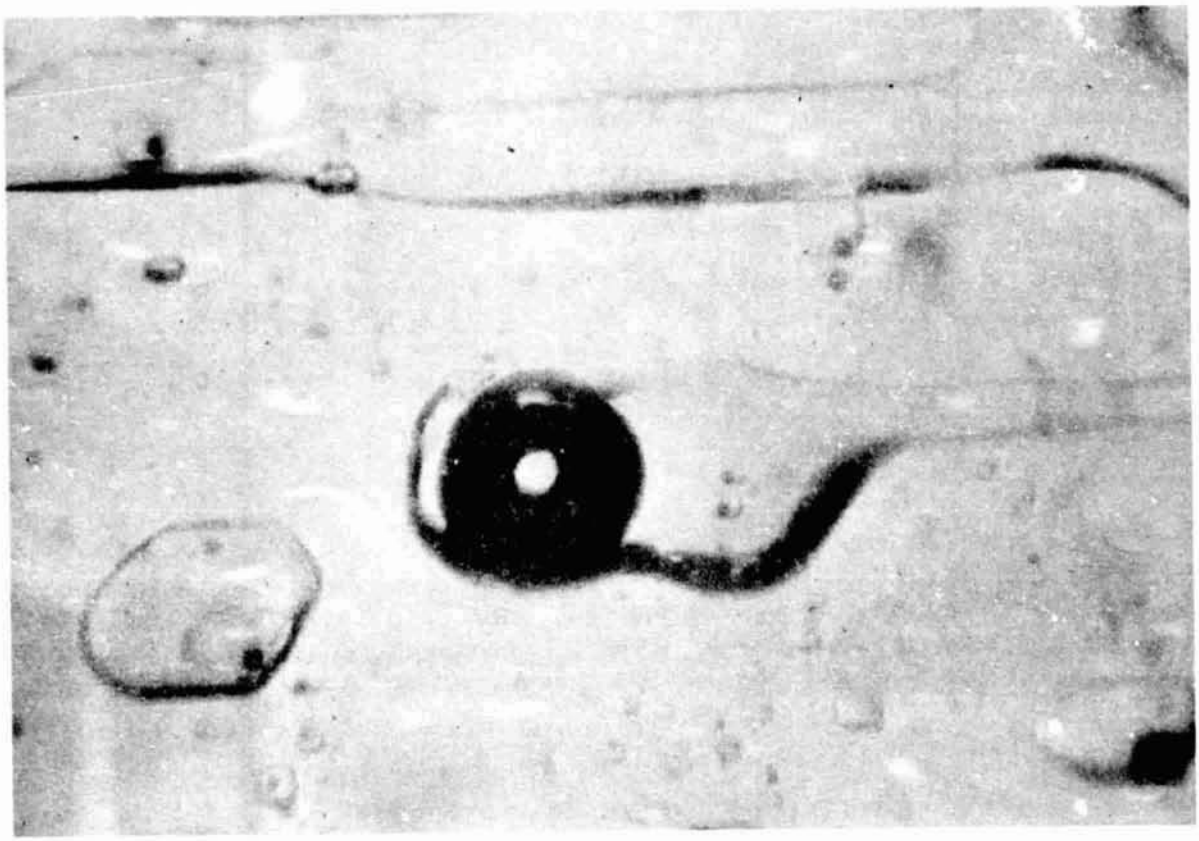

1 mm

appear to be cavities containing a sphere of solution. However, close inspection of the dark sphere reveals a bright ring inside. The ratio of the diameter of this ring to the diameter of the dark sphere is constant and equal to about 2/3. The bright spot in the center of the dark sphere is due to undeviated light passing through the center of the sphere.

Recently, some workers have examined the appearance of an air bubble inside a container filled with water.[20] They found that the air bubble looks like a dark sphere with a bright spot in the center and contains a bright ring whose radius is about 2/3 that of the dark sphere. Thus, it is possible that the defect shown in Fig. 61 is actually a solution-filled cavity containing an air bubble. For this reason further investigation is needed to tell if this is the case.

5.3 Procedure for Drilling in Crystals

During our studies on convection currents it became important to develop a technique for supporting the growing crystal in solution. A technique such as this would be especially important for growth experiments in a zero-gravity environment when one wishes to hold a crystal at a desired position in the solution. A crystal can be supported with a thin glass rod, if a small hole is drilled in it. This drilling is not an easy task, however, since crystals such as Rochelle salt are very fragile. For this reason Tom Hunter, Machinist for the Physics Department, designed a special machine and established the drilling procedure for fragile crystals. A paper on this work will appear in the Review of Scientific Instruments shortly.[21]

5.4 Nature of Ferroelectricity

Two ferroelectric crystals, Rochelle salt and TGS, were used in many experiments of this project. In spite of a great deal of study by many workers, the nature of ferroelectricity has not been clarified. This nature must be clarified eventually in order that the results obtained in the current project be fully utilized both industrially and scientifically. For this reason, some effort toward this direction was made during this project. With the use of electron-nuclear-double-resonance (ENDOR) technique, strong evidence was obtained which indicates that the ferroelectricity in TGS is associated with the quantum-tunneling of a proton in the crystal. A paper based on this study will appear in the Journal of Chemical Physics shortly.[22]

Section 6. Recommendations

In view of the results obtained in this investigation, the following is recommended.

(1) Further ground-based research in solution crystal growth.

A great deal of effort has been made in the last two decades to understand the mechanism of growth and doping of metal and semiconductor crystals. Compared to these efforts only a small amount of work has been done to understand the fundamental mechanisms of crystal growth from solutions; for example, no one had seriously investigated such subjects as the effect of growth rate on dopant concentration, microscopic cavities and effect of convection on their production and crystal growth in low-pressure environments until we studied these things in this project. Although many scientists have used solution-grown crystals, few people have studied growth techniques. Because of this lack of basic knowledge we recommend that long-range support be given for investigating solution crystal growth.

There are two other purely practical reasons why we believe solution crystal growth studies should be supported: First, in the temperature range where most solution crystal growth occurs, it is relatively easy to obtain 1% accuracy of temperature control. For example, if one works on between 25°C and 35°C, he can easily control the temperature with 0.2°C. At the high temperatures necessary for metal and semiconductor crystal growth, control of this accuracy is difficult to achieve. Hence greater reliability and consistency can be expected from solution crystal growth experiments. Second, we have seen how much information can be gained by observing the flow of convection currents around a growing crystal. In most cases, crystals which grow from solution can be properly illuminated so that

surrounding convection currents can be seen, but convection currents around crystals grown from a melt can usually only be imagined. Very sophisticated techniques could be used to make convection in melts visible, but almost any investigator may see convection in a water-solution system if he chooses. Thus, there is more potential information on the effect of convection to be gained from studying solution crystal growth.

(2) Future flight experiments

More zero-gravity solution crystal growth experiments are needed to understand the difference in crystals grown in zero and one gravity surroundings. Our preliminary experiment on Skylab-4 has definitely demonstrated the difference in cavity formation in Rochelle salt crystals grown in zero-gravity and those grown in one-gravity surroundings. Differences such as this need to be studied for several other materials. The Space Shuttle program should offer opportunities for this type of investigation.

Section 7. References

1. H. V. Malmstadt, C. G. Enke, and E. C. Toren, Jr., (W. A. Benjamin, Inc., New York, 1963), Chapter 8.

2. F. Jona and G. Shirane, "Ferroelectric Crystals" (The McMillan Company, New York, 1962).

3. P. G. Grodzka and T. C. Bannister, Science 176, 506 (1972).

4. "International Critical Tables of Numerical Data" (Ed. by C. D. Hogman, McGraw-Hill, New York, 1933).

5. "Handbook of Chemistry and Physics" (Ed. by C. D. Hogman, Chemical Rubber Publishing Co., Cleveland, Ohio, 1958).

6. G. Volkel and W. Windsch, Phys. Stat. Sol. (b) 43, 263 (1971).

7. Bob A. Wilkinson, Jr. and I. Miyagawa, J. Chem. Phys. 55, 2177 (1971).

8. I. Miyagawa, NASA Technical Summary Report, Contract Number NAS 8-28098, February 28, 1973.

9. "Pyroelectric Infrared Detectors", Royal Radar Establishment, Procurement Executive Ministry of Defense, 1973.

10. P. J. Lock, Appl. Phys. Lett. 19, 390 (1971).

11. H. C. Gatos, in a report given by R. Snyder at the George C. Marshall Space Flight Center, January 18, 1973.

12. Reported by W. Wilcox, Convection Conference, the George C. Marshall Space Flight Center, August 9, 1973.

13. K. L. Bye, P. W. Whipps, and E. T. Keve, Ferroelectrics 4, 253 (1972).

14. I. Miyagawa, Technical Summary Report, NASA Contract #NAS8-28098, May, 1974.

15. See, for example, for review, D. T. J. Hurle, J. Cryst. Growth 13, 39 (1972).

16. See, for example, reference 2, p. 282.

17. Electronic Design 22, 39 (March, 1974).

18. "Pyroelectric Infrared Detectors", Royal Radar Establishment, Procurement Executive Ministry of Defense, 1973.

19. I. Miyagawa, Progress Report, NAS 8-28098, August 7, 1974, Fig. 4 on p. 9.

20. D. McLachlan, Jr., and H. M. Cox, Rev. Sci. Instrum., 46, 80 (1975).

21. Tom Hunter, Rev. Sci. Instrum., December, 1975, in press.

22. Y. Kotake and I. Miyagawa, J. Chem. Phys., December 1, 1975, in press.